Changing land-use patterns are of great importance in environmental studies and critical for land use management decision-making over farming systems in arid and semi-arid regions. Unfortunately, ground data scarcity or inadequacy in many regions can cause large uncertainties during the characterization of phenological changes in arid and semi-arid regions, which can hamper tailored decision-making towards the best agricultural management practices. Alternatively, state-of-the-art methods for phenological metrics extraction and long-time series analysis techniques of multispectral remote sensing imagery provide a viable solution. In this context, this thesis aims to assess the relevance of phenology data and machine learning algorithms to characterize the changes over farming systems. It also investigates the strength and validity of phenology data combined with climate data to provide the first pheno-climatic classification of Morocco. To this end, four farming systems (FS) (Fallow (FA), Rainfed area, (RA) Irrigated Annual Crop (IAC), and Irrigated Perennial Crop (IPC)) in arid areas of Morocco were studied based on 13 phenological metrics (PhM). These metrics were derived from large MODIS-NDVI time-series between 2000 and 2020. For classification and change analysis purposes, 3 machine learning algorithms and a pixel-based change analysis method were investigated. Besides, long time series of climatic data (i.e., rainfall data and land surface temperature) and phenological metrics were used to produce the first pheno-climatic classification of Morocco at a scale of 500 m. The classification overall accuracy over the Beni Mellal-Khenifra region reached 88%, with a kappa coefficient of 0.83 and values of F1-score greater than 0.76. However, by comparing, the accuracy of the three classifiers (i.e., Support Vector Machine (SVM), Random Forest (RF), and k-Nearest Neighbour (K-NN)), the RF method showed the best performance with an overall accuracy of 0.97 and kappa coefficient of 0.96. Variations in FS have been found to be linked well with other indicators of local agricultural land management, as well as the historical agricultural drought changes over the study area. Results showed a significant dynamism of the plant cover linked to the behaviour of farmers who tend to cultivate intensively and to invest in high-income crops. More specifically, a relevant variability in fallow and rainfed areas closely linked to the weather conditions was found. In addition, a significant lag trends of the start (-6 days), end (+3 days) of season was found, and which indicate that the length of the season was related to spatio-temporal variability of rainfall. This study has also highlighted the potential of Multitemporal moderate spatial resolution data to accurately monitor agriculture and better manage land resources. In the meantime, for operationally implementing the use of such work in the field, we believe that it is essential to consider the perceptions, opinions, and mutual benefits of farmers and stakeholders to improve strategies and synergies whilst ensuring food, welfare, and sustainability.

Keywords: Morocco, Oum Er-Rbia, semi-arid, farming systems, NDVI, phenology, time-series, machine learning, pheno-climatic classification.

N° d'ordre : 418/22

Caractérisation et suivi à long terme de la phénologie des couverts agricoles par utilisation des modèles d'apprentissage automatique et les données spatiales à

LEBRINI YOUSSEF

N° d'ordre : 418/22

كلية العلوم والتقنيات ببني ملال
Faculté des Sciences et Techniques de Béni Mellal

UNIVERSITE SULTAN MOULAY SLIMANE

Faculté des Sciences et Techniques

Béni-Mellal

Centre d'Études Doctorales : ***Sciences et Techniques***

Formation Doctorale : **Ressources Naturelles, Environnement ET Santé**

THÈSE

Présentée par

LEBRINI YOUSSEF

Pour l'obtention du grade de

DOCTEUR

Discipline : **Sciences de la Terre**

Spécialité ***: Télédétection et Sciences des Données***

Caractérisation et suivi à long terme de la phénologie des couverts agricoles par utilisation des modèles d'apprentissage automatique et les données spatiales à moyenne résolution spatiale

Soutenue le Mardi 17 Mai 2022 à 10h devant la commission d'examen:

Abdelghani CHEHBOUNI	Professeur et program lead, Université Mohammed VI Polytechnique, Ben Guerir, Maroc.	Président
Abdelhamid FADIL	Professeur, Ecole Hassania des Travaux Publiques (EHTP), Casablanca, Maroc	Rapporteur
Nadya WAHID	Professeur, Faculté des Sciences et Techniques, Université Sultan Moulay Slimane, Béni Mellal, Maroc	Rapporteur
Salah ERRAKI	Professeur Faculté des Sciences et Techniques, Université Cadi Ayyad, Marrakech, Maroc	Rapporteur
Mustapha NAMOUS	Professeur, Faculté Polydisciplinaire, Université Sultan Moulay Slimane, Béni Mellal, Maroc	Examinateur
Malika OURRIBANE	Professeur, Ecole Supérieur de Technologie, Université Sultan Moulay Slimane, Béni Mellal, Maroc	Examinateur
Ahmed LAAMRANI	Professeur, Université Mohammed VI Polytechnique, Ben Guerir, Maroc.	Invité
Abdelghani BOUDHAR	Professeur, Faculté des Sciences et Techniques, Université Sultan Moulay Slimane, Béni Mellal, Maroc	Encadrant
Tarik BENABDELOUAHAB	Chercheur, Institut Nationale de Recherche Agronomique, Rabat, Maroc	Co-Encadrant

Thesis Presentation

Author:

LEBRINI Youssef

Data4Earth Lab, Faculty of Sciences and Techniques, Sultan Moulay Slimane University, Beni Mellal 23000, Morocco; E-mail: y.lebrini@usms.ma

Title:

Characterization and long-term monitoring of crop cover phenology using machine learning models and multitemporal moderate spatial resolution data

Specialty:

Remote Sensing and Data Science

Supervisor:

Pr. Abdelghani BOUDHAR

Data4Earth Lab, Faculty of Sciences and Technics, Sultan Moulay Slimane University, Beni Mellal 23000, Morocco.

Co-Supervisor:

Dr. Tarik Benabdelouahab

National Institute of Agronomic Research (INRA), Rabat, Morocco.

Cite as:

Lebrini Youssef (2022). Characterization and long-term monitoring of crop cover phenology using machine learning models and multitemporal moderate spatial resolution data. Ph.D., Sultan Moulay Slimane University, Beni Mellal, Morocco. p120.

Articles

Lebrini, Y., Boudhar, A., Laamrani, A., Htitiou, A., Lionboui, H., Salhi, A., Chehbouni, A., Benabdelouahab, T. Mapping and Characterization of Phenological Changes over Various Farming Systems in an Arid and Semi-Arid Region Using Multitemporal Moderate Spatial Resolution Data. *Remote Sens.* 2021, *13*, 578. https://doi.org/10.3390/rs13040578 **(SCOPUS and WoS, IF= 4.85)**

Lebrini Y., Boudhar A., Htitiou A., Hadria R., Lionboui H., Bounoua L., Benabdelouahab T., (2020). Remote monitoring of agricultural systems using NDVI time series and machine learning methods: a tool for an adaptive agricultural policy. *Arabian journal of Geosc*iences, 13. https://doi.org/10.1007/s12517-020-05789-7 **(SCOPUS, IF= 1.83)**

Lebrini Y., Boudhar A., Hadria R., Lionboui H., Elmansouri L., Arrach R., Ceccato P., Benabdelouahab T., (2019). Identifying Agricultural Systems Using SVM Classification Approach Based on Phenological Metrics in a Semi-arid Region of Morocco. *Earth Systems and Environment*, 3(2), 277-288. https://doi.org/10.1007/s41748-019-00106-z **(SCOPUS)**

Lebrini,Y., Benabdelouahab T., Boudhar A., Htitiou, A., Hadria, R., Lionboui, H., 2019. Farming systems monitoring using machine learning and trend analysis methods based on fitted NDVI time series data in a semi-arid region of Morocco, Proc. SPIE 11149, Remote Sensing for Agriculture, Ecosystems, and Hydrology XXI, 111490S, 21 October. https://doi.org/10.1117/12.2532928 **(SCOPUS)**

Benabdelouahab T., **Lebrini Y.**, Boudhar A., Hadria R., Htitiou A., Lionboui H., 2019. Monitoring spatial variability and trends of wheat grain yield over the main cereal regions in Morocco: a remote-based tool for planning and adjusting policies. *Geocarto International*.1-20. https://doi.org/10.1080/10106049.2019.1695960 **(SCOPUS, IF= 3.78)**

Salhi, A., Benabdelouahab, T., Martin-Vide, J., Okacha, A., El Hasnaoui, Y., El Mousaoui, M., El Morabit, A., Himi, M., Benabdelouahab, S., **Lebrini, Y.**, Boudhar, A., & Casas Ponsati, A. (2020). Bridging the gap of perception is the only way to align soil protection actions. *Science of The Total Environment*, 718, 137421. https://doi.org/10.1016/j.scitotenv.2020.137421 **(SCOPUS, IF= 7.96)**

Htitiou, A., Boudhar, A., **Lebrini, Y.**, Lionboui, H., Chehbouni, A., Benabdelouahab T., 2021. Classification and status monitoring of agricultural crops in central Morocco: a synergistic combination of OBIA approach and fused Landsat-Sentinel-2 data. Journal of Applied Remote Sensing 15(1). https://doi.org/10.1117/1.JRS.15.014504 **(SCOPUS, IF= 1.53)**

Benabdelouahab T., Gadouali F., Boudhar A., **Lebrini Y.,** Hadria R. & Salhi A. (2020). Analysis and trends of rainfall amounts and extreme events in the Western Mediterranean region. *Theoretical and Applied Climatology*. https://doi.org/10.1007/s00704-020-03205-4 **(SCOPUS, IF= 2.88)**

Lionboui H., Benabdelouahab T., Htitiou A., **Lebrini Y.**, Boudhar A., Hadria R., Elame F. 2020. Spatial assessment of losses in wheat production value: A need for an innovative approach to guide risk management policies. *Remote Sensing Applications: Society and Environment*. https://doi.org/10.1016/j.rsase.2020.100300 **(SCOPUS)**

Htitiou, A., Boudhar, A., **Lebrini, Y.**, Hadria, R., Lionboui H., Benabdelouahab T., 2020. A comparative analysis of different phenological information retrieved from Sentinel-2 time series images to improve crop classification: a machine learning approach, Geocarto International, https://doi.org/10.1080/10106049.2020.1768593 **(SCOPUS, IF= 3.78)**

Htitiou A., Boudhar A., **Lebrini Y.**, Hadria R., Lionboui H., Elmansouri L., Tychon B., Benabdelouahab T., 2019. The Performance of Random Forest Classification Based on Phenological Metrics Derived from Sentinel-2 and Landsat 8 to Map Crop Cover in an Irrigated Semi-arid Region. *Remote Sensing in Earth Systems Sciences*. https://doi.org/10.1007/s41976-019-00023-9 **(SCOPUS)**

Hadria R., Boudhar A., Ouatiki H., **Lebrini Y.**, Elmansouri L., Gadouali F., Lionboui H., Benabdelouahab T., 2019. Combining Use of TRMM and Ground Observations of Annual Precipitations for Meteorological Drought Trends Monitoring in Morocco, *American Journal of Remote Sensing*, 7(2): 25-34. https://doi.org/10.11648/j.ajrs.20190702.11

Hadria, R., Benabdelouahab, T., Elmansouri, L., Gadouali, F., Ouatiki, H., **Lebrini, Y.**, Boudhar, A., Salhi, A., & Lionboui, H. 2019. Derivation of air temperature of agricultural areas of Morocco from remotely land surface temperature based on the updated Köppen-Geiger climate classification. *Modeling Earth Systems and Environment*. https://doi.org/10.1007/s40808-019-00645-4 **(SCOPUS)**

Hadria R., Elmansouri L., Benabdelouahab T., Ouatiki H., **Lebrini Y.**, Htitiou A., Khellouk R., Recours aux satellites pour appuyer le management de l'eau d'irrigation : Estimation des besoins en eau des agrumes par télédétection dans la Plaine de Triffa-Berkane (Maroc), 2019, *African Journal of Land Policy and Geospatial Sciences*, Vol.2, No.2. https://doi.org/10.48346/IMIST.PRSM/ajlp-gs.v2i2.16334

Benabdelouahab, T., Derauw, D., Hayat, L., Tychon, B., Hadria, R., Boudhar, A., Balaghi, R., **Lebrini, Y.**, Maaroufi, H., & Barbier, C., 2019. Using SAR Data to Detect Wheat Irrigation Supply in an Irrigated Semi-arid Area. *Journal of Agricultural Science*. Vol. 11. https://doi.org/10.5539/jas.v11n1p21.

Book chapters

Boudhar, A., Ouatiki H., Bouamri H., **Lebrini Y.,** Karaoui I., Hssaisoune M., Arioua A., and Benabdelouahab T., 2020. Hydrological Response to Snow Cover Changes Using Remote Sensing over the Oum Er Rbia Upstream Basin, Morocco, edited by N. Rebai and M. Mastere, 95-102: Springer International Publishing. https://doi.org/10.1007/978-3-030-21166-0_9

Hadria R., Salhi A., Benabdelouahab T., Elmansouri L. , Lionboui H., Ouatiki H., **Lebrini Y.,** Htitiou A., Khellouk R., 2019. Evaluation of TRMM 3B42 V7 Rainfall Product over Morocco, In book: Recent advances in environmental Science from the Mediterranean region, Publisher: Springer - Advances in Science, Technology and Innovation (ASTI). https://doi.org/10.1007/978-3-030-51210-1_298

Presentations

Lebrini, Y., Benabdelouahab T., Boudhar, A., Htitiou, Lionboui, H., Assessment of MODIS phenological metrics performance to identify the behavior of agricultural systems. Oral Comm. 41st Canadian Symposium on Remote Sensing, 13-16 July 2020. (Online).

Lebrini Y., Benabdelouahab T., Boudhar A., Htitiou A., Hadria R., Lionboui H., Farming systems monitoring using machine learning and trend analysis methods based on fitted NDVI time series data in a semi-arid region of Morocco. Oral Comm., SPIE Remote Sensing for Agriculture, Ecosystems and Hydrology XXI, Strasbourg 9-13 September 2019, France.

Lebrini Y., Boudhar A., Hadria R., Lionboui H., BENABDELOUAHAB T., Oral Pres. Monitoring and analyzing vegetation dynamics over agricultural areas of Morocco using NDVI time-series. Afro-Mediterraniean Conference on Multidisciplinary Research & Applications, 7 & 8 july 2018, IAV, Rabat, Morocco.

Htitiou, A., Boudhar, A., **Lebrini, Y.,** Benabdelouahab T., Deep learning-based reconstruction of spatiotemporally fused satellite images for smart agriculture applications in a heterogeneous agricultural region. 5th International Conference on Smart City Applications. 7–8 October 2020, Virtual Safranbolu, Turkey (Online).

Htitiou A., Benabdelouahab T., Boudhar A., **Lebrini Y.**, Hadria R., Lionboui H., Oral Pres. A Phenology-Based Method for Operational Crop Type Mapping through a Combined Use of Landsat-8 and Sentinel-2A Data, International Symposium on Applied Geoinformatics (ISAG-2019) 7-9 November 2019, Istanbul, Turkey.

Hadria R., Salhi A., Benabdelouahab T., Elmansouri L., Lionboui H., Ouatiki H., **Lebrini Y.**, Htitiou A., Khellouk R., Evaluation of TRMM 3B42 V7 Rainfall Product over Morocco, Euro-Mediterranean Conference for Environmental Integration 10-13 Octobre 2019, Sousse, Tunisia.

Acknowledgment

The difficulty with thanks is that I must summarize a 4 years period of meetings and sharing of ideas, and try not to forget anyone.

My first words of thanks go to my supervisor Prof. Abdelghani BOUDHAR, for the opportunity offered to carry out this project within his team and the trust he placed in me. He has given me unfailing scientific support throughout this period of work. I thank him warmly for this.

I would also like to thank Doctor Tarik Benabdelouahab, my co-supervisor, for his strong contribution to the success of this work and for his welcome at the National Institute of Agronomic Research (INRA).

I express my gratitude to all spatial agencies around the world to NASA for providing free access to a large part of their satellite data.

My sincere thanks also go to the members of the jury for the interest they gave to this work by agreeing to examine it and enrich it with their comments.

Thanks to all members of the GEVARET team for their help and support during all the years that I have spent with the team.

I would like to especially thank my family who gave me the freedom to act and the wisdom to continue in this way. I thank them for encouraging me to pursue this adventure and for their support, morally and financially.

Finally, to all those whose help was not negligible.

Abstract

Changing land-use patterns are of great importance in environmental studies and critical for land use management decision-making over farming systems in arid and semi-arid regions. Unfortunately, ground data scarcity or inadequacy in many regions can cause large uncertainties during the characterization of phenological changes in arid and semi-arid regions, which can hamper tailored decision-making towards the best agricultural management practices. Alternatively, state-of-the-art methods for phenological metrics extraction and long-time series analysis techniques of multispectral remote sensing imagery provide a viable solution. In this context, this thesis aims to assess the relevance of phenology data and machine learning algorithms to characterize the changes over farming systems. It also investigates the strength and validity of phenology data combined with climate data to provide the first pheno-climatic classification of Morocco. To this end, four farming systems (FS) (Fallow (FA), Rainfed area, (RA) Irrigated Annual Crop (IAC), and Irrigated Perennial Crop (IPC)) in arid areas of Morocco were studied based on 13 phenological metrics (PhM). These metrics were derived from large MODIS-NDVI time-series between 2000 and 2020. For classification and change analysis purposes, 3 machine learning algorithms and a pixel-based change analysis method were investigated. Besides, long time series of climatic data (i.e., rainfall data and land surface temperature) and phenological metrics were used to produce the first pheno-climatic classification of Morocco at a scale of 500 m. The classification overall accuracy over the Beni Mellal-Khenifra region reached 88%, with a kappa coefficient of 0.83 and values of F1-score greater than 0.76. However, by comparing, the accuracy of the three classifiers (i.e., Support Vector Machine (SVM), Random Forest (RF), and k-Nearest Neighbour (K-NN)), the RF method showed the best performance with an overall accuracy of 0.97 and

kappa coefficient of 0.96. Variations in FS have been found to be linked well with other indicators of local agricultural land management, as well as the historical agricultural drought changes over the study area. Results showed a significant dynamism of the plant cover linked to the behaviour of farmers who tend to cultivate intensively and to invest in high-income crops. More specifically, a relevant variability in fallow and rainfed areas closely linked to the weather conditions was found. In addition, a significant lag trends of the start (-6 days), end (+3 days) of season was found, and which indicate that the length of the season was related to spatio-temporal variability of rainfall. This study has also highlighted the potential of Multitemporal moderate spatial resolution data to accurately monitor agriculture and better manage land resources. In the meantime, for operationally implementing the use of such work in the field, we believe that it is essential to consider the perceptions, opinions, and mutual benefits of farmers and stakeholders to improve strategies and synergies whilst ensuring food, welfare, and sustainability.

Keywords: Morocco, Oum Er-Rbia, semi-arid, farming systems, NDVI, phenology, time-series, machine learning, pheno-climatic classification.

ملخص

تغيير أنماط استخدام الأراضي له أهمية كبيرة في الدراسات البيئية وحاسمة لإدارة استخدام الأراضي في المناطق القاحلة وشبه القاحلة. لسوء الحظ، فإن ندرة البيانات الأرضية أو عدم كفايتها في العديد من المناطق يمكن أن تسبب شكوكًا كبيرة أثناء توصيف التغيرات الفينولوجية في المناطق القاحلة وشبه القاحلة، مما قد يعيق صنع القرار المصمم تجاه أفضل ممارسات الإدارة الزراعية. بدلاً من ذلك، توفر أحدث الأساليب لاستخراج المقاييس الفينولوجية وتقنيات تحليل السلاسل طويلة الأمد لصور الاستشعار عن بعد متعددة الأطياف حلاً قابلاً للتطبيق. في هذا السياق، تهدف هذه الأطروحة إلى تقييم أهمية بيانات علم الفينولوجيا وخوارزميات التعلم الآلي لتوصيف التغيرات في أنظمة الزراعة. كما تبحث في قوة وصحة بيانات الفينولوجيا جنبًا إلى جنب مع البيانات المناخية لتقديم أول تصنيف فينو-مناخي للمغرب. تحقيقا لهذه الغاية، تمت دراسة أربعة أنظمة زراعية: المنطقة المعشوشبة *(FA)* ، المنطقة البورية *(RA)* المنطقة المسقية *(IAC)* ، و المنطقة المسقية المعمرة *((IPC)* على أساس 13 مقياسًا فينولوجيًا .تم اشتقاق هذه المقاييس من سلاسل زمنية كبيرة لـ *MODIS-NDVI* بين عامي 2000 و2020. لأغراض التصنيف وتحليل التغيير، تم فحص 3 خوارزميات للتعلم الآلي وطريقة تحليل التغيير المعتمدة على البيكسل. إلى جانب ذلك، تم استخدام سلسلة زمنية طويلة من البيانات المناخية (أي بيانات هطول الأمطار ودرجة حرارة سطح الأرض) والمقاييس الفينولوجية لإنتاج أول تصنيف فينو-مناخي للمغرب بمقياس 500 متر. بلغت الدقة الكلية للتصنيف على منطقة بني ملال خنيفرة 88٪، مع معامل كابا 0.83 وقيم درجة *F1* أكبر من 0.76 أظهرت النتائج ديناميكية كبيرة للغطاء النباتي مرتبطة بسلوك المزارعين الذين يميلون إلى الزراعة بشكل مكثف والاستثمار في المحاصيل عالية الدخل. وبشكل أكثر تحديدًا، تم العثور على تنوع وثيق الصلة في المناطق البور والمعشوشبة المرتبطة بظروف الطقس. بالإضافة إلى ذلك، تم العثور على اتجاهات تأخر لبداية الموسم (-6 أيام)، ونهاية الموسم (+3 أيام)، والتي تشير إلى أن طول الموسم كان مرتبطًا بالتباين المكاني والزماني لهطول الأمطار. سلطت هذه الدراسة الضوء أيضًا على إمكانات بيانات الدقة المكانية المعتدلة متعددة الزمان لرصد الزراعة بدقة وإدارة موارد الأراضي بشكل أفضل. في غضون ذلك، من أجل التنفيذ العملي لاستخدام مثل هذا العمل في هذا المجال، نعتقد أنه من الضروري النظر في التصورات والآراء والمزايا المتبادلة للمزارعين وأصحاب المصلحة لتحسين الاستراتيجيات مع ضمان الغذاء والرفاهية والاستدامة.

الكلمات المفتاحية: المغرب، أم الربيع،مناخ شبه قاحل، نظم الزراعة، مؤشر*NDVI* ، علم الفينولوجيا، السلاسل الزمنية، التعلم الآلي، التصنيف الفينو-مناخي

Résumé

L'évolution des modes d'utilisation des terres est d'une grande importance dans les études environnementales et critique pour la gestion de l'utilisation des terres dans les régions arides et semi-arides. Malheureusement, la rareté ou l'inadéquation des données au sol dans de nombreuses régions peut entraîner de grandes incertitudes lors de la caractérisation des changements phénologiques dans les régions arides et semi-arides, ce qui peut entraver la prise de décision adaptée vers les meilleures pratiques de gestion agricole. Alternativement, les méthodes de pointe pour l'extraction de métriques phénologiques et les techniques d'analyse de longues séries temporelles d'images de télédétection multispectrales offrent une solution viable. Dans ce contexte, cette thèse vise à évaluer la pertinence des données phénologiques et des algorithmes d'apprentissage automatique pour caractériser les changements sur les systèmes agricoles. Elle étudie également la force et la validité des données phénologiques combinées aux données climatiques pour fournir le premier zonnage phéno-climatique du Maroc. À cette fin, quatre systèmes agricoles (jachère (FA), zone pluviale (RA), culture annuelle irriguée (IAC), et culture pérenne irriguée (IPC)) dans les zones arides du Maroc ont été étudiés sur la base de 13 paramètres phénologiques (PhM). Ces métriques ont été dérivées de grandes séries temporelles MODIS-NDVI entre 2000 et 2020. Pour la classification et l'analyse des changements, trois algorithmes d'apprentissage automatique et une méthode d'analyse des changements basés sur les pixels ont été étudiés. En outre, de longues séries chronologiques de données climatiques (c'est-à-dire les données pluviométriques et la température à la surface du sol) et de métriques phénologiques ont été utilisées pour produire la première classification phéno-climatique du Maroc à une échelle de 500 m. La précision globale de la classification sur la région de Beni Mellal-Khenifra a atteint 88 %, avec un coefficient de kappa de 0,83 et des valeurs de score F1 supérieures à 0,76. Cependant, en comparant la précision des trois classificateurs (Support vector Machine (SVM), la Random Forest (RF) et les K Nearest Neighbor (K-NN)), la méthode RF a montré la meilleure performance avec une précision globale de 0,97 et un coefficient de kappa de 0,96. Les variations du FS se sont avérées être bien liées à d'autres indicateurs de la gestion locale des terres agricoles, ainsi qu'aux changements historiques de la sécheresse agricole dans la zone d'étude. Les résultats ont montré un dynamisme significatif de la couverture végétale lié au

comportement des agriculteurs qui ont tendance à cultiver de manière intensive et à investir dans des cultures à haut revenu. Plus spécifiquement, une variabilité pertinente dans les zones de jachère et de culture pluviale étroitement liée aux conditions météorologiques a été trouvée. En outre, un décalage significatif entre le début (-6 jours) et la fin (+3 jours) de la saison a été constaté, ce qui indique que la durée de la saison est liée à la variabilité spatio-temporelle des précipitations. Cette étude a également mis en évidence le potentiel des données multitemporelles à résolution spatiale modérée pour surveiller avec précision l'agriculture et mieux gérer les ressources foncières. En attendant, pour mettre en œuvre de manière opérationnelle l'utilisation de ces travaux sur le terrain, nous pensons qu'il est essentiel de prendre en compte les perceptions, les opinions et les avantages mutuels des agriculteurs et des parties prenantes pour améliorer les stratégies et les synergies tout en assurant l'alimentation, le bien-être et la durabilité.

Mots-clés : Maroc, Oum Er-Rbia, climat semi-aride, systèmes agricoles, NDVI, phénologie, séries temporelles, apprentissage automatique, zonnage phéno-climatique.

Table of Contents

Acronyms

AVHHR:	Advanced Very High Resolution Radiometer
AOS:	Amplitude of Season
AS/FS:	Agricultural Systems/Farming Systems
BVAL:	Base Value
DIP:	Doukkala Irrigated Perimeter
EVI:	Enhanced vegetation index
EMS:	Electromagnetic spectrum
EOS:	End of Season
EOST:	End of Season Time
FIR:	Far InfraRed
FA:	Fallow
IPC:	irrigated Perennial Crop
IAC:	irrigated Annual Crop
K-NN:	K-nearest Neighbor
LST:	Land Surface Temperature
GINT:	Great Integral
LD:	Left Derivative
LSP:	Land Surface Phenology
LWIR:	Large Wave InfraRed
MWIR:	Mid Wave InfraRed
ML:	Machine Learning
MODIS:	Moderate Resolution Imaging Spectroradiometer
NDVI:	Normalized Difference Vegetation index
NIR:	Near InfraRed
NASA:	National Aeronautics and Space Administration
NGA:	National Geospatial-Intelligence Agency
OER-AGS:	Oum Er-Rbiaa Agency's Geographical Scop
PhM:	Phenological Metrics
RD:	Right Derivative
RA:	Rainfed Area
RF:	Random Forest
RGB:	Red, Green, Blue
SOS:	Start of Season
SOST:	Start of Season Time
SINT:	Short Integral
SVM:	Support Vector Machine
SWIR:	Short Wave InfraRed
TIP:	Tadla Irrigated Perimeter
JPL :	Jet Propulsion Laboratory

List of Figures

List of Tables

General introduction

Phenology is the study of natural cycles and repeating biological processes (Schwartz 2003). It's an integral discipline that can extend interactions to the population, community, and landscape scales while also providing essential insight into ecology at the individual level. (Cleland et al. 2007; Schwartz 2003). Spring season arrival starts a flood of green throughout vast swaths of the globe, when plants begin their phenological cycle of growth, reproduction, and senescence. Timing of these phenological stages is closely tied to temperature and climate through the phenological cycle (White et al. 2009a). Even though it does not seem apparent, modest variations in rainfall and temperature can cause significant differences in plant development timing. (Atzberger et al. 2013). In addition, the ecological connections that rely on the presence of plants might be affected by this temporal change. Phenology information, such as farming system type and development stages, has previously been proved as a viable alternative for agricultural management methods and identifying crop kinds and yields in the agricultural sector(Cui et al. 2019). Many studies have been conducted to investigate the use of machine learning methods for agricultural systems monitoring and vegetation cover mapping. Yu et al. (2018) have used KNN and SVM classifiers to evaluate the effects of a new method to extract information from neighborhood pixels on the improvement of Land Use Land Cover (LULC) classification. Wessel et al. (2018) have focused their study on the comparison of the object-based image analysis (OBIA) and pixel-based methods to evaluate RF and SVM classifiers in mapping tree species using Sentinel-2 data. Wang et al. (2018) have evaluated the performance of Landsat 8, Sentinel-2, and Pléiades-1 data in mapping mangrove species over the National Nature Reserve for mangroves in China. Finally, Jin et al. (2016) have determined a new approach to classify deforested areas based on phenological metrics and RF classification.

Studying phenology through time series data provides a vibrant alternative to traditional static methods (i.e, single date image analysis). They give a cohesive way to characterize the dynamic processes occurred through farming systems. In this regard, remote sensing provides good opportunities to accurately and repeatedly map this relevant

information, as it offers timeliness, global coverage, and objective observation. Nevertheless, the task of mapping farming systems is not a straightforward and simple matter since it requires specific data and particular analysis techniques. Rapid image acquisition from satellite sensors perceive inter- and intra-season phenological patterns, and assess ongoing trends in ecosystem responses to climate warming (Zhang et al. 2003). Phenology maps express the geographical distribution of the current stages, or phenophases, of plant development at a particular point in time. They provide a foundation for evaluating which species interactions are most sensitive to temperature, and help us understand how trophic mismatches can affect community dynamics, ecosystem services, and species conservation over time (Gill et al. 2019).

The pursuit of these objectives is presented in four independent research articles that fit together into a unified body of work. Chapter 3 works to develop an effective methodology for phenological metrics extraction over the Beni Mellal-Khenifra region. It explores the effectiveness of using phenological metrics in mapping farming systems over the studied region using machine learning algorithms. Chapter 4 aims to evaluate 3 machine learning algorithms for mapping farming systems over the Oum Er-Rbiaa (OER) basin. Therefor it investigates changes in farming systems over 20 years using a change analysis method. Chapter 5 develops a methodology to effectively map and characterize the behaviour of farming systems using phenological metrics and trend analysis tests. Using phenological and change analysis methodologies developed in the previous chapters, this chapter aims to map trends over farming systems for 20 years of coarse resolution satellite observations.

Finally, data of phenological metrics computed over Morocco, land surface temperature, rainfall and topography data were used to establish the first pheno-climatic classification of Morocco. Chapter 6 provides more details about the methodology and shows results of this pheno-climatic classification.

Chapter 1: Fundamental backgrounds

1.1 Phenology

The term "phenology" was derived from the Greek word "phainō" which means "to show" or "to appear" and the word "logos" which mean, "to study". This term (i.e., Phenology) was introduced by the Belgian botanist Charles Morren in 1853 (Hopp 1974; Lieth 1974). The term "phenology" indicates that phenology has been principally concerned with the dates of first occurrence of biological events in their annual cycle.

The phenology is an integrative discipline and could be defined as the study of the timing of recurring biological events, the causes of their timing with regard to biotic and abiotic effects, and the interrelation among phases of the same or different vegetation cover (Lieth 1974; Schwartz 2013). Phenophases can include vegetative phase, reproductive phase, and grain development phase (Wielgolaski 2001). Figure 1 shows an example of wheat crop phenophases during a cropping season.

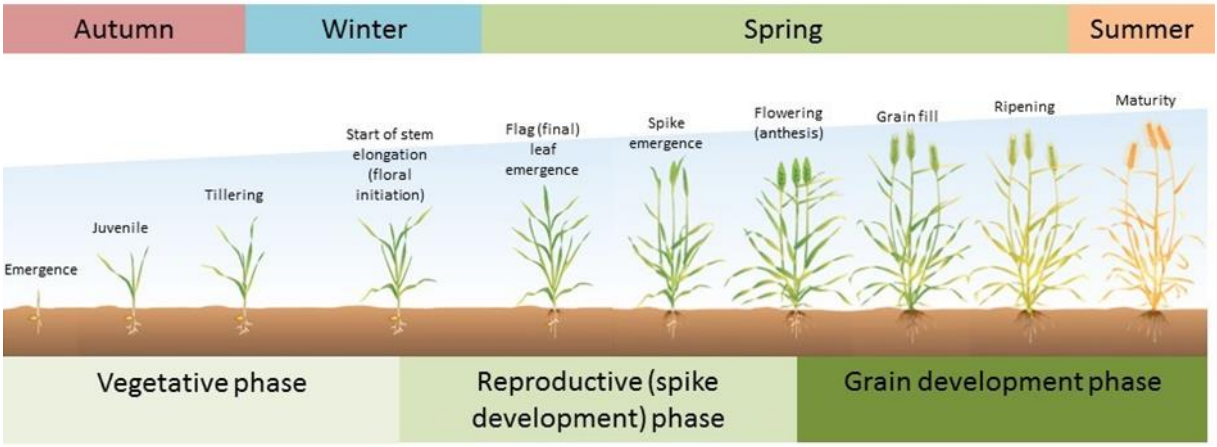

Figure 1: Illustration of phenological phases of vegetation cover (https://grdc.com.au)

The number of phenophases to be investigated deeply related to the field of the study,

observation method and the research applications (Laskin and McDermid 2016; Liang 2019). There are many subfield of phenology, the applications adopted within this research are in the sub-field of phytophenology, this sub-field interests to the study of plants seasonality (Defila and Clot 2001). Many factors affect the development stages of vegetation cover (i.e., temperature, photoperiod, moisture). As reported by Menzel et al. (2006) temperature has the greatest effect on vegetation seasonality. The quantity of heat remains constant each year, but the length of time between phenophases can vary due to variability in weather and surrounding ambient temperatures (Laskin et al. 2019; Schwartz 2013). This could be explained by the plant requirement in term of amount of accumulated heat energy in order to move from a phenological stage to another (Estrella et al. 2007).

Rainfall amounts and the variability of rainfall are two other factors, which affect the phenological stages of vegetation cover (Suepa et al. 2016). Low amounts of rainfall affect especially vegetation in rainfed area where no irrigation supply is provided. In addition, lack of precipitations have also an effect on vegetation cover over other farming systems (i.e., irrigated system). This effect could be manifested as the scarcity of water resources and succession of drought periods. Length of cropping season is also affected by geographic location. Based on hopkin's law phenological stages varies based on latitude and elevation. These variations in length of season are of 4 days per degree latitude or 120 m increase in elevation (Hopkins 1918).

1.2 Remote Sensing Basics

Remote sensing is the science of deriving information about an object without being in physical contact with it (Campbell and Wynne 2011). From a geoscience stand of point, remote sensing describes the science of collecting information about targets (object or phenomenon) from the Earth's terrestrial, atmospheric, and aquatic ecosystems using radiation sensors on-board aerospace ships (Campbell and Wynne 2011). Earlier, remote sensing of objects on earth surface started with cameras secured on tethered balloons back in the 1840s for topographic mapping. Platforms that are more sophisticated emerged over time (i.e., aircraft and spacecraft). The development of these platforms was mainly motivated by the need for military surveillance and reconnaissance (Campbell and Wynne 2011). Aerial photography

(cameras mounted on airplanes) was brought to existence by World War I, while spacecraft-based photography (cameras mounted on artificial satellites) started with the emergence of space programs in the 1960s (Campbell and Wynne 2011). Hence, remote sensing techniques have been used in numerous civil applications related to natural resources monitoring. Remote sensing includes the full process of illumination, atmospheric and target interactions, information recording by the sensors, and storage and data processing in the ground segment (e.g., reception units) (Figure 2). The targets must first be illuminated in order to be detected from space. This can be through electromagnetic radiation naturally produced by the sun (passive remote sensing) or artificially produced (active remote sensing) based on radar instruments (Campbell and Wynne 2011).

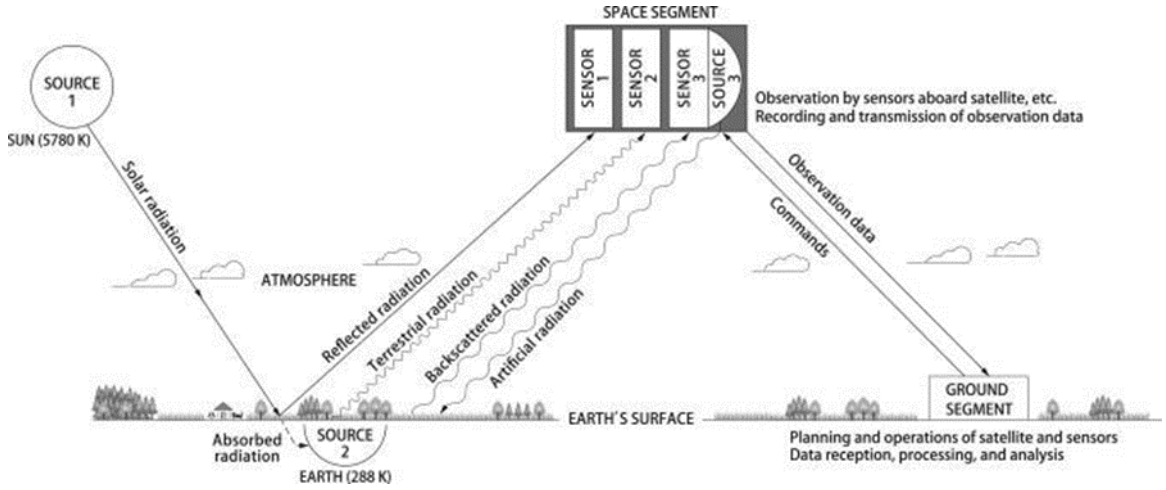

Figure 2: Remote sensing process (source: https://www.omnisci.com)

The electromagnetic radiation, a result of combined electric and magnetic waves, comprises multiple regions (Figure 3). The latter are categorized by the wavelength (the distance between successive wave crests, measured in Meters), or by the frequency (number of cycles of a wave per unit time, measured in Hertz) in what is called the electromagnetic spectrum (EMS). This EMS, range from the gamma radiation bands (the shortest wavelength and highest frequency) to the radio waves (the longest wavelengths and lowest frequencies). However, the radiation that is practical for remote sensing is limited to those regions lying between the visible wavelengths and the microwaves. The visible region of the electromagnetic spectrum, which occupies wavelengths between 0.4 and 0.7 μm, is the only part that is perceptible to the human eyes. Right after the visible region, there is the infrared radiation where the associated wavelength lies between 0.7 and 100 μm. The infrared

comprises five sub-regions, namely the near infrared (NIR), the short wave infrared (SWIR), the mid wave infrared (MWIR), the large wave infrared (LWIR), and the far infrared (FIR) (Figure 3). The NIR and MWIR waves (from 0.7 to 3 μm) are used the same way as the visible ones as all of them are captured by the sensors as reflected energy. The FIR (from 17 to 100 μm), on the other hand, is mostly the radiation released from the terrestrial targets as heat depending on the target's temperature, and thus recorded as thermal energy (Campbell and Wynne 2011). Above 100 μm until 1 m in wavelength, the radiation belongs to the microwave region.

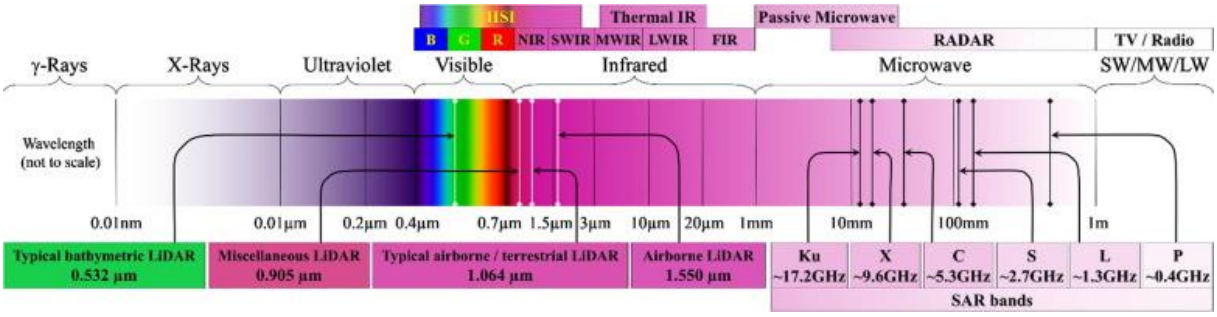

Figure 3: The electromagnetic spectrum (Toth and Jóźków 2016)

The microwave region can be divided into several bands (Ka, K, Ku, X, C, S, L, and P) that can be artificially produced and recorded by the radar systems (Figure 3). In the passive system, after the radiation reaches the surface, it interacts with the various terrestrial targets. Depending on the physical characteristics of the target, the radiation is either reflected towards the sensors or absorbed by the targets and later released in longer wavelength as heat (Campbell and Wynne 2011). However, during its travel through the atmosphere, the radiation interacts with the various atmospheric particles and molecules (aerosols) through the scattering and absorption phenomena. Both of these disturb the electromagnetic radiation when it travels from the sun towards the terrestrial targets and when it is reflected or emitted by these targets towards the sensors in orbit. They specifically take place when the aerosols are in the propagation path of the radiation. The radiation is subject to a change of trajectory or absorbed by the aerosols. The amount of radiation disturbed or blocked from attending the passive sensors depends on the wavelength of the incoming radiation and the density of aerosols in the atmospheric column the radiation is traveling through (Campbell and Wynne 2011). The atmospheric effect generally occurs when the aerosols are about the same or greater

size than the wavelength radiation. Aerosols of large sizes such as water droplets are capable to influence a wide range of wavelengths. Molecules constituting the atmosphere absorb the radiation at specific wavelengths. The absorption phenomenon is mainly caused by ozone, carbon dioxide, and water vapor. Each of these molecules absorbs specific radiation wavelengths at various regions of the electromagnetic spectrum (Figure 3). The Ozone-induced absorption mostly blocks the ultraviolet radiation from getting to the earth's surface. The carbon dioxide mostly absorbs radiation in the first half of the FIR preventing it from escaping the atmosphere. The water vapor presents various absorption windows throughout the electromagnetic spectrum. The most significant of these concerns the emitted radiation located in the second half of the FIR region and the shorter microwaves. The vast majority of remote sensing applications mainly rely on the electromagnetic radiation that belongs to the regions, called atmospheric bands, where the absorption is at its minimum. The weather applications, on the other hand, make use of both of the aforementioned atmospheric distortion phenomena.

1.3 Remote Sensing of Phenology

Despite it is an interdisciplinary field, phenology did not attract much attention before the age of satellites (Schwartz 2003). From this viewpoint, detection of phenology from the ground seems difficult if not impossible. Numerous platforms have been employed in the phenological analysis of vegetation since the early 1970's (Table 1). Some of these sensors, such as the popular Advanced Very High Resolution Radiometer (AVHRR) and Landsat, have extensive imagery archives for detecting long-term phenology patterns. The size and aims of the research are dictated by the different spatial and temporal resolutions of the numerous sensors. To some extent, image fusion has worked as a compromise in bridging this gap. (de Moura et al. 2017).The red edge of the electromagnetic spectrum is absorbed by chlorophyll in healthy vegetation for photosynthesis, it reflects strongly in the green and even more in near-infrared regions; this mismatch in reflectance is known as the red edge (Myneni et al. 1995). The sensors are sensitive to these wavelengths, and a popular index called the normalized difference vegetation index (NDVI) was developed to leverage the differences in the red visible and near-infrare (Rouse et al. 1973). Because it is directly related to the total density of healthy

vegetation on the planet's surface, the NDVI is frequently employed as a proxy for vegetation cover (Tucker 1979; Tucker et al. 1983). By creating a ratio between the red and near-infrared bands, much of the inherent signal variation due to calibration, noise, and atmospheric effects are minimized (Xiaoyang Zhang et al. 2003). However, NDVI is limited by saturation in high biomass regions such as the tropics, the amount of soil brightness, and is intrinsically nonlinear.

Table 1: Satellite sensors and datasets used for phenological research.

Platform	Sensor	Operation	Resolution	Frequency
Landsat	MSS	1973-1985	79 m	18 days
Landsat	TM	1984-present	30 m	16 days
Landsat	OLI-TIRS	2013-present	30 m	16 days
Landsat	ETM+	1999-present	30 m	16 days
Sentinel-2	MSI	2015-present	10-60 m	5 days
NOAA	AVHRR	1982-present	8 km	twice
NOAA	AVHRR	1989-present	1 km	twice monthly
SPOT	Vegetation	1999-present	1 km	1-2 days
Terra	MODIS	2000-present	250 m, 500 m, 1 km	1-2 days
Aqua	MODIS	2002-present	250 m, 500 m, 1 km	1-2 days

Schwartz and Reed (1999) worked to refine the observed timing between satellites derived Start of Season (SOS) and ground green-up. A fundamental problem described by Schwartz et al. (1997) and White et al. (1997) was how to accurately relate satellite observations to phenological events: a necessary factor in describing the processes affecting SOS. The Moderate Resolution Imaging Spectroradiometer (MODIS) was introduced in 1999 and has remained the standard sensor for phenology research ever since. It is mounted on two platforms in near polar, sun-synchronous orbit with two daily equatorial crossings each (Terra AM and Aqua PM, launched in 2002).

The advent of remote sensing data provides easy and common solutions to map agricultural systems and to characterize crop phenological information at both local and regional scales (Hadria et al. 2019; Htitiou et al. 2019a; Htitiou et al. 2020b; Kariyeva and van Leeuwen 2012). Several studies have explored the use of phenological metrics for monitoring agricultural systems using different data sources and methods (Adole et al. 2018; Lebrini et al. 2019a). Many studies have confirmed that time series of vegetation indices used to produce phenological parameters provides accurate and robust results compared to traditional

methods based on single-image processing (Atkinson et al. 2012; Hao et al. 2015; Jönsson et al. 2018). Indeed, satellite-derived phenological metrics provide the ability to monitor and discriminate vegetation cover from local to large scale based on contrasted differences observed in the phenological profiles (Atzberger et al. 2013; Bachoo and Archibald 2007; Lieth 1974; Schwartz 2003; Wessels et al. 2009). Whether it is used to map agricultural systems (Alcantara et al. 2012; Qiu et al. 2017), to analyze the response of phenological metrics to climate events (Cui et al. 2017) or to extract seasonal cropping patterns (Jönsson et al. 2018), remote sensing-derived phenological metrics have improved agricultural monitoring. Because of its spatio-temporal continuity, MODIS data provides an excellent opportunity to characterize and to monitor the spatiotemporal variability of vegetation (Friedl et al. 2010). The high spectral and temporal resolutions and its data availability since 2000 allow constructions of useful time series of vegetation indices (VIs) (Akhtar et al. 2017; Suepa et al. 2016). This high temporal resolution paired with moderate spatial resolution of 250 m is ideal for regional and global phenology assessments. MODIS provides a suite of high-quality vegetation products that undergo rigorous quality assessments before release. MODIS also provides a land surface temperature (LST) product that has been effective in modeling land surface phenology.

An enduring remote sensing problem indirectly solved by MODIS is the issue of surface reflectance in the visible and infrared bands being absorbed by cloud cover. Imagery contaminated by clouds punctuates the time-series dataset, interrupting the phenological sequence. The solution is to group daily imagery into 8- and 16-day composites and average the clear NDVI or LST values at each pixel location. These temporal composites work to create a trending seasonal curve from which significant phenological metrics can be extracted. These metrics predominantly include Start of Season, Large Integral, maximum NDVI, end of season, and length of growing season. These are important indicators of phenological trends and shifts from climate change, but there is a pressing need to characterize successive stages within the continuous progression of plant development(Reed et al. 1994).

Land surface phenology (LSP) is defined as the seasonal pattern of variation in vegetated land surfaces observed using remote sensing (White et al. 2005). The challenges of linking species-specific phenophases observed on the ground to satellite imagery are

multifarious. The main obstacle being extrapolating observations at the level of individual plants across space and determining the scales at which this is possible (Badeck et al. 2004).

Chapter 2: Data and Methods

2.1 Study areas

2.1.1 Beni Mellal-Khenifra region

The study area is located in centre of Morocco, with a total area of 28374 km2 that represent about 4 % of the national territory (Figure 4). In the Geo-morphological aspect the region includes four geographical units; the Atlas Mountains, the foothill area that represents the transition between the Mountain and the Tadla plain, the phosphate plateau and the irrigated perimeter of Tadla. The study area topography ranges from 300 m above sea level, in the plan to 3890 m in the Mountain. About half the region is Mountainous (from 900 to 3890 m) while the other half consists of plains and plateaus (around 600 m).

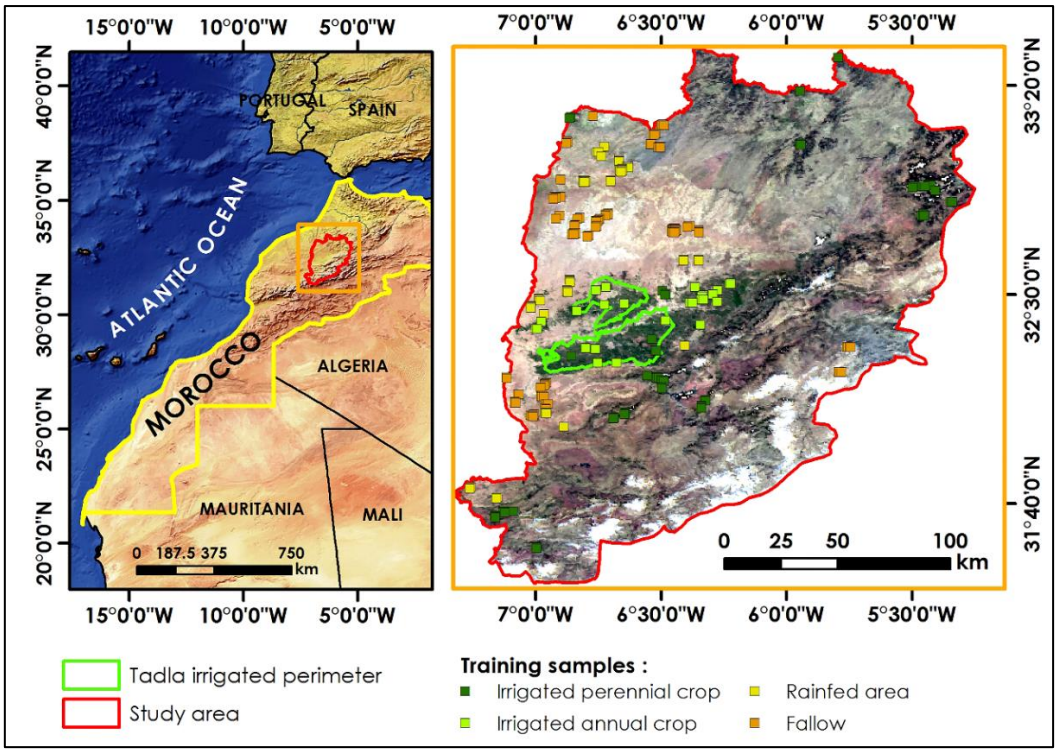

Figure 4: Localisation of the Beni Mellal-Khenifra region and the training samples

The main agricultural classes present in this region are the irrigated perimeter, the rainfed area (no irrigated), the fallow, and the foothill zone (trees and forest). Climate is variable from humid in the high Mountains to semi-arid in the plain, with an intense cold winter and very hot summers. In addition, the annual average rainfall is characterized by significant variations, with a rainfall average amount of 230 mm in the plain and 1000 mm in the high Mountains (Marchane et al. 2015; Ouatiki et al. 2019b). The average annual temperatures varies between a maximum of 46 °C in August and a minimum of -2°C in January (Ouatiki et al. 2017). The agricultural sector is one of the most promising sectors in the region and constitutes the main economic activity. The useful agricultural area in the region is about 948,397 ha of which 212,000 ha is irrigated (CRI 2015). The region is characterized by a large irrigation scheme covering about 100,000 ha and a small and medium hydraulic zone (foothill area) with an approximate surface area of 81,787 ha (Lionboui et al. 2016a).

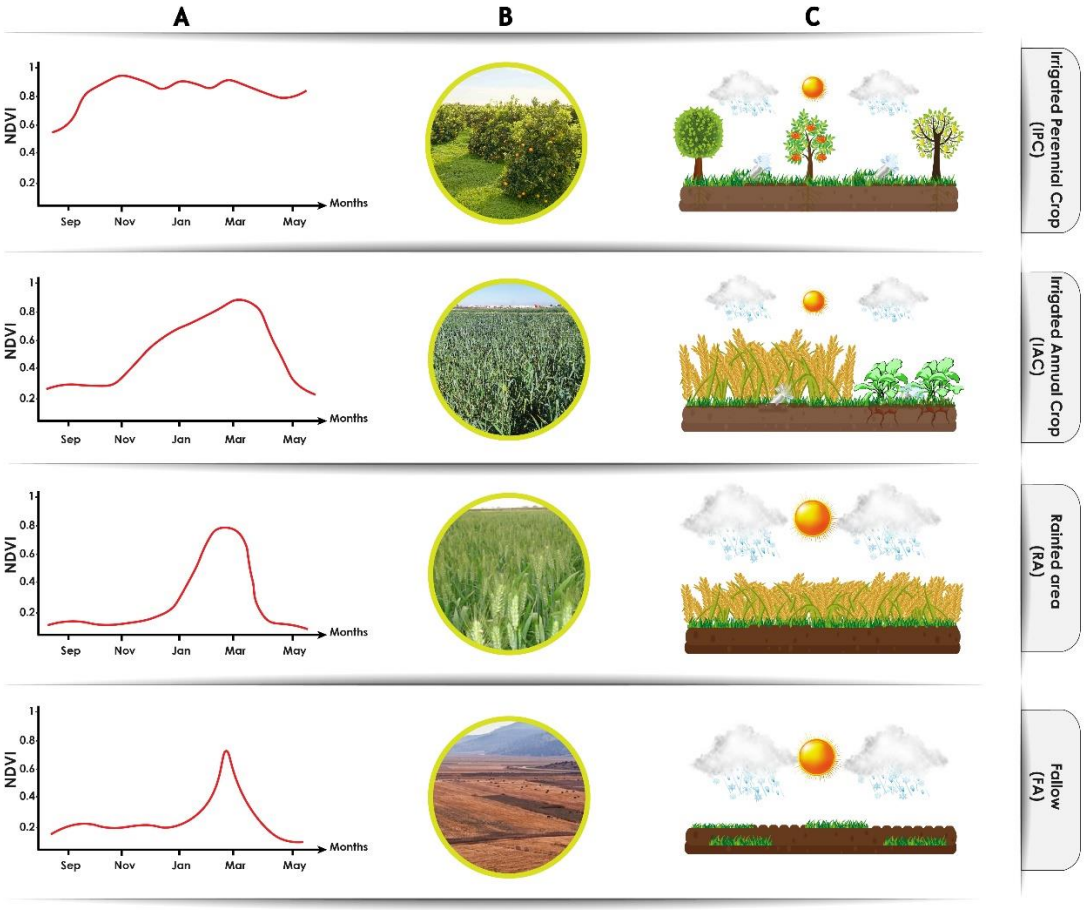

Figure 5: Farming systems encountered in the study area, A) Typical NDVI profile, B) On ground view, C) Farming systems illustration.

In this study, four farming systems types (Figure 5) have been selected to evaluate the

effectiveness of phenological metrics in the characterization of changes. The farming systems are named, (i) Irrigated Perennial Crop (IPC), (ii) Irrigated Annual Crop (IAC), (iii) Rainfed Area (RA), and (iv) Fallow (FA).

The phenology of IPC farming system is characterized by a permanent vegetative activity during the cropping season, and a high biomass production (Figure 5). IAC represents a high inter-annual variability with a high amplitude with a rapid growth and senescence moments. The IAC farming system described with a high vegetative activity with a maximum of NDVI generally in March, low dependency on climate conditions and soil type, and a maintained growth cycle from seed to harvest time. RA and FA farming systems are a typical semi-arid lands, were the start of vegetative activity depend on the climate conditions, especially the first rainfall. Figure 5 gives deep informative illustrations of the four farming systems investigated in this study.

2.1.2 Oum Er-Rbiaa Agency's Geographical Scop (OER-AGS)

The study area for chapter 4 and 5 is the Oum Rr-Rbia Agency's Geographical Scop (OER-AGS), in West-central Morocco, between 31°15'-33°22' N and 5°08'-8°23' W (Figure 6). The OER basin covers an area of 38,000 km^2, while its administrative area is around 50,000 km^2. The OER basin is made up of five geographical units form: the Atlas Mountains, the foothill areas, the plain, the phosphate plateau and the coastal area (Lebrini et al. 2020). A combination of flat and mountain terrains generally characterize The topography of the basin. Elevation ranges between 100 m (e.g., in the western and coastal zone) and 3890 m (e.g., in the eastern zone) above sea level (Ouatiki et al. 2020) (Figure 6). The OER River sources are located in the Mountainous upstream zones and the river covers a distance of 550 km overpassing the Tadla Irrigated Perimeter (TIP), the coastal areas, the northern zone of the Doukkala Irrigated Perimeter (DIP) and flows into the Atlantic Ocean at the Azemmour city (Lebrini et al. 2020). The climate is variable from humid in coastal and mountainous zones to semi-arid in the plains, with cold winters and dry summers (Ouatiki et al. 2020). Annual rainfall average varies from 230 mm to 1000 mm in the plains and the Atlas Mountains, respectively (Boudhar et al. 2020). The agricultural season generally occur between September and June, while the most important amount of rainfall is received between October and May (i.e., 70 to 80 % of the annual rainfall).

The annual temperature varies between a maximum of 46 °C in August and a minimum of -3°C in January. The investigated areas are primarily agricultural, with irrigated crops (i.e., cereals, sugar beet, and alfalfa) and rainfed area (wheat). The study area dominated also by tree cultivations especially, the pomegranate and the citrus, which presents a permanent activity during the season (Figure 6).

The OER-AGS includes 11 dams; the most important of which are Al Massira and Bin El Ouidane. In the Tadla plain, lies the Tadla Irrigated Perimeter (TIP). According to the Regional Office of Agricultural Development in Tadla (ORMVAT), the productive agricultural areas extend over superficies of 259.600 ha, of which 132.396 ha are rainfed and 127.204 ha are irrigated (Benabdelouahab et al. 2015). Mobilized irrigation water comes mainly from the Bin El Ouidane dam, the floodway from OER River, sources, and pumping. The main agricultural areas are irrigated crops, rainfed, and rangeland. The DIP is located in the downstream portion of the OER-AGS, at about 130 m in elevation, and represents 96.000 ha, out of 428.000 ha of the useful agricultural area in the plain of Doukkala, according to the Regional Office of Agricultural Development in Doukkala (ORMVAD).

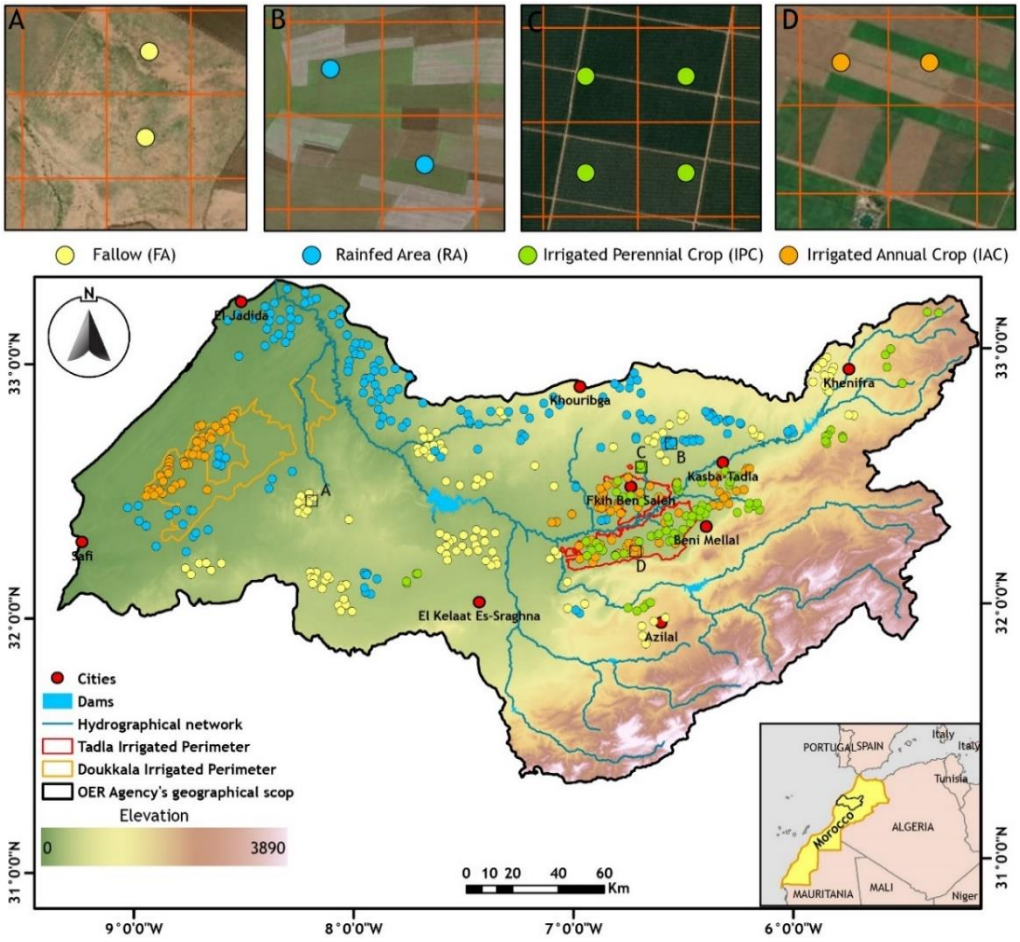

Figure 6: Map of the study area including the major irrigated areas (Tadla and Doukalla irrigated perimeters, respectively in red and orange) and the reference data localization: A) Fallow, B) Rainfed area C) Irrigated Perennial Crop and D) Irrigated Annual Crop

2.1.3 National-scale territory

The study site concerns the total area of Morocco between 21°N and 36°N latitude and between 1°W and 17°W longitude. Its area extends approximately 710 850km2, where 62% is located in the pre-Saharan and Saharan area (Figure 7).

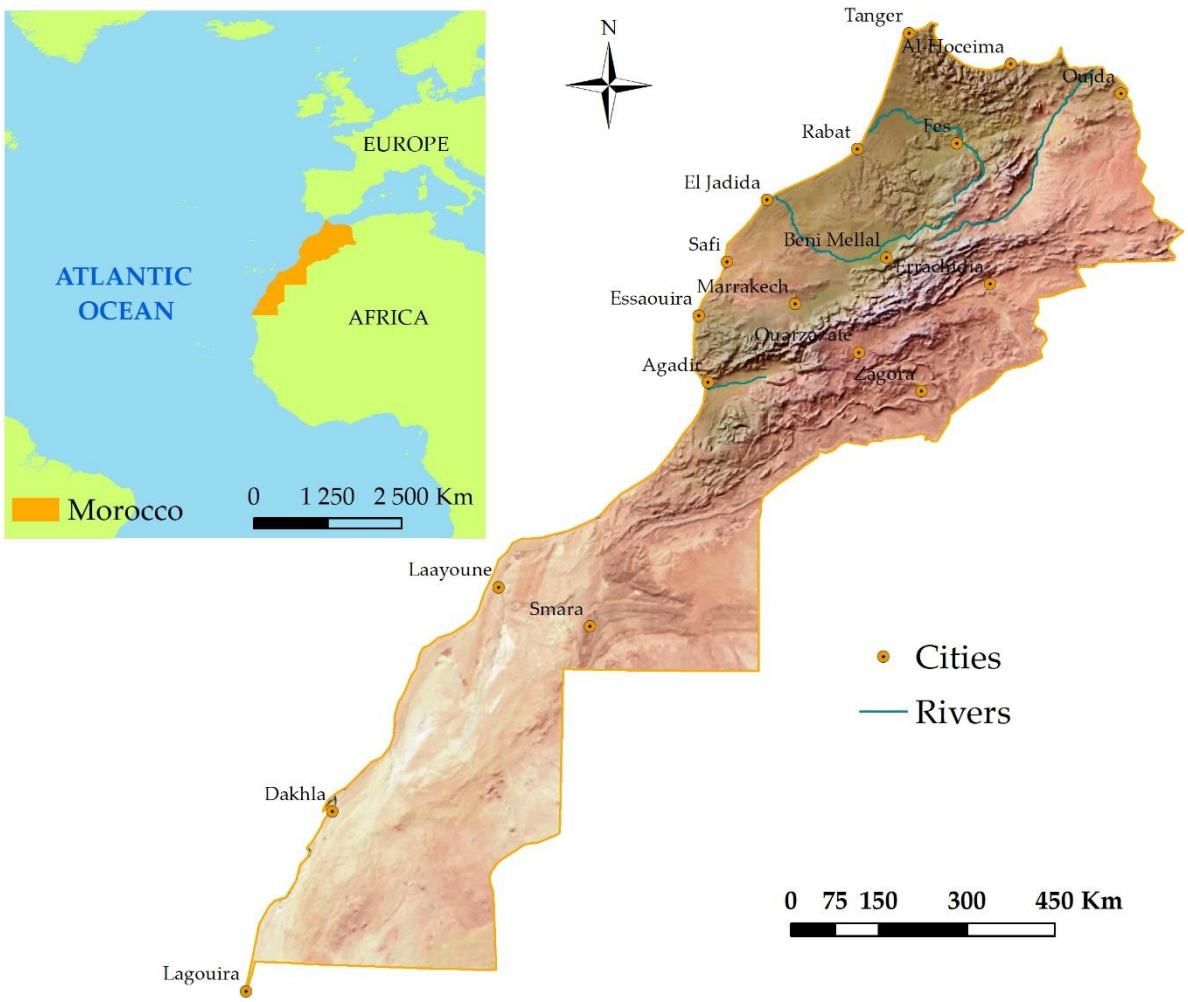

Figure 7: Geographic location of Morocco

This particular geographical position gives the area a great bioclimatic diversity. The climate varies from humid and sub-humid to Saharan and desert. It also includ arid, semiarid and high mountain regions over the Rif, Middle Atlas and High Atlas, where altitudes surpass 2500m, 3000m and 4000m respectively (Figure 7). The Mediterranean climate of the area is characterized essentially by two seasons: a hot and dry summer and a short winter with concentrated precipitation (Schilling et al. 2012). The climate is also variable according to region and marked by strong annual and inter-annual irregularity. Thus, the yearly average temperature reaches 10° C, whereas the average maximum can reach 45° C in the centre of the country and 50° C inside the Saharan regions. The minimum annual average temperatures vary from 5° C to 15° C according to region, with the absolute minimum of the order of 4° C to 0° C in mountainous and neighbouring regions. Precipitation in general diminishes from the north toward the south (Gadouali et al. 2020). Over Morocco, the forest zones occupy 12.6%

of the area. The grasslands cover more than 54 Mha. In most cases, these lands are of marginal use for annual cultivation due to drought and erosion and insufficient soil fertility (Sobrino and Raissouni 2000).

2.2 Remote sensing data

2.2.1 Moderate Resolution Imaging Spectro-radiometer (MODIS)

Moderate Resolution Imaging Spectro-radiometer (MODIS) was used to characterize the spatio-temporal dynamics of phenological metrics. A time series of MOD13Q1 16-day composites product at 250 m resolution and MOD13A1 at a spatial resolution of 500m covering the study area have been acquired between 2000 and 2020 (23 images per year). MODIS sensor is onboard two space-platforms, Terra and Aqua. The orbit of Terra around the Earth is scheduled to pass from north to south across the equator at about 10:30 a.m. and p.m. local solar time while Aqua passes in the opposite direction from south to north over the equator at about 1:30 a.m. and p.m.

All images have been downloaded through the United States Geological Survey (USGS) reverb tool (NASA LP DAAC). MOD13Q1 and MOD13A1 product were calculated from the Level-2G daily surface reflectance gridded data (MOD09 and MYD09 8-day composites series) using the Constrained View angle-Maximum Value Composite method (CV-MVC) (Didan 2015). MODIS-Terra is a near-polar orbiting satellite operated by NASA and has many spectral bands, NDVI, EVI, Bleu, NIR, Red, MIR and quality bands (Didan 2015). For the overall studied seasons, NDVI layers were used to produce NDVI time series. This choice is based on the sensitivity of this index to vegetation canopy variations in areas characterized by a low plant density, unlike other indices such as EVI (Enhanced Vegetation Index) (Ji and Peters 2007). The study concerns different agricultural production units with low (fallow), medium (rainfed) and high (irrigated area) crop density and growth potential. Normalization methods is another advantage of this index, which allows the minimization of shadow effects, noise related to the atmospheric conditions and the solar angle change (Matsushita et al. 2007). NDVI takes advantage of the degree of absorption by chlorophyll in the red and the scattering of leaves in the near infrared radiation of which is proportional to

vegetative development (Tucker et al. 1983).

The land cover map originated from Glob Cover (Hadria et al. 2018; Kaptué et al. 2011), was served as a mask for the agricultural zones in the study area. This map was developed by the Flemish Institute for Technological Research, Belgium (VITO), in the E-AGRI project (http://www.e-agri.info).

2.2.2 Climate Hazards group Infrared Precipitation with Stations (CHIRPS) product

Rainfall data from Climate Hazards group Infrared Precipitation with Stations (CHIRPS) (CHIRPS 2020) available from 1981 has been summed over the OER basin for every year within the MOD13Q1 product period. The CHIRPS data are delivered at two spatial resolution levels, 0.05 and 0.25°.

The CHIRPS v2.0 rainfall product is developed by the USGS and CHC in collaboration with NASA, USAID, and NOAA (Liu et al. 2019). The dataset was developed to provide long-term rainfall data for trend and drought monitoring to support early warning systems (such as the FEWS-NET framework). The CHIRPS algorithm combines thermal IR, PMW, and RGs rainfall data to produce daily, pentanal, and monthly rainfall estimates at 0.05° x 0.05° spatial resolution. It works in a three steps estimation process that involves the computation of the CHPclim, the CHIRP, and the CHIRPS estimates. First, the CHPclim is created based on long-term monthly means from FAO and GHCN rainfall historical records, TRMM 2B31 rainfall estimates, CMORPH rainfall estimates, IR, MODIS LST in addition to physiographic and geographic information (Liu et al. 2019). The CHIRPS rainfall product is available from 1981 to present at daily, pentanal, and monthly time resolutions. With a quasi-global spatial coverage (50°S-50°N), the dataset is provided at 0.05° x 0.05° (CHIRPSp5) and 0.25° x 0.25° (CHIRPSp25) spatial resolutions. In this research, the CHIRPSp5 data with a spatial resolution of 0.05° were used.

2.2.3 MODIS Land Surface Temperature (LST)

The LST product used in this research is the land surface temperatures (LST) at 500 m spatial resolution derived from the Moderate Resolution Imaging Spectroradiometer (MODIS) sensors on board Terra satellite. The Land Surface Temperature (LST) 8-day data are retrieved

at 1Km pixels by the generalized split-window algorithm. The data were resampled to 500m of spatial resolution. The MODIS land surface temperature (LST) is derived from two thermal infrared band channels, i.e. 31 (10.78–11.28 μm) and 32 (11.77–12.27 μm) using the split-window algorithm (Vancutsem et al. 2010) which corrects for atmospheric effects and emissivity using a look-up table based on global land surface emissivity in the thermal infrared(Vancutsem et al. 2010). The product is comprised of LSTs, quality assessment, observation time, view angles, and emissivity. In this work, Terra 8-day Land Surface Temperature data was considered.

2.2.4 Shuttle Radar Topography Mission (SRTM) Digital Elevation Model (DEM)

The Shuttle Radar Topography Mission (SRTM) is an international project supported by the National Geospatial-Intelligence Agency (NGA) and NASA in February 2000 (Farr et al. 2007). During its 11-day mission 12.3 Tbyte of terrain data were collected covering land areas between 56°S and 60°N. Two InSAR instruments were used: a C-band radar provided by the Jet Propulsion Laboratory (JPL) and an X-band radar provided by the German and Italian space agencies (O'Loughlin et al. 2016). Kinematic GPS, corner reflector arrays, ground control points (GCPs) from NGA and JPL, and optical imagery DEMs were used in system calibration and accuracy assessment (Farr et al. 2007). Table 7 provide a summarize of the dataset used during this thesis research.

Table 2: Spatial and temporal characteristics of data used in this research

Feature	Product	Variable name	Time range (MM/YYYY)	Unit	Temporal resolution	Spatial resolution
Climate	CHIRPS	Rainfall	01/2000 – 12/2020	mm	Monthly	5.4km
	MOD11A2	LST	02/2000 – 03/2020	°C	8 days	1km
Phenology	MOD13Q1	NDVI	01/2000 – 12/2020	NDVI	16 days	250 m
	MOD13A1	NDVI	01/2000 – 12/2020	NDVI		500 m
Topography	SRTMGL3	DEM	2000	m	-	90 m
	SRTMGL3	Slope		%	-	

2.3 Data time series filtering and phenological metrics extraction

Filtering noisy time series of NDVI and phenological metrics extraction has been performed with TIMESAT program (Jönsson and Eklundh 2004). TIMESAT is one of the most advanced programs and widely used for smoothing time series data and estimating seasonal

phenological metrics. There are two essential steps to extract phenological metrics from NDVI profiles: First, filtering abnormal values from NDVI profiles to produce smoothed time series, and second the application of various algorithms for the computing phenological metrics (Table 3). In order to obtain high quality time series and fill the gaps in data TIMESAT implements three different smoothing methods, which are Savitzky-Golay (SG) (Chen et al. 2004), asymmetric Gaussian (AG) (Bachoo and Archibald 2007; Chen et al. 2006) and double logistic (DL) (Geng et al. 2014). The AG filtering method is less sensitive to noise than the other approaches (Jönsson and Eklundh 2002; Jönsson and Eklundh 2004). The study performed by Fu et al. (2018) shows the robustness of this algorithm in smoothing time series and preserving the characteristics of NDVI profile, contrary to DL and SG methods. The AG method can generate a smoothed NDVI profile while describing minor changes in the NDVI sequence data (Gao et al. 2008). Therefore, the AG method was chosen as the time series reconstruction method to be used in this study. Table 3 shows the setting used for NDVI time series processing in TIMESAT. More details on the filtering approach used and phenological metrics extraction for this study could be found in Lebrini et al. (2020).

Table 3: Input setting for NDVI time series processing in TIMESAT used in this study, as recommended by (Eklundh and Jönsson 2015).

Parameter	Description	Value
Spike method	Two values: 1 for median filter and 2 for decomposition by Loess	1
Spike value	Degree of spike removal.	1.8
Amplitude cutoff value	Data with amplitude below this value are masked.	0.1
Valid data range	Data range of time series to be processed	0-1
Season parameter	The study area contains one cropping season.	1
Number of envelope iterations	Number of iterations for envelope adaptation	2
Adaptation strength	Strength of the envelope adaptation.	3

The second step is PhM extraction; such measurements are usually calculated using a common method based on value thresholds of the seasonal vegetation amplitude, assuming that a particular phenomenon has started when the NDVI values surpass a given threshold (Figure 8). Our study has then been carried out by setting the proportion of the seasonal amplitude to 10% measured from the left and right minimum values, respectively (Jönsson and Eklundh 2004). In general, four PhM were extracted using TIMESAT program for trend

analysis. Definitions of PhM used in this study are explicitly defined in Table 4.

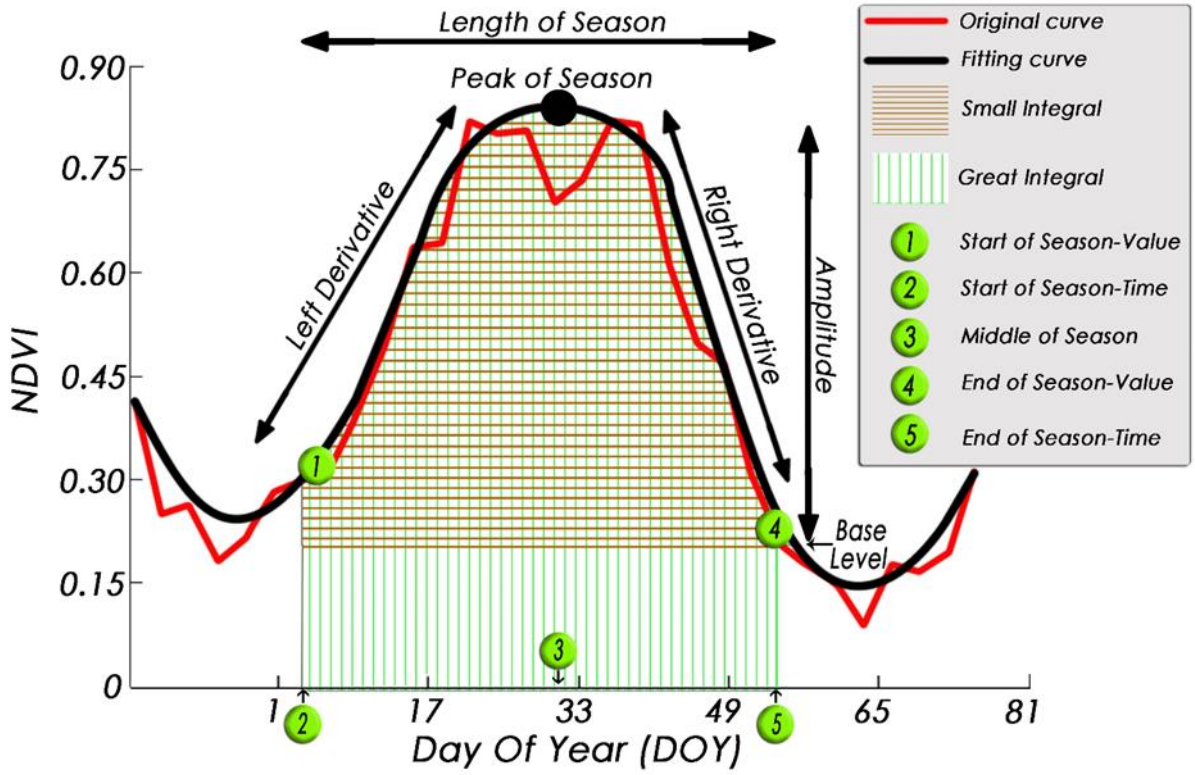

Figure 8: Phenological metrics extracted from NDVI time series

After filtering and reconstructing of NDVI time series for each agricultural season, thirteen phenological metrics were extracted using TIMESAT (Figure 8). These phenological metrics allowed discrimination between different phenological areas. The definitions of the phenological metrics used in this study are explicitly defined in Table 4.

Table 4: Definition of computed phenological metrics (Eklundh and Jönsson 2015; Reed et al. 1994)

Phenological metric	Phenological definition (for cropping season)
1) Start of season – time (TSOS)	Beginning date of photosynthesis activity in the vegetation canopy
2) End of season – time (TEOS)	End date of photosynthesis activity in the vegetation canopy
3) Start of season – value (SOSV)	NDVI value at the beginning date of photosynthesis activity in the vegetation canopy
4) End of season – value (EOSV)	NDVI value at the end date of photosynthesis activity in the vegetation canopy
5) Length of season (LOS)	Length of photosynthetic activity during the cropping season
6) Peak of season (PS)	Maximum level of photosynthetic activity of cropping season
7) Middle value of season	Mean value of the times for which the left edge increase to

(MVS)	90% and the right edge decrease to 90%
8) Great integral (GINT)	Canopy photosynthetic activity across the entire growing season
9) Small integral (SINT)	Canopy photosynthetic activity between the function describing the season and the base level
10) Amplitude (AMP)	Maximum increase in canopy photosynthetic activity above the baseline
11) Base level (BSL)	The average of the left and the right minimum values
12) Right derivative	Rate of decrease at the EOS between the right 10% and 90% of the amplitude.
13) Left derivative	Rate of increase at the SOS between the left 10% and 90% of the amplitude.

The general methodology is summarized in Figure 9. More details are provided within chapters of this thesis.

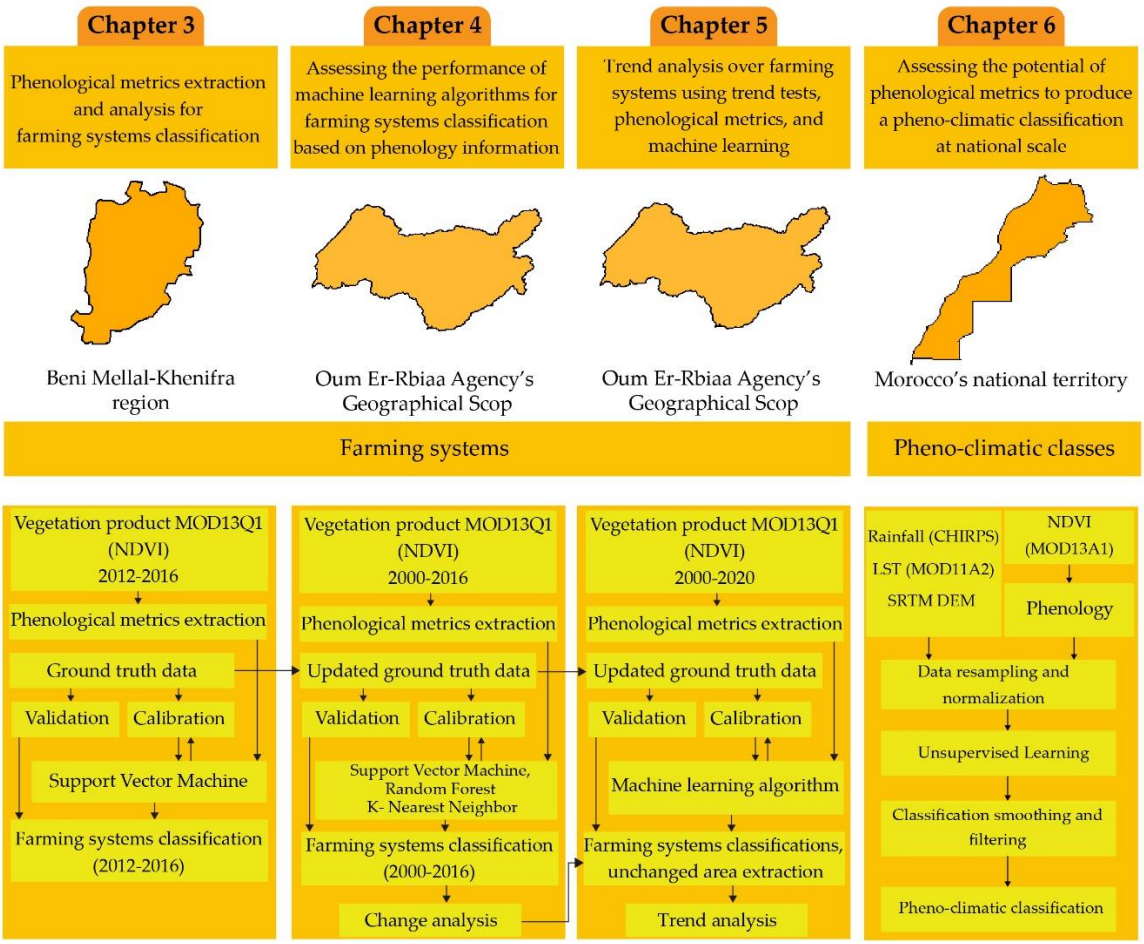

Figure 9: flowchart of the general methodology of the thesis.

Chapter 3: Identifying agricultural systems using SVM classification approach based on phenological metrics in a semi-arid region of Morocco

Lebrini Y., Boudhar A., Hadria R., Lionboui H., Elmansouri L., Arrach R., Ceccato P., Benabdelouahab T., (2019). Identifying Agricultural Systems Using SVM Classification Approach Based on Phenological Metrics in a Semi-arid Region of Morocco. *Earth Systems and Environment*, 3(2), 277-288. https://doi.org/10.1007/s41748-019-00106-z

3.1 Introduction

In arid and semi-arid regions, the effects of climate change can be dramatic on agriculture whose production depends largely on the quantity and distribution of annual rainfall (Almazroui et al. 2017b; DeFries et al. 1999; Dixon et al. 1994). The global changes in land cover are at the origin of the disturbances observed in the agricultural cycle. In the semi-arid context, successive droughts and floods affect the land cover and the socio-economic development, especially in arid and semi-arid regions (Almazroui et al. 2017a; Barakat et al. 2019; Lionboui et al. 2014). In these areas, agricultural production depends on the spatio-temporal distribution of the rainfall amount (Benabdelouahab et al. 2016; René and Nathalie 2007). Hence, evaluating and monitoring land cover is an essential element for global changes (DeFries et al. 1999; Jung et al. 2006; Lambin et al. 2001).

The monitoring of vegetation cover variability during agricultural seasons allows managers and policy makers to manage agricultural systems (Löw et al. 2013). In this context, remote sensing can provide essential tools to support large scale agricultural monitoring systems through vegetation indices. Many studies affirmed that vegetation indices used to produce phenological parameters based on time series data provide accurate and robust classification

results compared to traditional methods that use a single image (Alcantara et al. 2012; Pal and Mather 2005).

Phenological parameters provide information on plants periodicity, as well as the monitoring of the appearance and occurrence of phenological events, such as onset, senescence, length of season and peak of biomass production (Lieth 1974; Schmidt et al. 2015; Schwartz 2003). Remote sensing time series analysis based on NDVI can be one of the most reliable tools for mapping and characterizing the vegetative development behaviors among cropping seasons. Many studies used phenological parameters extracted along one or several seasons in different applications: i) for crop mapping (Arvor et al. 2011; Lessel and Ceccato 2016; Wardlow et al. 2007), ii) crop yield and agricultural production (Mottaleb et al. 2015; Shahriar et al. 2014; Zhao et al. 2017), iii) analyzing the spatio-temporal trends of the vegetation linked to climate (Evrendilek and Gulbeyaz 2011; Peng et al. 2013; Vrieling et al. 2011), iv) extracting pheno-regions and biomass quantification (Diouf et al. 2014; Diouf et al. 2015) and monitoring drought dynamics effects on agriculture (McVicar and Jupp 1998; Winkler et al. 2017; Wu et al. 2015).

Phenological observations (e.g. biomass accumulation, peak of greenness, period of leaf development) in agriculture provide valuable information to improve yield prediction models (Hadria et al. 2006; 2007; Viña et al. 2004). Therefore, it is important to be able to monitor and determine accurately the spatio-temporal variability of phenological metrics (e.g. length, start and end of the agricultural season) and to analyze their behavior in arid and semi-arid regions. This study is crucial in filling the gap of information to monitor agricultural area using phenological metrics and to help managers and decision makers to analyse the agricultural policies impact and to optimize the land use choices.

The aim of the present chapter is twofold: 1) spatio-temporal analysis of phenological parameters patterns using 4 seasons of NDVI time series obtained from MODIS satellite data, 2) map the main phenological classes through phenology-based classification approach.

3.2 Methods

Three steps were carried out to map farming systems over the study area using phenological metrics extracted from the NDVI time-series data (Figure 10). Concerning this chapter, nine phenological metrics, which are start of season, end of season, amplitude value, middle of season, peak of season, small integral, large integral, base value of season, and right derivative were extracted. The phenological metrics values were extracted for the sampled pixels. These values were analyzed using a statistical method to display the distribution of data based on the extremes, first quartile, median and third quartile (boxplot) (McGill et al. 1978). The boxplots help to make comparisons across phenological parameters in order to analyse the behavior of the phenological metrics in terms of agricultural systems. Details on phenological metrics extraction are presented in chapter 2.

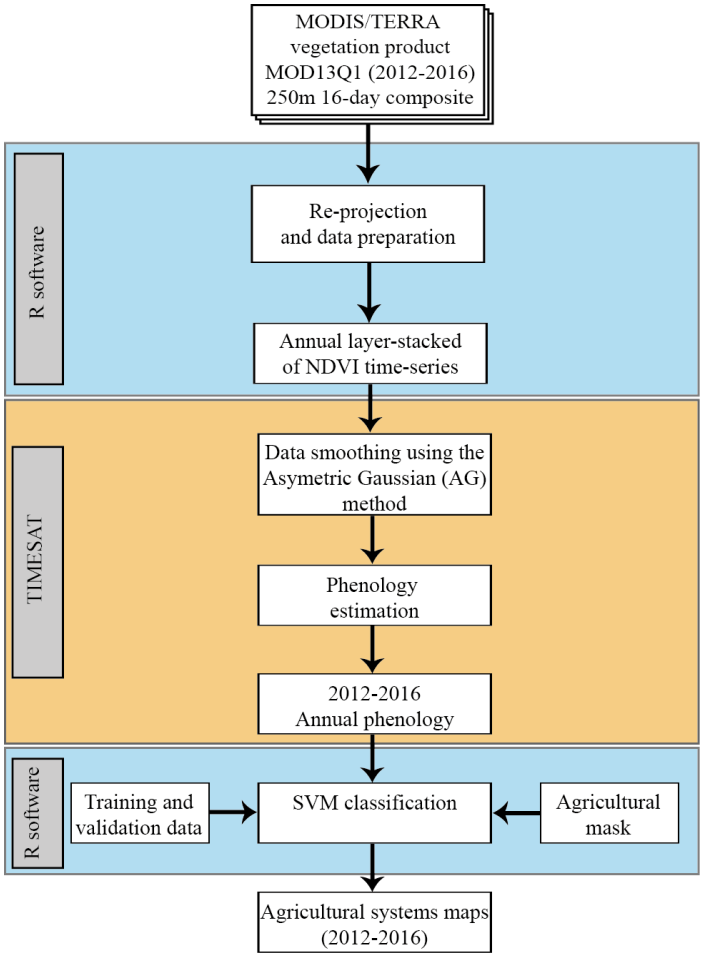

Figure 10: Schematic diagram illustrating the research methodology adopted in this chapter.

3.2.1 Classification of time-series data

In this chapter, Support Vector Machine (SVM), which is a supervised nonparametric statistical technique, was used as a classification method. SVM is a mathematical technique for solving the classification problems with a high generalization capability from small training samples and a high potentiality for regional characterization study (Shao and Lunetta 2012; Vapnik 2006). The open-source R language and software was used to implement the SVM classification using the "CARET" package (Jed Wing et al. 2018; R Core Team 2017). Four classes were considered, namely irrigated annual crop, irrigated perennial crop, rainfed area and fallow (Figure 5). The accuracy assessment was carried out using overall accuracy, producer and user accuracy, F1 score, and the Kappa coefficient.

SVM with Radial Basis Function (RBF) kernel was used due to his robustness and effectiveness for remote sensing data classification (Mountrakis et al. 2011). Defining Kernel function parameters (g and C) are required to use the SVM method. The optimal choice of these parameters was performed using the "CARET" package. The tuning step was performed based on 2015/2016 data. Then, the optimal model was defined and used to classify farming systems over the study area.

3.2.2 Field data

We selected four land cover types: irrigated perennial crop, irrigated annual crop, rainfed area and fallow, in order to evaluate the effectiveness of the curve fit for remotely sensed NDVI data within the Beni Mellal-Khenifra Region. Farming systems truth data were identified and selected within 2016 cropping season (Table 5). For the period from 2012 to 2016, a verification step was carried out using ground truth data from field survey and Google Earth images to confirm the no-change of the agricultural system type. Type localities consist of 40 irrigated annual crop locations containing 210 pixels, 40 irrigated perennial crop locations containing 301 pixels, 40 rainfed crop locations containing total pixels of 254 and 40 fallow locations containing 441 pixels (Table 5). Time series of an arbitrarily selected pixel from each land cover type are shown in Figure11.

Table 5: Classes and size of the training dataset

Class name	number of training samples (pixel)
Irrigated annual crop	210
Irrigated perennial crop	301
Rainfed area	254
Fallow	441
Total	1206

Irrigated annual crop represents a high degree of inter-annual variability with a high amplitude and abrupt growth and senescence. The irrigated perennial crop was selected as representative of a high base and weak amplitude. Rainfed crop and fallow were selected as representative of typical semi-arid land cover, which depends on climate conditions and may not have a pronounced phenology.

3.3 Results and discussions

3.3.1 NDVI profile analysis

In this step, NDVI profile responses were represented in Figure 11 at the pixel-level in the time-series MODIS data for each agricultural system class which are; the irrigated perennial crop (Figure 11-a), the irrigated annual crop (Figure 11-b), the rainfed area (Figure 11-.c) and the Fallow (Figure 11-d). The multi-temporal NDVI profile of a specific agricultural system reflects its phenological characteristics (e.g., start, end and length of season).

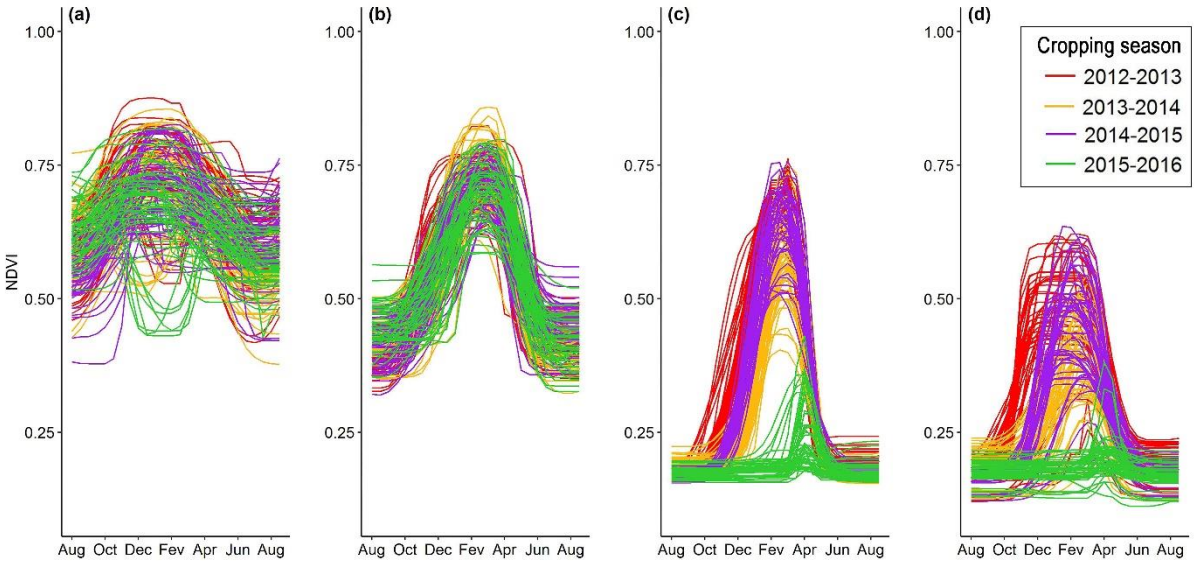

Figure 11: NDVI profiles for land surface phenology in the study area a) Irrigated perennial crop b) Irrigated annual crop c) Rainfed area d) Fallow

Figure 11 shows four different categories of profiles, which are characterized by a well-defined shape. For each category, the phenological metrics values depend on the NDVI profile size and dimensions. Figure 11-a and Figure 11-b are discriminated by their high values of the NDVI peak ranges from 0.7 to 0.9, unlike that for Fig. 4.d and partially for Figure 11-c. The NDVI profile in Figure 11-a is characterized by its high base value, which indicates a perennial crop zone with high and permanent photosynthetic activity. The opposed profiles observed in IPC agricultural system were originated from the phenological cycle of certain irrigated perennial crops (e.g., pomegranate), which starts the photosynthetic activity in late March and reach the maximum on around June (Figure 11-a). The length of the cropping season (LOS) lasts longer for Figure 11-a and Figure 11-b where the season length takes more than 8 months, in contrast to other two profiles where LOS takes less than 5 months.

NDVI profiles for the rainfed area (Figure 11-c), and fallow (Figure 11-d) show an important internal variability linked to the cropping season climate conditions. Accordingly, all phenological parameters in these areas are directly influenced by the local climate fluctuations; mainly the water amount available from rainfall events over each season.

Regarding the start of season criteria, NDVI values in irrigated zones are heterogeneous (Figure 11-a, Figure 11-b). This observed heterogeneity is due to the farmer decision about sowing dates and the irrigation water supplies moments. Adversely, the start of season in the rainfed area, as showed in Figure 11-c and Figure 11-d, is homogeneous due to the crop

dependence to the first rainfall event. For the amplitude parameter, as shown in Figure 11-a and Figure 11-b, irrigated perennial crop zones are characterized by lowest amplitude values, contrary, highest amplitude values are observed in the irrigated annual crops profile.

3.3.2 Phenological parameters analysis

The phenological metrics were computed for each pixel on the basis of the NDVI profile. The distribution of these metrics was analyzed using boxplot representation to study their behavior regarding the agricultural system classes.

Figure 12-a to Figure 12-i, represent statistics of the studied phenological metrics for each phenological classes. The amplitude and small integral metrics confound irrigated perennial crops and fallow (Figure 12-a, Figure 12-g). Similarly, the rainfed area and fallow classes are not separable when just using the base level and the end of season metrics (Figure 12-b). The middle of season and the end of season confounded between the irrigated annual crops, rainfed area and fallow (Figure 12-f, Figure 12-h).

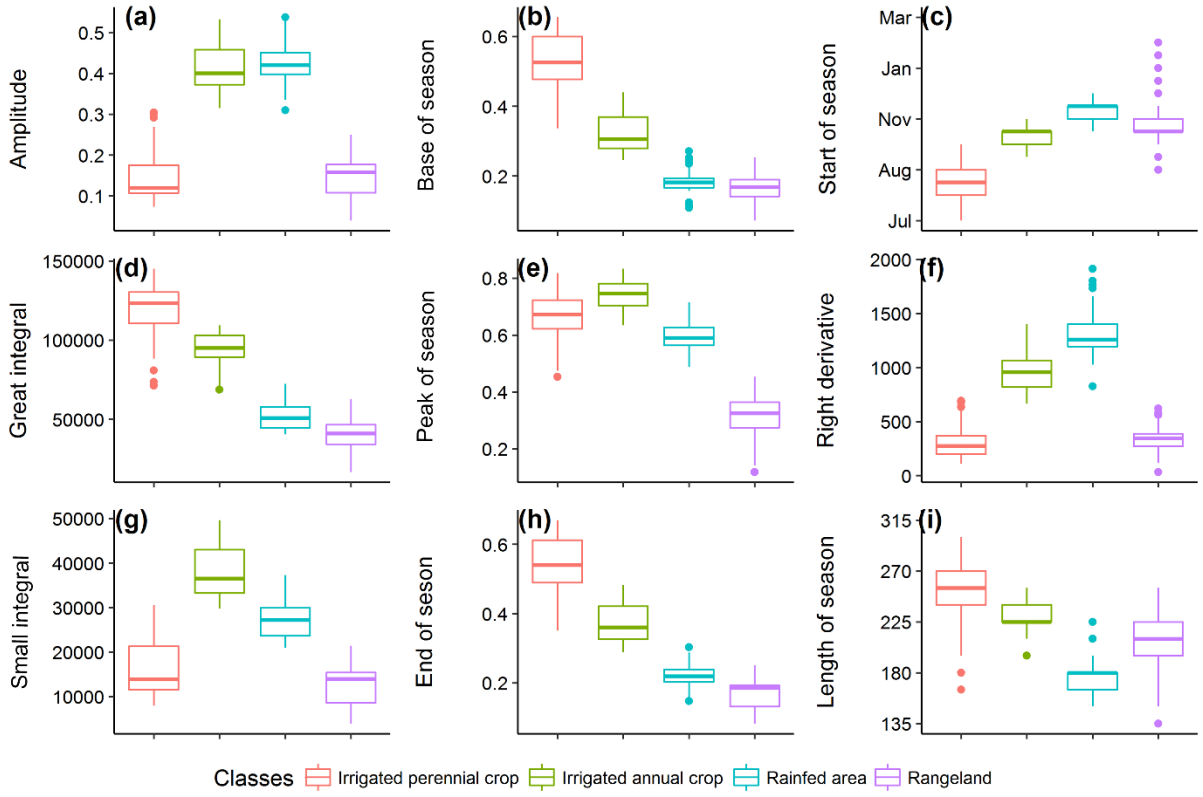

Figure 12: Boxplot presenting the phenological parameters behaviour in the study area

Unlike previously cited indicators, the great integral, the start of season, the peak and

the length of the season parameters provide valuable information to discriminate between surface classes (Figure 12-d, Figure 12-c, Figure 12-e, and Figure 12-i).

Based on these results, we focused on the spatial analysis of the phenological metrics for the 2015/2016 season (Figure 13). The parameters showed high spatial variability and a contrasting level of phenological responses. Indeed, according to Jönsson and Eklundh (2002), the great integral (GINT) indicates the level of plant biomass production. This production is strongly related to water availability in the arid and semi-arid areas (Benabdelouahab et al. 2015). Similarly, in the irrigated area (irrigated and pumping zone) the length of the season (LOS) parameter takes a longer period compared to the non-irrigated area due to the irrigation water supplies during the critical periods of crop development (Figure 12 and Figure 13). Since the LOS parameter was calculated based on the difference between the end (Fig. 6.h) and the start of the cropping season (Figure 13-c), it plays a key role to observe the length of the biomass production period.

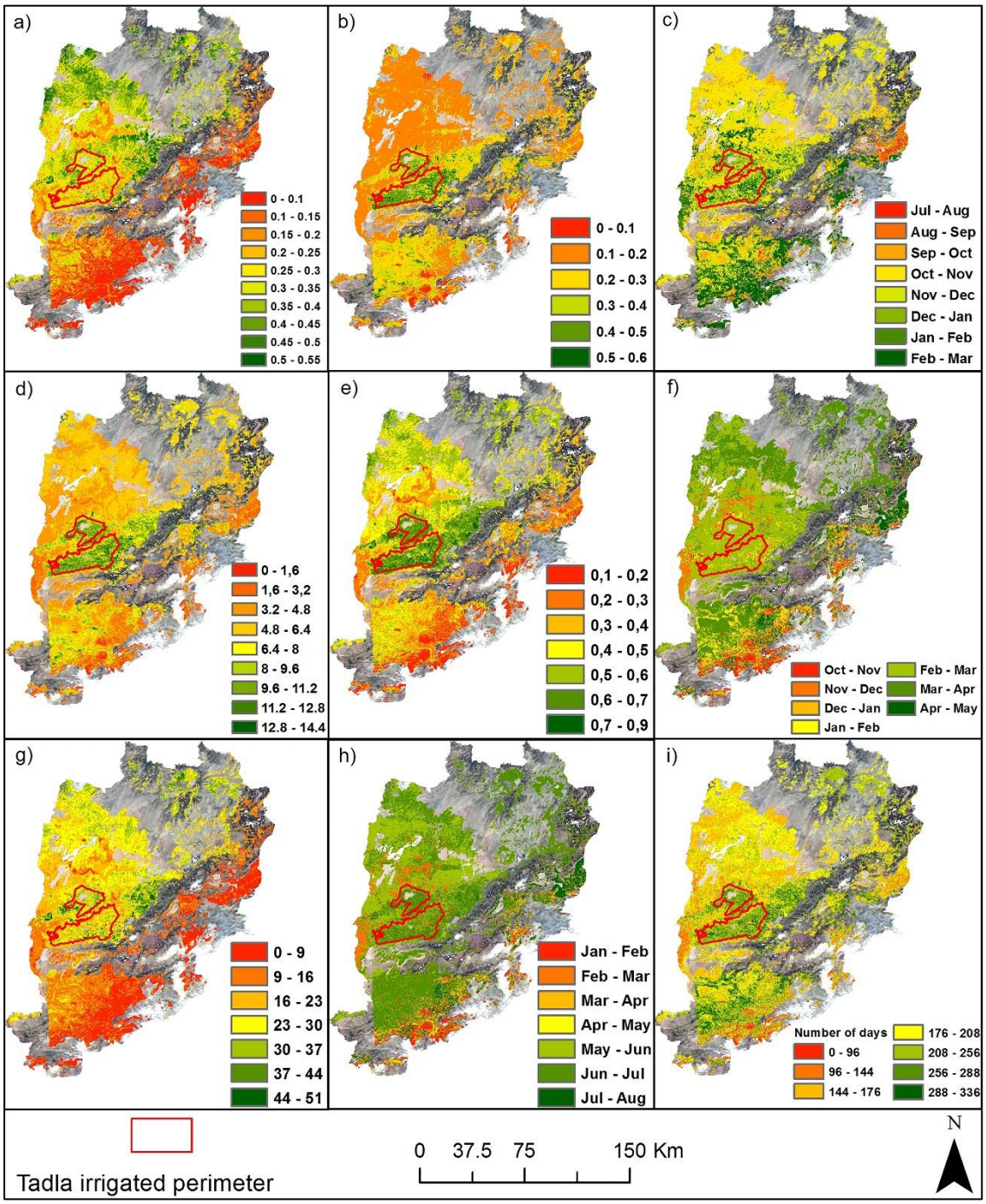

Figure 13: Seasonality maps of the nine phenological parameters: a) amplitude, b) Base, c) end of season, d) Great integral, e) peak, f) middle, g) small integral, h) end of season, i) length of season. The background is an RGB image composite of MODIS.

For the case of irrigated area of the studied zone (Tadla irrigated perimeter, foothill area, and pumping area), the values of GINT, LOS, and the Base level are high and range from 11.2 to 14.4, 256 to 288 days and from 0.4 to 0.6, respectively (Figure 13-b, Figure 13-d, Figure 13-i). The peak of season parameter indicates the highest level of NDVI values in the irrigated

area with values ranging between 0.6 and 0.9 (Figure 13-e). Adversely, the rainfed area and fallow zones are characterized by the lowest GINT, LOS, and peak values with less than 6.4, 208 days and 0.4, respectively, but are more distinguished by amplitude and middle of season metrics (Figure 13-a, Figure 13-f). Regarding the short integral metrics (SINT), the high values observed correspond to the perennial crops characterized by high biomass production during the cropping season (Figure 13-g). As seen by these results, phenological parameters values in the rainfed area and fallow zones depend on the cropping season climate conditions. The nine phenological parameters are considered as keys parameters to discriminate the different phenological zones (Figure 13).

3.3.3 SVM classification

The specific objective of this step is to classify, at the overall study zone, the discriminated area combining the nine phenological parameters, discussed previously, as input to the SVM classifier. The optimal model was selected based on the tuning step of the classifier since it ensures the highest accuracy (C= 8 and g =0.274). In order to evaluate the accuracy of the classification, a confusion matrix was established by comparing classification results with reference data essentially based on ground truth data (Table 6).

Table 6: Confusion matrix obtained from the SVM classifier for the 2015/2016 agricultural season

Class	Producer accuracy (%)	User accuracy (%)	F1 score	Commission error	Omission error
Fallow	91.3	88.42	0.88	0.08	0.09
Irrigated annual crop	92.59	86.21	0.91	0.02	0.07
Irrigated perennial crop	92.98	94.64	0.95	0.02	0.07
Rainfed area	81.25	88.64	0.77	0.03	0.19
Overall accuracy	88.7%				
Kappa coefficient	0.83				

The confusion matrix results are 88.7% and 0.83 for overall accuracy and kappa coefficients, respectively. For the irrigated annual crop class, it was accurately classified with 92.59% and 86.21% for producer and user accuracy, respectively (Table 6). Concerning the irrigated perennial crop class, it was mapped correctly with 92.98% of producer accuracy that has been ranked correctly considering the reference data and user accuracy of 94.64% that has been mapped with the classification algorithm (Table 6). For this class, about 6% of the pixels

were committed to other classes. Producer accuracy for the Rainfed area class is about 81.25%, as long as it is about 88.64% for the user accuracy, i.e. 11.36% of the rainfed area class have been classified inaccurately (Table 6). Rainfall area class results show a high omission error value of around 0.18. This is justified by the behavior of rainfed crops in relation to the climatic conditions of the agricultural season. An extremely dry year will condition the rainfall area to behave as a fallow area. Contrary to the good climatic conditions, which allow the rainfed areas to have a phenological behavior relatively similar to the irrigated crops. The fallow class has accuracy values of 91.30% and 88.42% for the producer and user accuracy, respectively (Table 6).

Phenological parameters extracted in this study showed high spatio-temporal heterogeneity over the study area. The contrasting differences between the derived parameters could be explained by the complex relationship between the rainfall anomalies and vegetation cover. The heterogeneous behavior of the vegetation cover is also influenced by climatic conditions, natural resources availability and land use practices such as rainfall amount and distribution, amount of irrigation water supply and access mode, soil quality and technical itinerary (Benabdelouahab et al. 2016).

The obtained classification results for the 2014/2015 cropping season was compared to the official statistics from the Regional Investment Centre (CRI) to assess the ability of the proposed classification method to predict the agricultural system superficies over the region (CRI 2015) (Figure 14 and Figure 15).

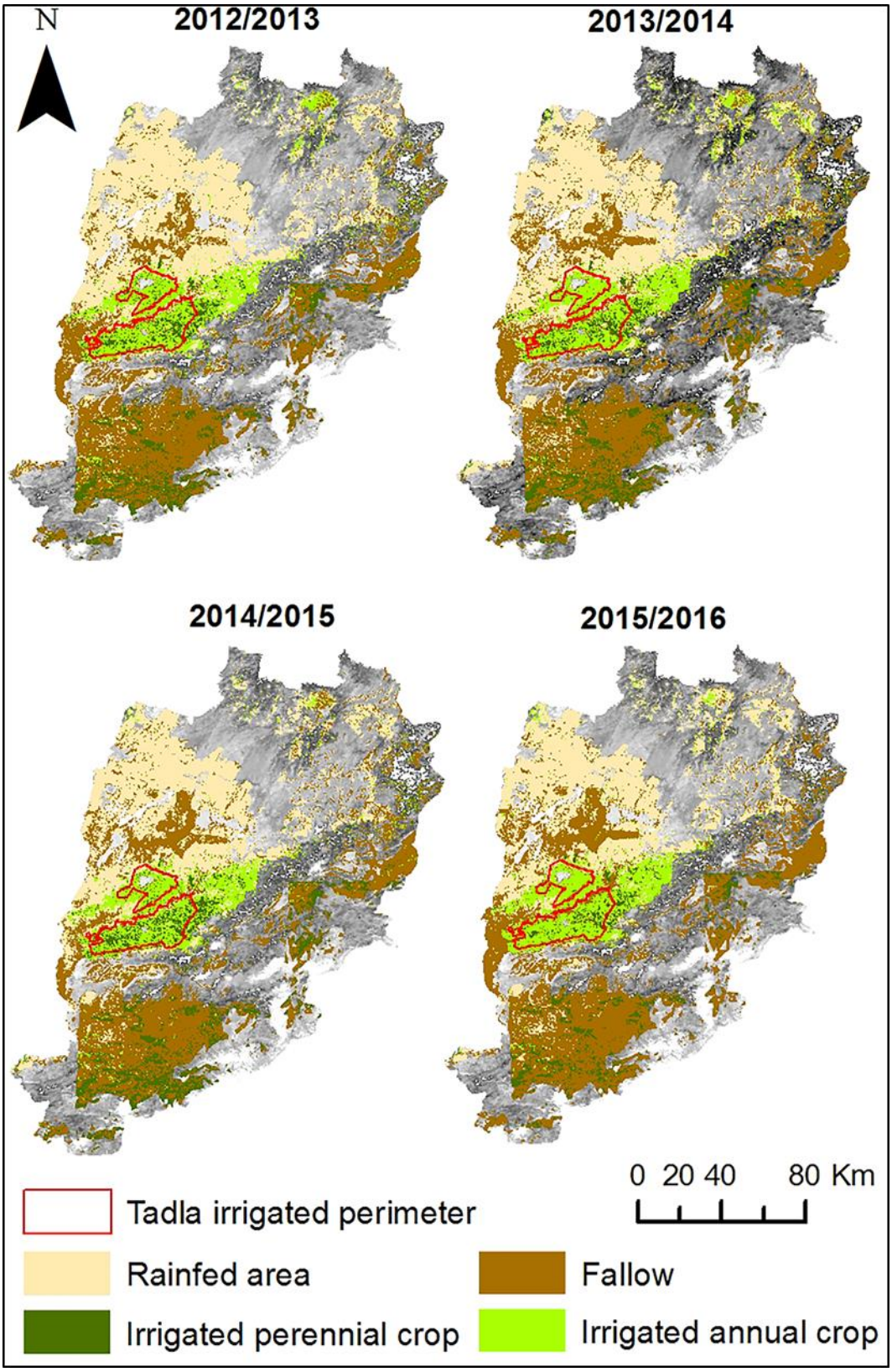

Figure 14: Classification results of the agricultural system classes. The background is a RGB composite of MODIS image.

The total irrigated class superficies is about 414,081 ha compared to 212,000 ha of the

irrigated area estimated by CRI (CRI 2015). This gap is due essentially to the no-controlled pumping area that is not involved in the official statistics. The pumping area can be detected and estimated using the developed classification approach based on phenological remotely sensed data. This approach constitutes a relevant way, for local policy makers and managers, to monitor and control the irrigated and the rainfed agricultural zones (Lionboui et al. 2016a).

Furthermore, superficies estimation errors can be also related to the low-resolution of the MOD13Q1 data product used in this study. In this case, one pixel can represent a mixture of two classes or more due to the short cover type change (Biggs et al. 2006; Boschetti et al. 2009). The dominant class will be retained, given its influence on the phenological behavior for each pixel (Sun et al. 2012).

Concerning the change in agricultural superficies, the fallow class has raised from 1,256,000 ha in 2014/2015 to 1,506,000 ha in the 2015/2016 cropping season (Figure 15). The increase of fallow superficies observed in the 2013/2014 (1,308,682 ha) and 2015/2016 (1,505,873 ha) cropping seasons is strongly related to rainfall with an average amount of 232 mm and 128 mm, respectively. Adversely, the fallow superficies are less than 1,260,000 ha, i.e., 2012/2013 and 2014/2015 cropping seasons, with an average amount of rainfall higher than 380 mm (Figure 15). For the same reason, the rainfed class area has decreased and classified as fallow area due to the lack of rainfall during the 2015/2016 cropping season. Irrigated areas are partially independent of climatic conditions. Except for the extremely dry years where managers can apply restrictions on access to irrigation water(Lionboui et al. 2016a). As a result, they give priority to the maintenance of orchards without a production goal and limit the areas of annual crops. This is reflected in the stability of the perennial crops superficies, unlike annual crops superficies that regress (Figure 15). Farmers in the study area practice supplementary irrigation. During a dry year, the farmer using pumping as the main source of irrigation will abandon his land or give up cultivation given the very high energy cost. This implies a reduction in the superficies of the irrigated annual crops by pumping. This is the case of 2015/2016 cropping season with an average of rainfall amount of 128 mm and a superficies of 534,081 ha. Adversely, cropping seasons with an average rainfall amount higher than 370mm, e.g., 2014/2015 cropping season, reach superficies greater than 580,890 ha (Figure 15).

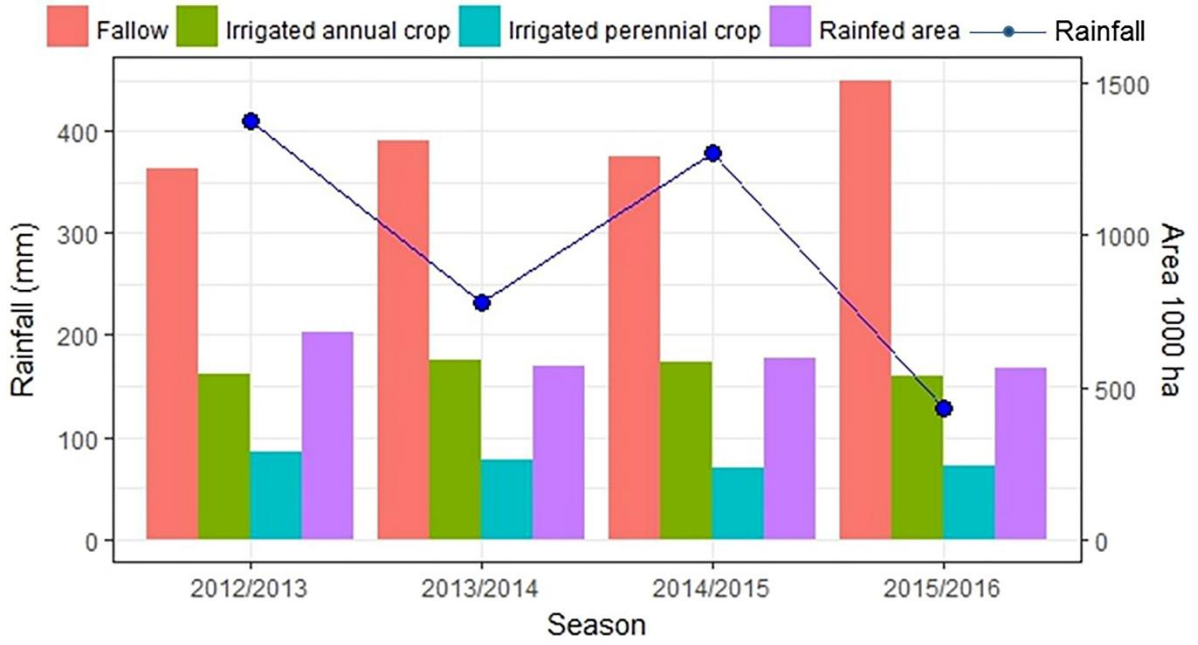

Figure 15: Area of phenological classes predicted by the SVM classifier shown against average rainfall amount in the study area

Although, the classification of agricultural systems based on phenological parameters as an input of the classification algorithm meet the objective to map the main phenological classes at large scale (Figure 14). This approach based on the low spatial resolution data can be seen as a preliminary step before moving on to higher resolution products.

Over inter-annual time scales, phenological patterns of rainfed crop areas depend strongly on the spatio-temporal fluctuations of rainfall and dry periods. Therefore, the phenological analysis provides information to deep our understanding about the spatio-temporal variability of land surface phenology in arid and semi-arid area on one hand, and on the other hand, to improve agricultural system monitoring that allows managers and policy makers to optimize the agricultural vocation and land suitability. These fluctuations in rainfall amount has a negative impact on agricultural systems, especially in arid and semi-arid region like the soil degradation (e.g., soil salinity, nutrient depletion) and the quality and depth of groundwater. Furthermore, the proportion of groundwater used for irrigation of croplands, increases in parallel with the overall decline in rainfall, which decreases the groundwater amount and leads to the degradation of croplands

3.4 Conclusion

This study examines the use of remote sensing data to characterize and map the spatio-temporal phenological metrics variability through Beni-Mellal-Khenifra region between 2012 and 2016. Phenology-based classification approach showed a high ability to identify and monitor the main agricultural system in the study area. The classification overall accuracy reached 88%, with a kappa coefficient of 0.83. The F1-score values for all classes were greater than 0.76. Analyzing the results, the rainfed area shows a dependence to the spatio-temporal fluctuations of rainfall, this result can be extended in further studies on the characterization of drought in agricultural zones. Therefore, the phenological analysis provides information to deep our understanding of the spatio-temporal variability of land surface phenology in arid and semi-arid area. In perspective, Asses environmental, agronomic and socio-economic consequences of phenological changes can improve the awareness of stakeholders to adapt it to take decisions to limit the impacts of change on ecosystems and society. The results demonstrated the ability of phenological parameters to identify and monitor the main agricultural system classes in the study area and to control the illegal pumping zones and the irrigated area.

Chapter 4: Remote monitoring of agricultural systems using NDVI time series and machine learning methods: a tool for an adaptive agricultural policy

Lebrini Y., Boudhar A., Htitiou A., Hadria R., Lionboui H., Bounoua L., Benabdelouahab T., (2020). Remote monitoring of agricultural systems using NDVI time series and machine learning methods: a tool for an adaptive agricultural policy. *Arabian journal of Geosc*iences, 13. https://doi.org/10.1007/s12517-020-05789-7

4.1 Introduction

Monitoring farming systems (FS) is a major task, particularly in arid and semi-arid regions where water scarcity and droughts are frequent (Benabdelouahab et al. 2020; Gu et al. 2007; Winkler et al. 2017). However, large-scale information about agricultural systems is essential for land use monitoring and management besides making an informed decision on food security and sustainability (Benabdelouahab et al. 2019b; Hentze et al. 2016; Lebrini et al. 2019b; Li et al. 2014; Salhi et al. 2020).

The advent of remote sensing data provides easy and common solutions to map agricultural systems and to characterize crop phenological information at both local and regional scales (Hadria et al. 2019; Htitiou et al. 2019a; Htitiou et al. 2020b; Kariyeva and van Leeuwen 2012). Several studies have explored the use of phenological metrics for monitoring agricultural systems using different data sources and methods (Adole et al. 2018; Lebrini et al. 2019a). Many studies have confirmed that time series of vegetation indices used to produce phenological parameters provides accurate and robust results compared to traditional methods based on single-image processing (Atkinson et al. 2012; Hao

et al. 2015; Jönsson et al. 2018). Indeed, satellite-derived phenological metrics provide the ability to monitor and discriminate vegetation cover from local to large scale based on contrasted differences observed in the phenological profiles (Atzberger et al. 2013; Bachoo and Archibald 2007; Lieth 1974; Schwartz 2003; Wessels et al. 2009). Whether it is used to map agricultural systems (Alcantara et al. 2012; Qiu et al. 2017), to analyze the response of phenological metrics to climate events (Cui et al. 2017) or to extract seasonal cropping patterns (Jönsson et al. 2018), remote sensing-derived phenological metrics have improved agricultural monitoring. Because of its spatio-temporal continuity, MODIS data provides an excellent opportunity to characterize and to monitor the spatiotemporal variability of vegetation (Friedl et al. 2010). The high spectral and temporal resolutions and its data availability since 2000 allow constructions of useful time series of vegetation indices (VIs) (Akhtar et al. 2017; Suepa et al. 2016).

Classification approaches based on remote sensing data are widely used in AS monitoring and numerous algorithms have been used to solve complex classification problems (Meyer et al. 2018). This includes Random Forest (RF), Support Vector Machine (SVM), Artificial Neural Networks (ANN), K-Nearest Neighbor (KNN), and Decision Trees (DT). These algorithms are also known as machine learning algorithms, which are data-based approaches that learn the relationships between the predictor and response (Breiman 2001). Compared to statistical methods, these algorithms are not parametric since they do not depend on a theory related to the distribution of the data (Qian et al. 2014).

Many studies have been conducted to investigate the use of machine learning methods for agricultural systems monitoring and vegetation cover mapping. Yu et al. (2018) have used KNN and SVM classifiers to evaluate the effects of a new method to extract information from neighborhood pixels on the improvement of Land Use Land Cover (LULC) classification. Wessel et al. (2018) have focused their study on the comparison of the object-based image analysis (OBIA) and pixel-based methods to evaluate RF and SVM classifiers in mapping tree species using Sentinel-2 data. Wang et al. (2018) have evaluated the performance of Landsat 8, Sentinel-2, and Pléiades-1 data in mapping mangrove species over the National Nature Reserve for mangroves in China. Finally, Jin et al. (2016) have determined a new approach to classify deforested areas based on phenological metrics and RF classification.

In the context of climate change, water supply is the main driver of crop growth variability in arid and semi-arid regions like Morocco (Benabdelouahab et al. 2019a). Therefore, to advance the involvement of stakeholders in agricultural management and to improve socio-economic conditions in vulnerable areas such as the Oum Er-Rbia Agency's Geographical Scope (OER-AGS), the adoption of a remote sensing derived phenology method is prime in facilitating decision-making and has the potential to improve land management and yield production in the region (Lionboui et al. 2020). Towards this objective, in this chapter, we present an analysis of long-term changes in agricultural systems over the Oum Er-Rbia Agency's Geographical Scope (OER-AGS) in Morocco. The study intends to (1) monitor and investigate changes in four agricultural systems using phenological metrics of long-term remote sensing data (2) investigate the performance of machine learning methods in the mapping of agricultural systems at large spatial scale.

4.2 Methods

4.2.1 Reference data collection

Four land cover types were selected: Irrigated Perennial Crop (IPC), Irrigated Annual Crop (IAC), rainfed area (RA) and fallow (FA), to evaluate the effectiveness of phenological metrics in discriminating farming systems within the OER-AGS and monitoring change over the studied period. The reference data for training and validation were collected through ground-based fieldwork during the 2015/2016 season (Table 7). Additional reference data were collected using high resolution Google Earth images.

Table 7 : Reference data plots

Agricultural System class	Code	Reference data (number of Pixels)
Irrigated annual crop	IAC	210
Irrigated perennial crop	IPC	301
Rainfed area	RA	254
Fallow area	FA	441

4.2.2 Phenological metrics classification

In this study, three machine-learning classifiers were used based on CARET package within R (Kuhn 2008; R Core Team 2017), which are: Support Vector Machine (SVM), Random Forest (RF) and K-Nearest Neighbor (KNN).

The SVM classification method is a supervised nonparametric technique derived from statistical learning theory for solving classification problems (Vapnik 2006). The most interesting properties of the SVM classification are the generalization capability from small training data and the high potentiality for large scale studies (Shao and Lunetta 2012). The principal approach of the SVM classification method is the concept of drawing vectors into a multidimensional space which is achieved through a kernel function and then searching for the optimal separation plan (i.e., hyperplane) that divides classes (Huang et al. 2010). The choice of the separation plan is based on the concept of maximum margin, which represents the distance between the hyperplane and the closest samples, these samples are known as the support vectors. Several kernel functions are used in the literature. According to Hsu et al. (2003) and supported by many other authors (Carrão et al. 2008; Clauss et al. 2016; Duro et al. 2012), the advantages of the Gaussian Radial Basis Function (RBF) kernel consist on his capability to works in a multidimensional space with minimum parameters configuration contrary to other kernels (e.g., linear, polynomial). In this study, the regularization parameter C and the kernel parameter λ for the SVM classifier were selected randomly using the tuning function in the CARET package. On the other hand, the RF classifier is a machine learning algorithm, considered as a special case of bagging approaches (bootstrap aggregation). The selection of many bootstrapped samples operation based on training data result with a number of trees (ntree) (Breiman 2001). In addition to bootstrap aggregation, each resulted tree is based on a random subset which represents two-thirds of the input variables (mtry), the remaining one-third that are not present in the calibration subset (i.e., out of bag samples) are used to obtain the out-of-bag (OOB) error of predictions (Rodriguez-Galiano et al. 2012). In this study, default values are used to train the RF classifier (Breiman 2001). Besides, the mean decrease in accuracy was calculated to assess the relative importance of each feature on the prediction for all classes. The variable importance is an important output that indicates the weight of a feature in the discrimination of a specific class (Pal 2005). Finally, we tested the KNN approach,

which is a supervised non-parametric classification technique used frequently in statistical applications (Samworth 2012). KNN classification methods consist of the finding of k training samples which are closest to training data according to a distance function based on these k samples (Sun et al. 2018). Nearest neighbors contribute more in the discrimination of a class than distant neighbors In this classification method, the k play an important role in the parameterization of the KNN algorithm and the delineation of classes (Qian et al. 2014). Regardless of the choice of classifiers, accuracy assessment was performed using the confusion matrix to compute the overall accuracy (OA), user's accuracy (UA), producer's accuracy (PA), kappa coefficient, and F1-score metric.

Based on the best classification result, AS class changes were mapped over the study area. The classification model performed within the 2015/2016 agricultural season has been applied to classify AS classes for 2000/2001, 2004/2005, 2008/2009, and 2012/2013 cropping seasons. Furthermore, AS maps obtained from 2000/2001 and 2015/2016 cropping seasons were used to map changes occurred in this period over the study area, these changes represent the dynamics between the principal four classes which are IPC, IAC, RA, and FA. The possible change types in the four AS classes comprise 12 classes that represent transition (i.e., from a class to another one.) and 4 classes with a static state.

4.3 Results and discussion

4.3.1 NDVI profile analysis

Figure 16 shows the spatiotemporal variation of NDVI values extracted from the reference data collected during field survey operations compared to the rainfall average over the studied region. A visual analysis of the NDVI temporal profiles shows four different patterns associated with each AS class, which are characterized by a well-defined range of NDVI values and describe the seasonality of each AS class. IPC class NDVI values range between 0.4 and 0.7 during the entire period and are characteristic of the high and permanent photosynthetic activity of irrigated perennial crops (Figure 16-B). The use of MODIS data at 250 m leads to a class mixture at the pixel level, which affects the mean NDVI value. This mixture attenuates during the study period due to tree growing extension encouraged by the

Green Morocco Plan (GMP). In fact, the dynamic tree-growth generated by the GMP over the region justifies the positive trend of the IPC NDVI observed beginning in 2000/2011 and which materializes by increases in both the minimum and maximum NDVI values and the length of photosynthetic activity through the cropping seasons (Figure 16-B).

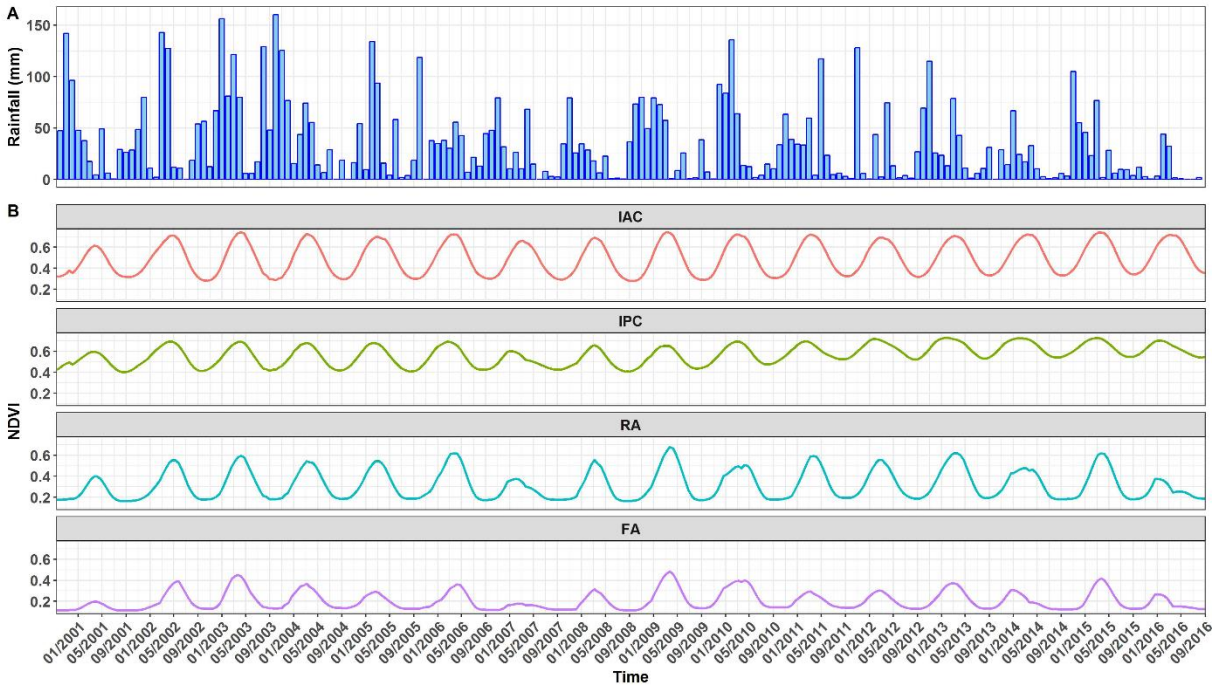

Figure 16: A) Monthly average rainfall; B) NDVI temporal profiles of the four agricultural system classes over the study area between 2000 and 2016.

The irrigated Annual Crop (IAC) NDVI values range from 0.3 to 0.8 with no much interannual variability in the maximum NDVI (Figure 16-B). This was expected as the IAC receives irrigation water supplies during the growing season. Indeed the average maximum NDVI is 0.65 (+/- 0.1). The small standard deviation indicates the independence of the rainfall interannual variation. The rainfed (RA) class NDVI varied from 0.2 to 0.7 for wet seasons (e.g. 09/2009 – 05/2010) and between 0.2 and 0.4 for dry seasons (09/2006 – 05/2007), with smaller maxima than the IPC. The RA time evolution shows significant variation over the studied period with an apparent time lag between the maximum precipitation and its maximum amplitude. A similar pattern is observed for the FA class though with much less NDVI amplitude than that of the RA.

Figure 17 summarizes the inter-annual variation of the mean, maximum, and minimum NDVI values for all AS classes over the study area between 2000/2001 and 2015/2016 cropping seasons. These results confirm the strong link of the vegetation's growth response in

the RA and FA classes to the temporal variability of rainfall presented in Figure 16-A. Concerning the length of the cropping season, it lasts longer for IAC where the mean season length is around 7-8 months, compared to the RA and FA classes where the mean season length is around five and three months, respectively (Figure 17). The variability in season length for the RA and FA classes is a response to seasonal rainfall variability both in frequency and in amount during the cropping season. In this case, a short rainy season causes an earlier end of the growing season. Regarding the start of season time (TSOS) of the NDVI cropping season, there is a significant variation between classes (Figure 17). The mean NDVI values presented in Figure 17 reveal an earlier TSOS for IAC class (i.e., between November and December) while for RA, TSOS is around the first of January. This delay in the start of season time is directly related to the time of occurrence of the first rainfall, which affects the sowing dates in rainfed regions. On the other hand, the earlier start of the season in the IAC is due to the impact of controlled irrigation frequency.

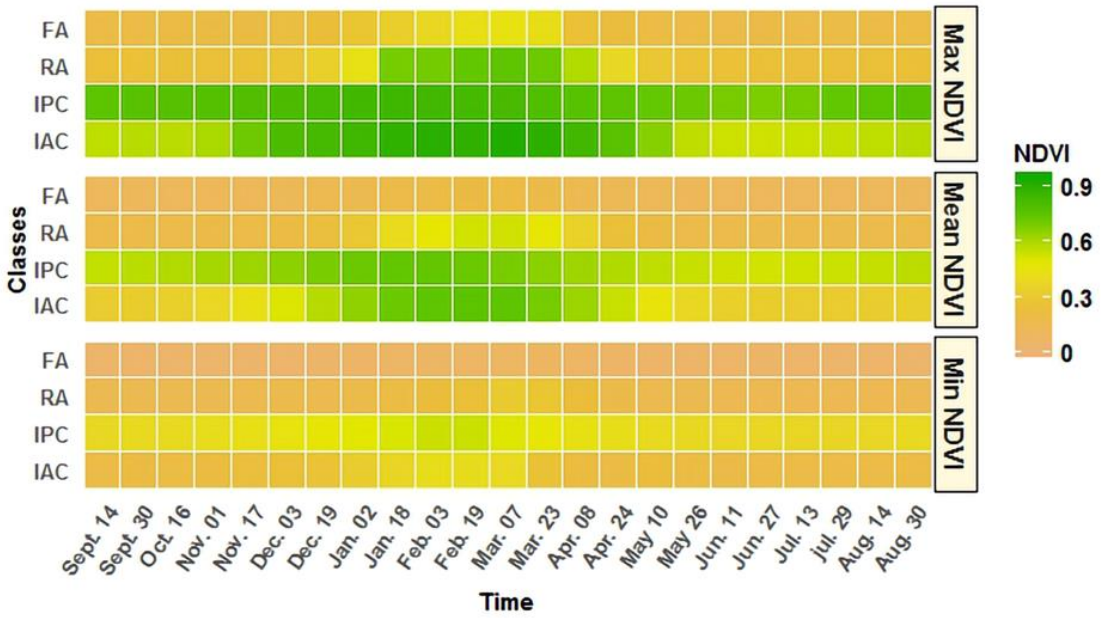

Figure 17: Heat-map of AS classes based on NDVI Maximum, Mean and Minimum values

4.3.2 Farming systems classification

The classification provides a better understanding of the spatial patterns of agricultural systems in the Oum Er-Rbia Agency's Geographical Scope (OER-AGS), which are important for food production, livelihoods, and food security in this area.

The classifications of agricultural systems, over the OER-AGS, depicted in Figure 18, were produced from the implementation of SVM, RF, and KNN classifiers based on phenological metrics. The three classifiers have been evaluated and the results are summarized in Table 8. In terms of individual accuracy, significant differences are obtained between the three classifiers. RF-based AS classification presented not only higher overall accuracy but also a much more balanced producer and user accuracy.

The RF classifier had a higher accuracy than the SVM and KNN classifier. The overall accuracy for RF was 97%, with a kappa value of 0.96 (Table 8). In general, all AS classes achieved over 90% user's accuracy. The RF classifier also produced over 90% producer's accuracy for most AS classes. Using this classifier, the FA class was slightly confused with RA. The KNN classifier generated relatively lower overall accuracy than RF classifier, with 95% and 0.91 for overall accuracy and kappa value, respectively. For the KNN classification, all

classes achieved over 90% user's accuracy, except for IPC, which had 88%. In terms of confusion between classes, the IPC class was confused with IAC.

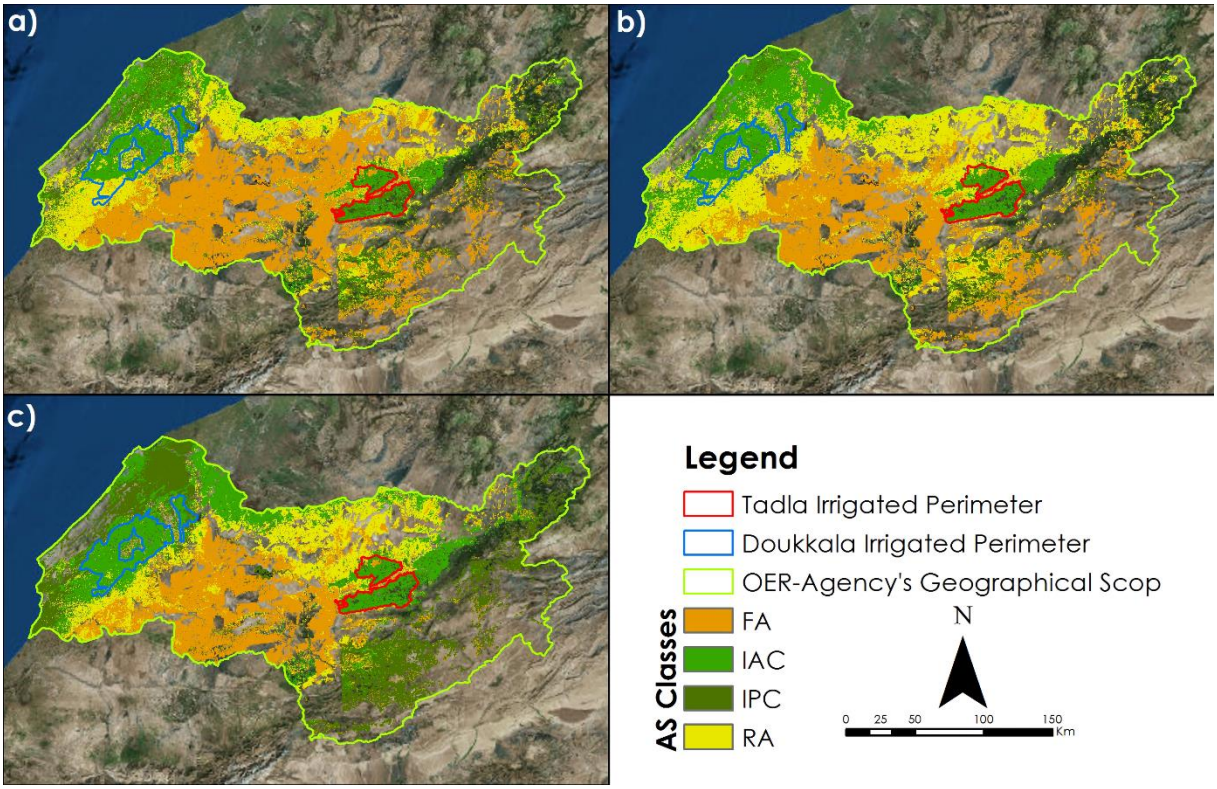

Figure 18: Agricultural System classification maps over the OER-AGS, a) Random Forest b) K-Nearest Neighbor and c) Support Vector Machine.

Finally, the SVM generated a relatively lower overall accuracy of 94% and a similar kappa value of 0.90. The producer's accuracy for IPC and RA classes was less than 90% while the user's accuracy was superior to 90%. There was confusion between IAC and IPC, RA and IAC, and FA and RA. Overall, the Random Forest method resulted in the best classification of AS classes. Furthermore, we tested the importance of the phenological metrics in mapping the four AS classes over the OER-AGS using the RF algorithm, the results are presented in the Figure 18.

Table 8: Confusion matrix of the three AS maps classification and accuracy assessment results

Classifiers	**RF**				**SVM**				**KNN**			
AS Class	**IAC**	**IPC**	**RA**	**FA**	**IAC**	**IPC**	**RA**	**FA**	**IAC**	**IPC**	**RA**	**FA**
IAC	127	1	0	0	128	5	4	0	121	3	0	0
IPC	1	48	0	0	1	44	2	0	6	45	0	0
RA	1	0	45	2	0	0	39	2	2	1	45	2
FA	0	0	0	15	0	0	0	18	0	0	0	18
PA	0.98	0.98	0.99	0.90	0.99	0.89	0.86	0.90	0.93	0.91	0.99	0.90
UA	0.99	0.97	0.93	0.99	0.93	0.93	0.95	0.99	0.97	0.88	0.90	0.99
F1	0.97	0.95	0.96	0.97	0.96	0.88	0.84	0.99	0.96	0.93	0.97	0.99
OA	0.97				0.94				0.95			
Kappa	0.96				0.90				0.91			

The result further indicated that the GINT metric had the highest mean decreasing accuracy, with the lowest mean decreasing accuracy obtained with the LD metric. For this reason, we also measured the importance of each phenological metrics in discriminating individual FS classes among the other classes (Figure 19). The results indicate that the GINT metric is important in separating FA and RA from the other classes. In addition, the VEOS and MIDDLE metrics are important in discriminating IPC and IAC classes, respectively. On the other hand, the MIDDLE metric has no significant importance in separating the FA class from others while LD has a smaller influence in separating the IPC and IAC classes. However, in the RA class, the importance of the TSOS metric is the least significant.

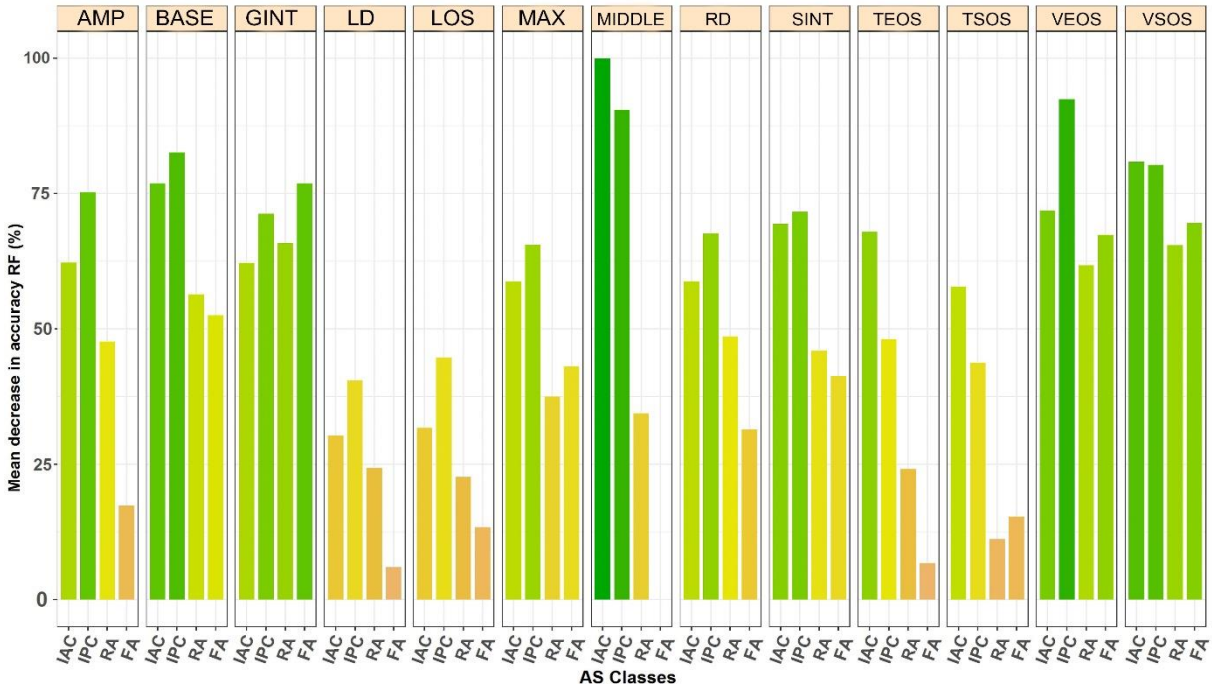

Figure 19: Relative importance comparison of each phenological metric using the mean decrease in accuracy

4.3.3 AS area change

In a context marked by climate change, the challenge is more serious for the arid and semiarid regions, like the OER-AGS, where water resources are facing several constraints. The interest for spatiotemporal monitoring of the AS area led us to study their changes through superficies and AS changes among cropping seasons of 2000/2001, 2004/2005, 2008/2009, 2012/2013, and 2015/2016 (Figure 20 and Figure 21).

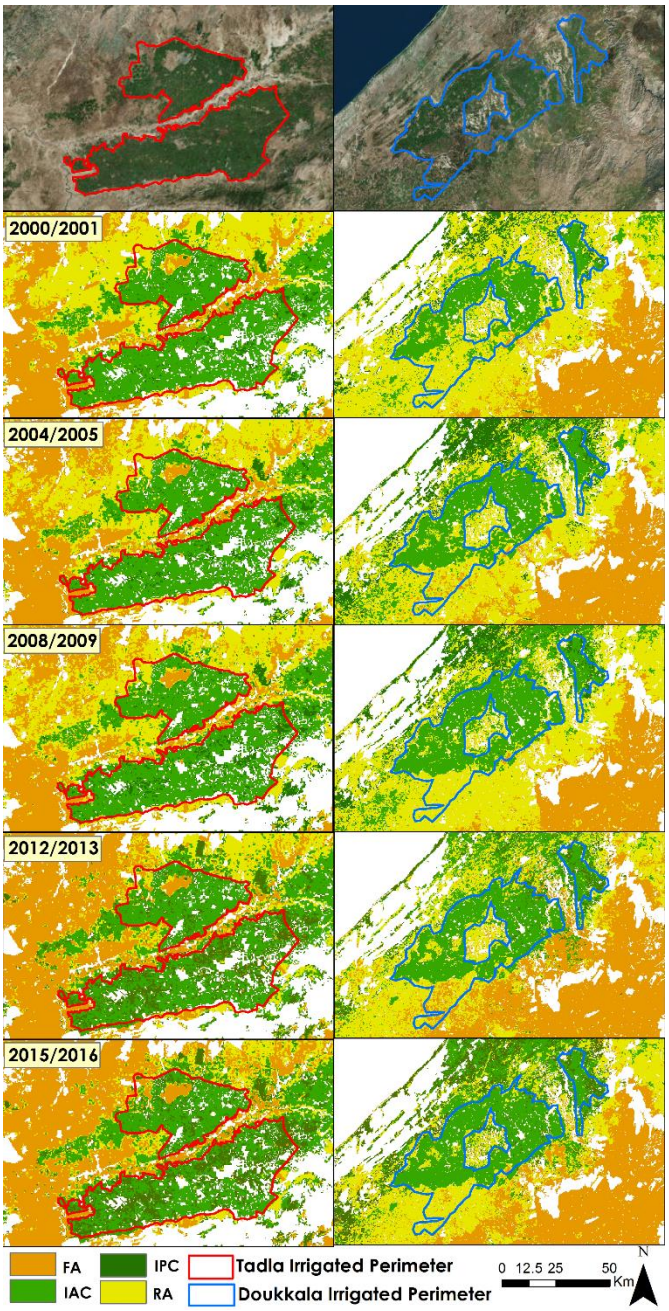

Figure 20: Changes in AS classes from 2000 to 2016 over the Tadla irrigated perimeter (left column) and Doukkala irrigated perimeter (right column).

The change detection results reveal an important dynamic between the different AS in the studied region. Concerning the IPC superficies, it has increased from 255,589 ha in 2001 to 342,000 ha in 2016 (26%). To understand this expansion, the transition map between 2000/2001 and 2015/2016, shows that there has been a marked change in AS classes over the study area. During the study period, a large area of IAC class has been converted to IPC, this happened near, and around the Tadla Irrigated Perimeter and around the northern part of the Doukkala

Irrigated perimeter (Figure 20, Figure 22-A, Figure 22-B). FA and RA classes were also transformed to IPC around the Tadla Irrigated Perimeter (Figure 22-A). Concerning the change towards IAC class, RA and FA were converted in a wide part of the DIP especially in the south part of the perimeter to IAC class (Figure 22-B).

The transition from RA to FA was observed around the TIP (Figure 22-B). The transition to IAC class is originated to the extension of irrigated perimeters, as observed in the pumping areas in the northern part of the TIP (Figure 20, Figure 22-A). The same result was observed in the south part of the DIP (Figure 20, Figure 22-B). The IAC class area has raised by about 28.5% from 374,150 ha in 2001 to 552,608 ha in 2016 (Figure 21).

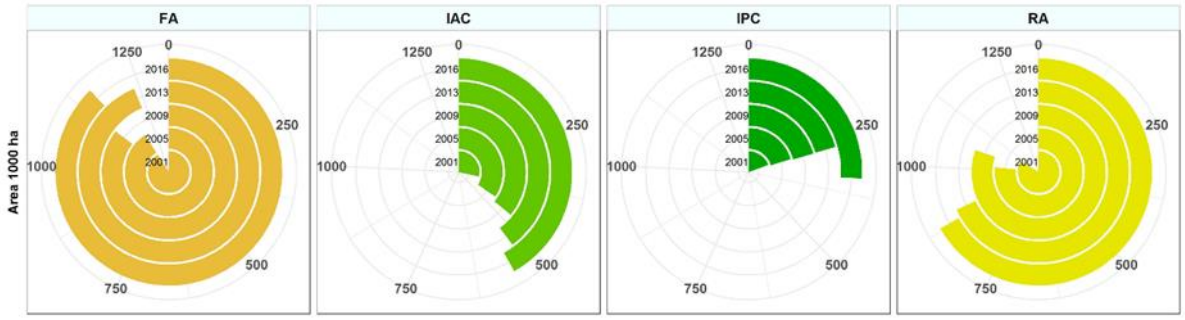

Figure 21: AS area change from 2000 to 2016

In this area, we observed the extension of IAC and IPC classes, outside irrigated perimeters (TIP and DIP), which indicates the development of groundwater pumping in these areas. The conversion from FA, RA, and IAC classes to IPC was encouraged by the availability of groundwater throughout the year, on one hand, and on the other hand by agricultural policies supporting the implementation of new irrigation techniques and high value-added crops (Lionboui et al. 2018). In addition, cultivating plants with higher value-added was an important orientation of the Moroccan government since the beginning of the Green Morocco Plan projects in the OER-AGS, from where the augmentation in IPC and IAC class is observed over the studied period. However, the increase of the IPC and IAC areas shown in the results may indicate a high pressure applied to the groundwater whose levels drop by 1 to 3 meters annually according to the Oum Er-Rbia Watershed Agency. Nevertheless, irregular changes in superficies were observed for the RA and FA classes over the studied period (Figure 21). RA class decreased from 1,104,687 ha in 2001 to 1,013,299 ha in 2005 (-16%) then increased in 2009 to 1,127,132 ha (7.6%) and decreased in 2016 to 880,500 ha (-42.1%) (Figure 21). The same

statement was observed for the FA class where the superficies is variable between 1,199,051 ha, 1,127,132 ha and 1,158,369 ha for 2001, 2009 (-6.2%) and 2016 (17.1%) years, respectively (Figure 21). The observed fluctuations in superficies of the RA and FA classes are strongly related to rainfall amount, which varies with climate and directly affects the extent of the cultivated area (Figure 22-A). For a dry season, a major part of the RA class changed into the FA class and during a wet season, a portion of the FA class is transformed into RA class (Figure 22).

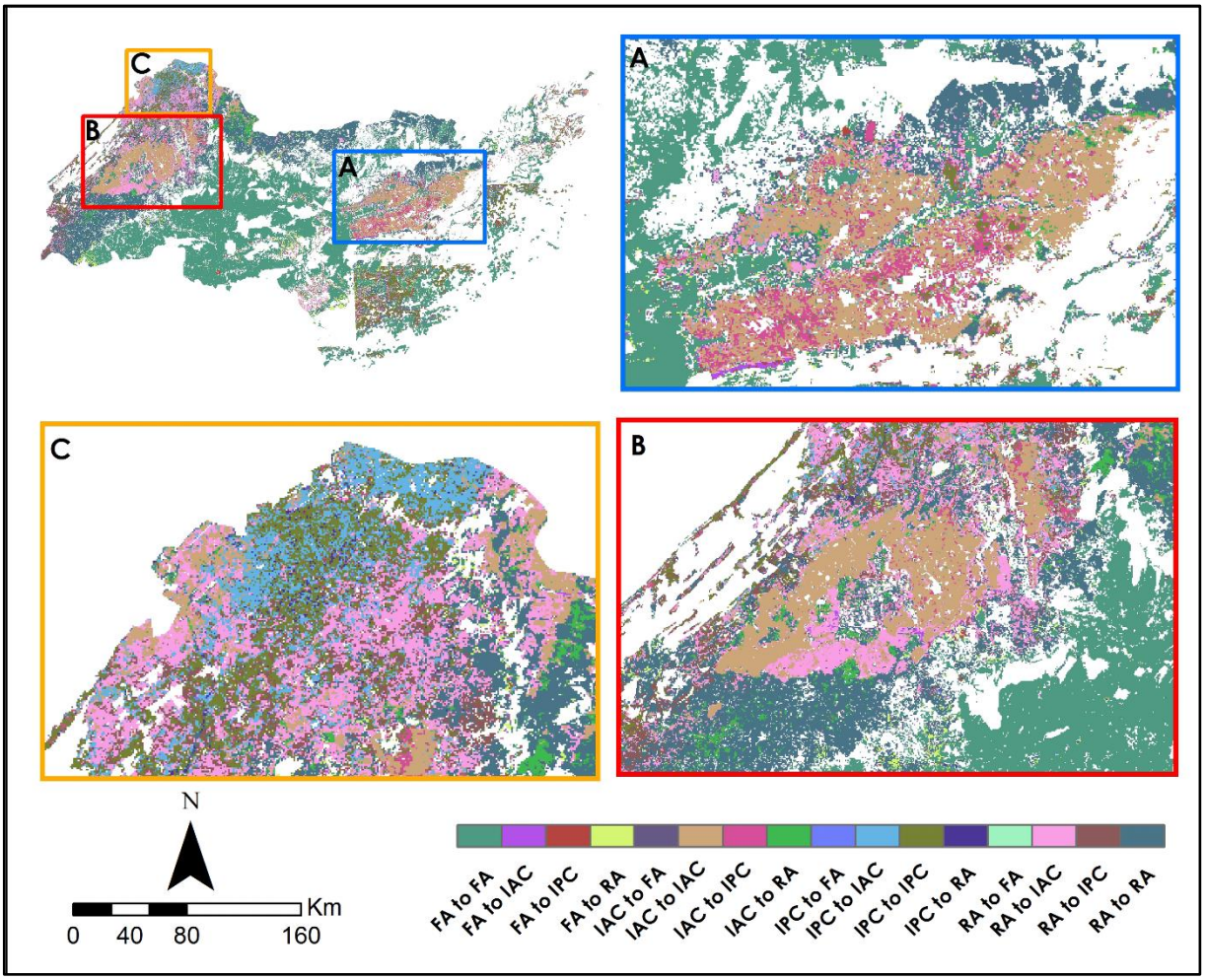

Figure 22: Transition map of AS classes from 2001 to 2016 over the OER-AGS

On the other side, the result shows the transition from IAC and IPC classes to FA and RA (Figure 22-B, Figure 22-C). These transitions are explained by many reasons, particularly human-induced soil degradation (e.g., soil salinity, nutrient depletion) and the quality and depth of groundwater. GLASOD (Global Assessment of Human-Induced Soil Degradation), indicated that 494 million hectares (Mha) of the African countries are degraded, in which 45 Mha degraded by nutrient depletion and 15 Mha degraded by soil salinity phenomena (Bai et

al. 2008). The Moroccan territory is concerned by 15.09 % of soil degradation, essentially soil salinity and erosion (Bai et al. 2008). As approved by del Barrio et al. (2016), semi-arid zones are the most vulnerable. Furthermore, the proportion of groundwater used for irrigation of croplands, increases in parallel with the overall decline in rainfall (Lionboui et al. 2016a), such type of exploitation decreases the groundwater amount and leads to the degradation of croplands. Hence, sustainable water management, in irrigated perimeters and the pumping area, is a crucial issue to ensure a stable irrigation water supply and to maintain a sustainable relationship between irrigation practices and environment over agricultural systems.

4.4 Conclusion

Agriculture is increasingly benefiting from the geo-spatial technologies, which can make a substantial contribution to the monitoring and the management of agricultural systems as providing accurate information at a large spatial scale. Data on semi-arid AS phenology are scarce and somehow difficult to produce, essentially because of lack of sufficient data. For this reason, the use of phenological metrics time series appears more efficient. The classification of agricultural systems may facilitate better decision making around food production, livelihoods, and food security in the OER-AGS. Thereby, phenological metrics of AS classes were mapped and studied over the OER-AGS area. Among the three classifiers, the RF classifier produced satisfactory accuracies. Mapping changes over the study area revealed important results, especially on the dynamics and the effect of regional policy on agricultural system changes. The use of satellite phenological metrics to classify AS and map changes over the sixteen years proved the ability of phenological metrics in characterizing the spatiotemporal changes over a large extent and a relatively long period. The production of such results, in the appropriate time and with accurate way is important for decision-makers and the management of agricultural practices to help the most vulnerable farms to continue their agricultural activities in the context of food insecurity and climate change and even crop insurance. However, further studies are still required to analyse trends of phenological metrics and to explore their linkages to surface climatic indices.

Chapter 5: Mapping and Characterization of Phenological Changes over Various Farming Systems in Arid and Semi-arid Region using Multitemporal moderate spatial resolution data

Lebrini, Y., Boudhar, A., Laamrani, A., Htitiou, A., Lionboui, H., Salhi, A., Chehbouni, A., Benabdelouahab, T. Mapping and Characterization of Phenological Changes over Various Farming Systems in an Arid and Semi-Arid Region Using Multitemporal Moderate Spatial Resolution Data. *Remote Sens.* 2021, *13*, 578. https://doi.org/10.3390/rs13040578

5.1 Introduction

Accurate monitoring of land use changes in arid landscapes and understanding of these changes drivers is crucial in arid environment research. Especially, since changes in farming systems affect directly socioeconomic as well as environmental sectors. Improving global food security will need a good understanding of the behavior of farming systems and their responses to climate and human induced factors (Benabdelouahab et al. 2019b; Lionboui et al. 2020). In African arid and semi-arid regions, there is a pressing need for characterizing the behavior and the distribution of farming systems for better monitoring of agricultural lands and thus managing land resources. In this context, accurate management and monitoring of farming systems particularly at large scale can substantially benefit from geo-spatial technologies and remote sensing data (Sishodia et al. 2020). However, on semi-arid regions, phenological data are scarce and difficult to produce due to the lack of sufficient ground information and limited studies (Lebrini et al. 2020). Therefore, the use of remotely sensed Phenological metrics (PhM) may provide viable alternative to costly and time-

consuming field sampling (Atzberger et al. 2013; Schreier et al. 2020). In addition, the change analysis of PhM could provide valuable information that would identify current trends as quickly as possible, and would be easily understandable by political authorities as well as by land managers to take actions quickly for better control of agricultural lands. In the same context, information on vegetation cover provide an insight on changes occurred and could be a potential indicator on food security and sustainability (Benabdelouahab et al. 2015; Benabdelouahab et al. 2018; Hentze et al. 2016; Li et al. 2014). To this end, the use of remote sensing has demonstrated a strong potential for understanding and detecting phenological changes because of consistent and frequent coverage (Lu et al. 2004). Data from remote sensing satellites provide large and continuous observations that characterize the changes occurred on the earth (Coppin P 2004; Lu et al. 2004). Indeed, time-series of satellite data are suitable to monitor the spatiotemporal behavior of plant phenology (Htitiou et al. 2020a; Htitiou et al. 2019b; Salhi et al. 2020). These issues motivate studying changes in farming systems to characterize the spatiotemporal variability that occurred over long periods and related to different drivers, i.e. short and long term weather events, public policy.

Many studies have proved the existence of a consistent relationship between vegetation indices and weather indices (i.e., temperature, precipitation) (Castro et al. 2009; Cleland et al. 2007; Hanamean Jr. et al. 2003; Moulin et al. 1997; White et al. 2009b; Zhou et al. 2001). During the last decades, scientific community have investigated the impact of land management on specific indices (e.g. Normalized Difference Vegetation Index, NDVI) in order to link vegetation changes to anthropogenic actions (DeFries et al. 1999). With this in mind, many researchers went further in studying changes in vegetation cover, based on satellite derived products, by developing techniques and tools for extracting and analyzing PhM, especially for monitoring farming systems (Adole et al. 2018; Atzberger et al. 2013; Chandola et al. 2010; Lebrini et al. 2019b). They demonstrated the ability of these metrics to monitor and differentiate vegetation cover based on the contrasted phenological profiles (Archibald and Scholes 2007; Atzberger et al. 2013; Bachoo and Archibald 2007; Schwartz 2003; Wessels et al. 2009). Consequently, remote sensing-derived PhM have improved agricultural monitoring whether it is to map farming systems (Alcantara et al. 2012; Qiu et al. 2017), to analyze the

dependence of vegetation cover to climate events (Cui et al. 2017) or to characterize the behavior of vegetation cover from different data sources (Jönsson et al. 2018).

Indeed, the use of Moderate resolution Imaging Spectroradiometer (MODIS) data provides an opportunity to characterize the spatiotemporal variability of vegetation cover at large scale (Bai et al. 2019; Lebrini et al. 2019a). It allows the construction of time series of vegetation indices (VIs) (e.g., NDVI, EVI…), by taking advantages of the combination of accurate reflectance, frequent coverage, moderate spatial resolution and the relatively long period of data availability since 2000 (Suepa et al. 2016).

In the scope of farming systems monitoring, different algorithms have been used. This includes Random Forest (RF) Wang et al. (2018), Support Vector Machine (SVM) Wessel et al. (2018), Artificial Neural Networks (ANN), and K-Nearest Neighbor (KNN) Yu et al. (2018). It is worthwhile noting that all of the above-mentioned algorithms are considered as machine learning algorithms, which are based on the automatic learning from dataset to find the relationships between the predictor and the response (Breiman 2001). Among all of them, the Random Forest (RF) (Breiman 2001) which will provide powerful classification of farming systems. It has several advantages including the ability of running efficiently on large volume of input variables, resisting to noise or over-fitting, being relatively robust concerning outliers, and requiring fewer parameters (James et al. 2014; Jin et al. 2016). These advantages makes of this algorithm the best choice for running out the classifications of farming systems.

At present, many studies based on limited observations over some irrigated zones in the Oum Er-Rbia (OER) basin are conducted, but fewer focused on large scale analysis. Investigating the changes in farming systems at large scale in the OER basin will have a far-reaching impact on agricultural sector development and how the system is adapting or not to climate changes. In this context, the present chapter sought to (i) use phenological metrics derived from twenty years of NDVI MODIS datasets (i.e., 2000-2019) to map and monitor changes in selected farming systems over a large arid-to-semi-arid region in Morocco (i.e., OER basin); (ii) Investigate trends in selected farming systems at large scale in the study area to evaluate how the systems are adapting or not to changes? ; and (iii) Provide information on farming systems changes for stakeholders to adopt more accurate and efficient strategies.

5.2 Methods

5.2.1 Random Forest classification and change analysis

To characterize the main cropping systems, the ground data used in this research were collected through ground truthing exercises over farming systems during the 2018-2019 cropping season. The collected data were reported using a GPS receiver, with a positional error of less than 2 m to generate data for classification training and accuracy assessments for 2018/2019 dataset. The reference points were collected in a way to represent the full variety of farming systems elements in the study area. Accuracy assessment of other classification result was performed using similar or near similar ancillary data from MODIS and Google Earth images and high-resolution aerial photographs. The land cover map originated from Glob Cover, was used to mask the agricultural zones over the study area (Hadria et al. 2018; Lebrini et al. 2020). A summary of the ground data is given in Table 9.

Table 9: Ground truthing data

Farming system class	Number of polygons	Training area (Ha)
Irrigated Perennial Crop (IPC)	80	1626.71
Irrigated Annual Crop (IAC)	105	1889.12
Rainfed Area (RA)	160	3617.76
Fallow (FA)	125	2661.06
Total	470	9794.65

To classify farming systems over the OER basin, supervised Random Forest (RF) classifier was used based on CARET package within R (R Core Team 2017). The RF is a non-parametric machine learning classifier that combines a random selection of training subsets of data with an ensemble of trees. Recent studies reveled the effectiveness of the RF classifier in remote sensing field, including land phenology mapping (Belgiu and Drăguţ 2016; Breiman 2001; Hao et al. 2015; Immitzer et al. 2012). For measuring the accuracies of the classification results using the RF classifier, Truth data were split into two sets of training (80%) and testing (20%) samples using a spatial cross-validation approach with 5 folds from the CAST package in R (Meyer et al. 2018). This spatial cross validation help to make sure that the truth sample

of the same field will be either in the test or in the training data in order to avoid over-fitting. The accuracy assessment was done by calculation of many accuracy metrics for the classifications results, including overall accuracy (OA), Kappa coefficient, producer's accuracy (PA), user's accuracy (UA) and F1-score. The classification of 2000/2001 was generated using "predict" function from CARET package in R (R Core Team 2017) . In order to increase the reliability and validity of our RF classification model and as an additional check of the resultant information of study-area-specific classification accuracy, a second accuracy assessment was performed for the 2000/2001 classification map using the same methods as in the accuracy assessment for the 2018/2019 classification map. In order to update testing polygons based on 2000/2001 situation. We have used the testing polygons from the 2018/2019 data and plotted them against smoothed NDVI profile from MODIS data and google earth images. From the MODIS time series we investigate the correspondence between NDVI profile of each testing polygon and the farming system. From imagery, we have added needed polygons to perform the accuracy assessment. Furthermore, FS maps obtained from the 2000/2001 and 2018/2019 classification result were used to map changes occurred over the study area. The transition between FS classes revealed by comparing the classification results was used to extract unchanged FS during the study period. In order to have significant and robust results of the further trend analysis, we opted to compute trend on unchanged farming systems resulted from the change analysis step. Figure 23 shows a detailed flowchart of the adopted methodology in this study.

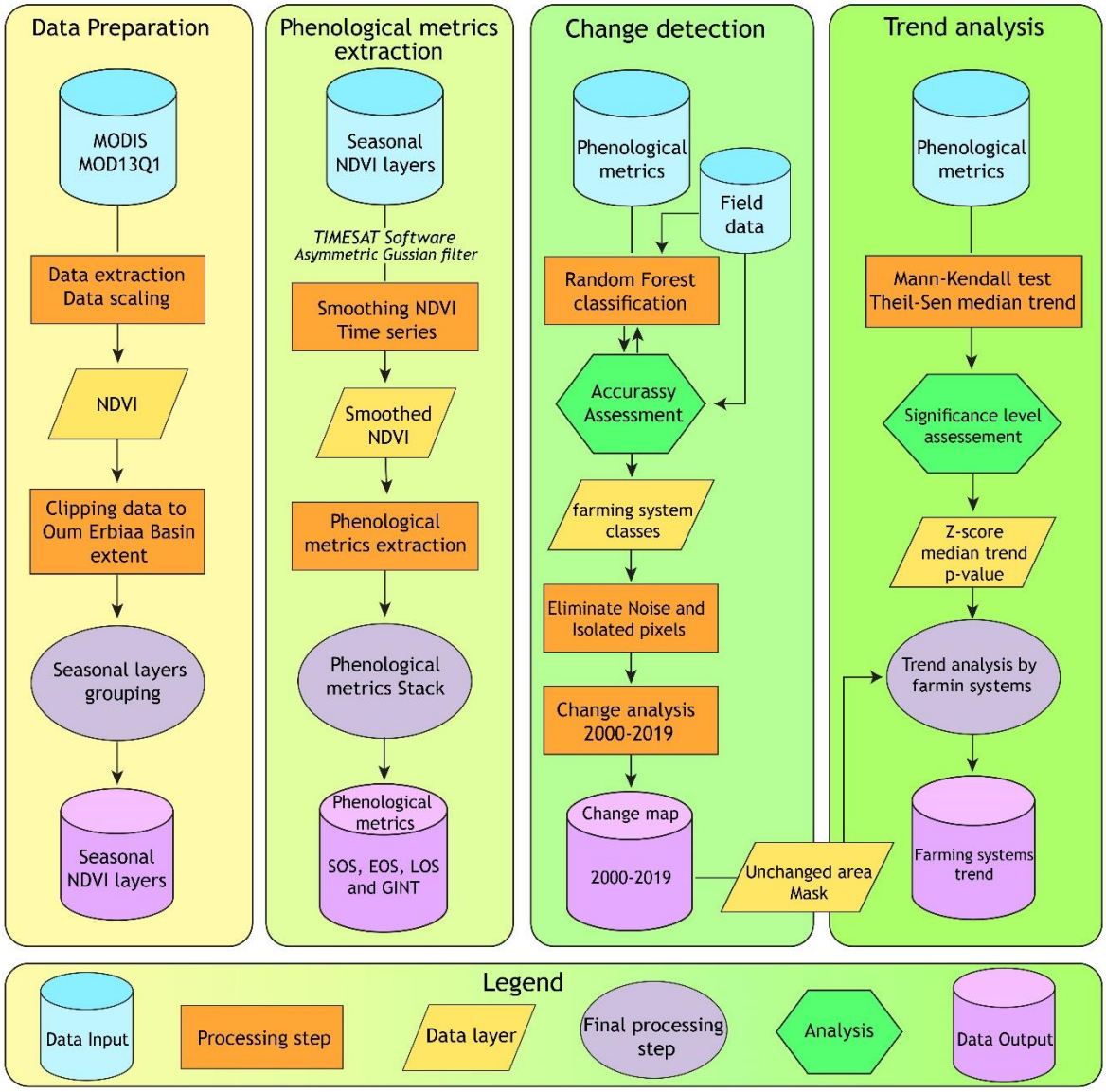

Figure 23: Overview of the methodology adopted in this study.

5.2.2 Variability and trend analysis

From the annual PhM previously retrieved, we calculated their per-pixel temporal mean and coefficient of variation (CV). In order to assess the spatial distribution of PhM showing improvement (positive change) or degradation (negative change), we employed the non-parametric Mann-Kendall (MK) trend test (Kendall 1975) to determine trends on PhM over the OER basin between 2000 and 2019 (Lebrini et al. 2019a).

The Z statistic follows the standard normal distribution with zero mean and unit variance under the null hypothesis of no trend. A positive Z value indicates an upward trend

whereas a negative value indicates a downward trend. Probability (p) represents the measure for evidence to reject the Null hypothesis and positive p values show a negative trend whereas positive p shows a positive trend. We calculated the MK trend test separately for every pixel for start and end of season, length of season, and great integral over the OER basin. These parameters are crucial indicators of seasonal productivity. The Mann-Kendall statistical trend Z was determined as follow:

$$S = \sum_{k=1}^{n-1} \sum_{j=k+1}^{n} sign(X_j - X_k) \ , \ where\ j > k \qquad (1)$$

Where n is the length of time series data, X_k and X_j are the observation at k and j time, respectively.

and

$$sign(X_j - X_k) = \begin{cases} 1 & if \ \ (X_j - X_k) > 0 \\ 0 & if \ \ (X_j - X_k) = 0 \\ -1 & if \ \ (X_j - X_k) < 0 \end{cases} \qquad (2)$$

The probability linked to the Mann-Kendall statistic 'S' and the selected n-data were determined to quantify the level of significance of the trend. The VAR(S) was calculated and then the normalized test statistic Z was computed using the following equations:

$$Var(S) = \frac{1}{18}(n(n-1)(2n+5) - \sum_t ft(ft-1)(2ft+5)) \qquad (3)$$

Where t varies over the set of tied ranks and ft is the number of times that the rank t appears (i.e. frequency). The equation used to calculate the Mann-Kendall significance Z-score is as follows:

$$Z = \begin{cases} \frac{S-1}{\sqrt{Var(S)}} & for\ S > 0 \\ 0 & for\ S = 0 \\ \frac{S+1}{\sqrt{Var(S)}} & for\ S < 0 \end{cases} \qquad (4)$$

Where, $Var(S)$ is the variance of the data set and n is the number of data points. The equation used to estimate Theil-Sen (TS) median trend is:

$$TS = Median(\frac{X_j - X_k}{t_j + t_k}) \quad (5)$$

This robust non-parametric trend operator is highly recommended for assessing the rate of change in time-series data. It is calculated by determining the slope between every pairwise combination and then finding the median value. Using the Mann-Kendall test and Theil-Sen median trend analysis, the trends in PhM were described accordingly, the significance level of the changes in NDVI trends was determined using the Z-score at p-value below 0.1 significance level.

5.3 Results and discussions

5.3.1 NDVI and rainfall time series analysis

Given the importance of the NDVI in monitoring vegetation cover, the spatio-temporal variation of this index was assessed based on reference data collected from fieldwork over farming systems types between 2000/2001 and 2018/2019 cropping seasons and the average rainfall over the OER basin for the same period (Figure 24).

A visual analysis of the temporal NDVI values shows different patterns associated with each farming system type. These patterns were characterized by a specific range of NDVI values and represent the seasonality and the growth cycle of each farming system. The NDVI values for IPC range between 0.45 and 0.9, which is an indicator of the permanent photosynthetic activity of perennial systems (Figure 24). The studied irrigated tree crops are generally carried out in intensive systems. Owing to their received quantities of water and their long life cycle, this farming system shows a unique character of persistence during the growing season from 2000 to 2019. The IAC class has some identical patterns to the IPC farming system, like water supply and the high value of production. The IAC farming system shows NDVI values that range from 0.3 to 0.8. The NDVI values start increasing in September and decrease in May of each agricultural season. Their variability in length of the growing season is mainly related to sowing's timing, the management of agricultural land, and other plant physiological disease problems.

For the RA farming system, the NDVI values varied from 0.2 to 0.7 for wet seasons and between 0.2 and 0.4 for dry seasons (i.e., 2006/2007 and 2008/2009 cropping seasons). In general, their NDVI response to rainfall is systematic. Indeed, agricultural lands in the RA farming system are entirely dependent on rainfall, which varies in amount from one year to the next and directly affects agricultural productivity. Indeed, in semi-arid regions, this relationship between rainfall and NDVI has been demonstrated in numerous researches (Barbosa et al. 2019; Davenport and Nicholson 1993; Lotsch et al. 2003). Thereby, the RA farming system shows high variability in terms of the start, end of season, and the length of season. This variability is linked to the strong dependency of this farming system on the climatic conditions especially the rainfall amount. The vegetative activity begins earlier in the case of a wet season and later for a dry season, and the same pattern could be observed for the end of the vegetative activity. A similar pattern could be observed in the FA farming system where the climatic conditions have more effects on the vegetative activity. These effects of rainfall could be well spotted in the 2009/2010 cropping season over FA and RA farming systems, we can observe precisely the start of the vegetative activity after receiving an important amount of rainfall (Figure 24). Through the coming pages, the paper explores more the behavior of farming systems using trend analysis techniques.

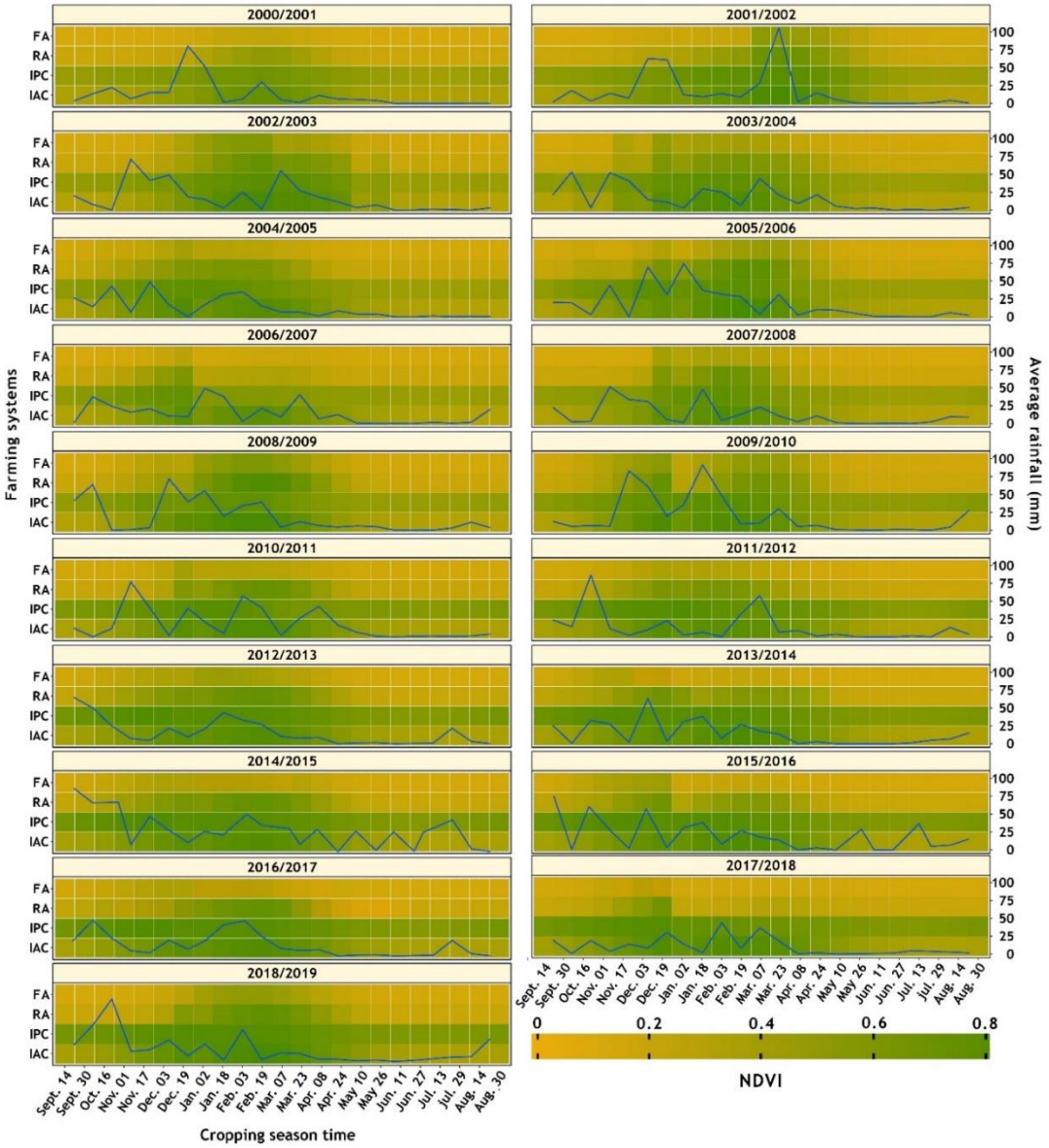

Figure 24: NDVI variability over the four farming systems over the OER basin between 2000 and 2019. NDVI presents the average values extracted from reference data; rainfall were retrieved from CHIRPS (CHIRPS 2020) over the OER basin.

5.3.2 Spatial Patterns of Phenological Metrics

To mutually characterize PhM behavior (i.e, TSOS, TEOS, LOS, and GINT) and their variability, we combined them with their coefficients of variation (CV), which is used as a measure of reliability, into the bivariate maps shown in Figure 6. These bivariate maps provide simultaneously a spatial representation of (1) where high or low variability in PhM are expressed for each farming system, and (2) the risk involved in the future management and

seeding in these farming systems. This combination of factors can assist in developing knowledge about which farming systems can be cultivated in an average year all with considering that in such regions, farming systems choices are largely based on the potential for attaining good yields, and the risk of season failure (Vrieling et al. 2013).

Figure 25-D, shows that areas located inside the irrigated perimeters with a start of the season (TSOS) that occurred between February and June generally have a CV below 0.1. Encouraged by the availability of irrigation water throughout the year, farmers in these areas are diversifying and intensifying their agriculture, thus putting a larger area under crops with high added value, whatever their water consumption (Lionboui et al. 2016b). Outside the irrigated perimeters, especially the center of the study area, strong variability is apparent (i.e., variability above 0.2). This high variability is more accentuated by moving towards the mountainous zones. Farmers prefer not to invest excessively in these zones, in order to avoid the risks associated with drought related mainly to the less stability of TSOS and therefore the rainfall amount and distribution. Areas outside the irrigated perimeters with TSOS between August and September have CV values between 0.1 and 0.3 for practically all locations. Nonetheless, the declining availability of water during the studied period causes a decrease in productivity and leads farmers to opt for crops that require less water but offer good margins, in order to maximize their profits and avoid the risk of season failure. Other regions outside the irrigated perimeters with a TSOS between 242 and 365 day of year have a CV below 0.15. Since these areas may present a low-risk investment opportunity, they could be a good choice for the implementation of new farming systems. Towards the western part of the basin, low variability is apparent (Figure 25-D).

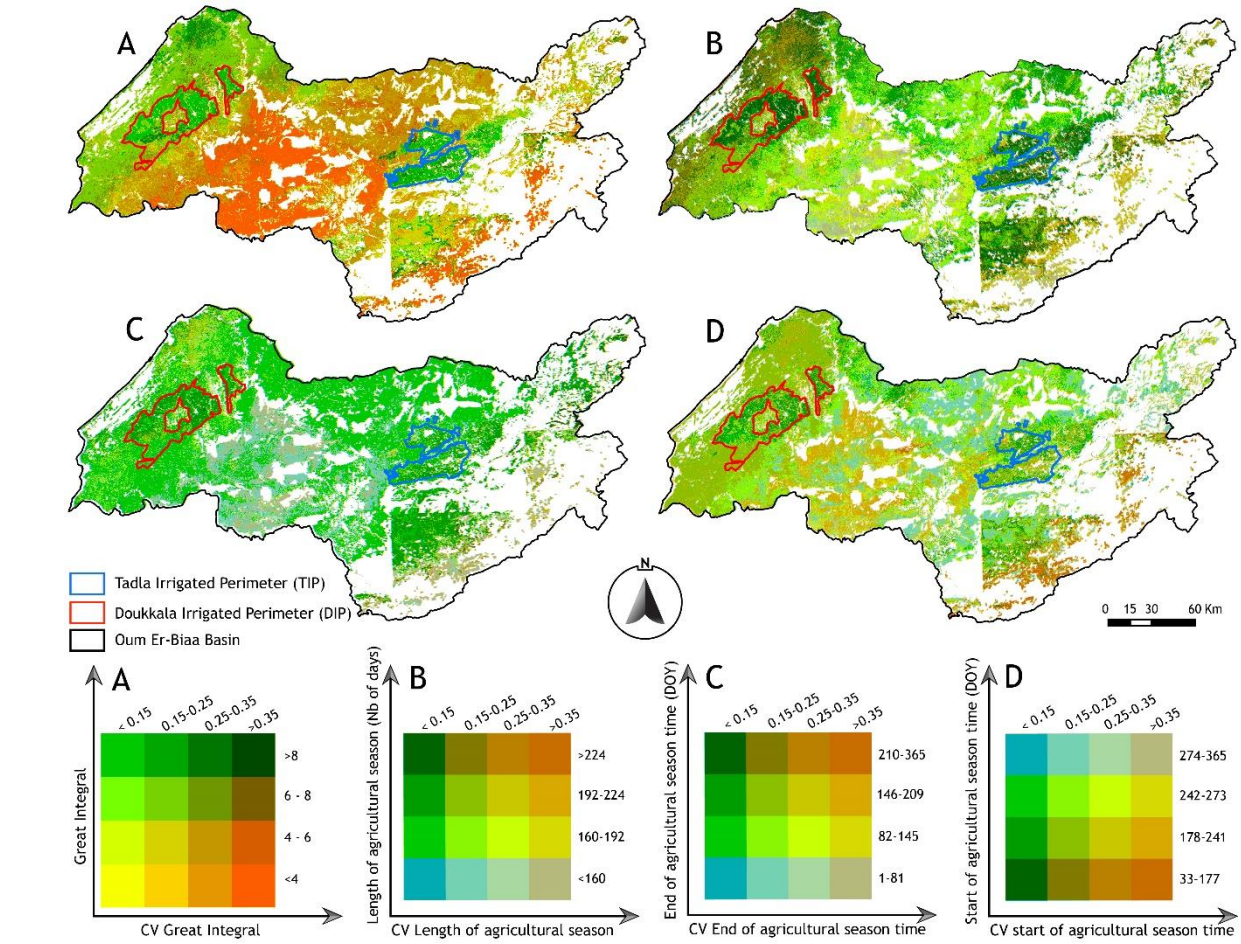

Figure 25: Bivariate map showing simultaneously the great integral (A), length (B), end (C), and the satrt (D) of season and their coefficients of variation. High resolution coresponding figures are provided with the supplementary materials.

On the other hand, areas located outside the irrigated perimeters with an end of season (TEOS) occurred between the DOY 33 and 177 express two degrees of variability, the first with a CV below 0.15 the second with a CV above 0.35. The majority of area, that has TEOS between 178 and 241, has a low variability with CV below 0.15. Inside the irrigated perimeters, low variability is expressed with a CV below 0.15 for areas having the TEOS between 178 and 241 and between 242 and 273. The high variability in term of CV observed for the TSOS and TEOS could be related to the dependence of the start of cropping season to climatic condition, in rainfed farming systems the season could not start without the first rainfall. Adversely, the end of cropping season depends on the climatic conditions but also depend on the physiological properties of the plant and its persistence (Figure 25-C).

Considering the phenological metric LOS, the results of this research show that the variability is inversely proportional to the value of length of the season, without regard to particulars or exceptions. Hence, the areas with a LOS value below 160 days have generally a CV value above 0.35 and the areas with a LOS value between 160 and 192 days have CV values between 0.15 and 0.35 especially in the center of the study area. However, these areas may express a deficit in agricultural production during years with low rainfall amount. The low variability is mostly located inside the irrigated perimeters where the LOS is above 224 days. These zones shows a CV values are below 0.15. Various areas in the western part of the basin also show a high CV values which are above 0.28 (Figure 25-B).

Finally, by combining the fourth phenological metric, explored during this study with its CV values (GINT), our results can help in the characterization of the biomass variability of farming systems encountered in this study area (Figure 25-A). The areas having a GINT values below 4 have a CV values above 0.35. These zones are generally rainfed area and fallow, where climatic conditions take effect. Generally, these areas are not recommended for the seeding of plants with high values of production. Instead, areas of GINT values above 8 have a CV values between 0.15 and 0.25. This moderate variability in biomass productivity could be considered as normal, knowing the differences in crop types over the irrigated parameters (i.e. alfalfa, sugar beet, wheat…). Other zones in the OER basin remain with low to moderate biomass productivity with high variability of GINT metric.

5.3.3 Determination of unchanged farming systems area

The RF classification offers a powerful algorithm to classify the spatial patterns of farming systems in the study area. In this study, the classification of farming systems, were produced from the implementation of the Random Forest (RF) classifier based on PhM. In terms of the individual accuracy, the results presents higher overall accuracy and much more balanced producer/user accuracy. The overall accuracy for RF was 97% and 93%, with a kappa value of 0.95 and 0.91, for 2018/2019 and 2000/2001 copping seasons, respectively. In general, all farming system classes achieved over 90% user's accuracy. The RF classifier also produced over 90% producer's accuracy for most farming system classes. The change detection results from 2000–2019 reveal an important dynamic between the different FS in the studied region.

The transition between FS from 2000/2001 to 2018/2019, shows that there has been a marked change in FS classes over the study area (Figure 26). To evaluate trends over the study area, we only considered the unchanged classes during the studied period.

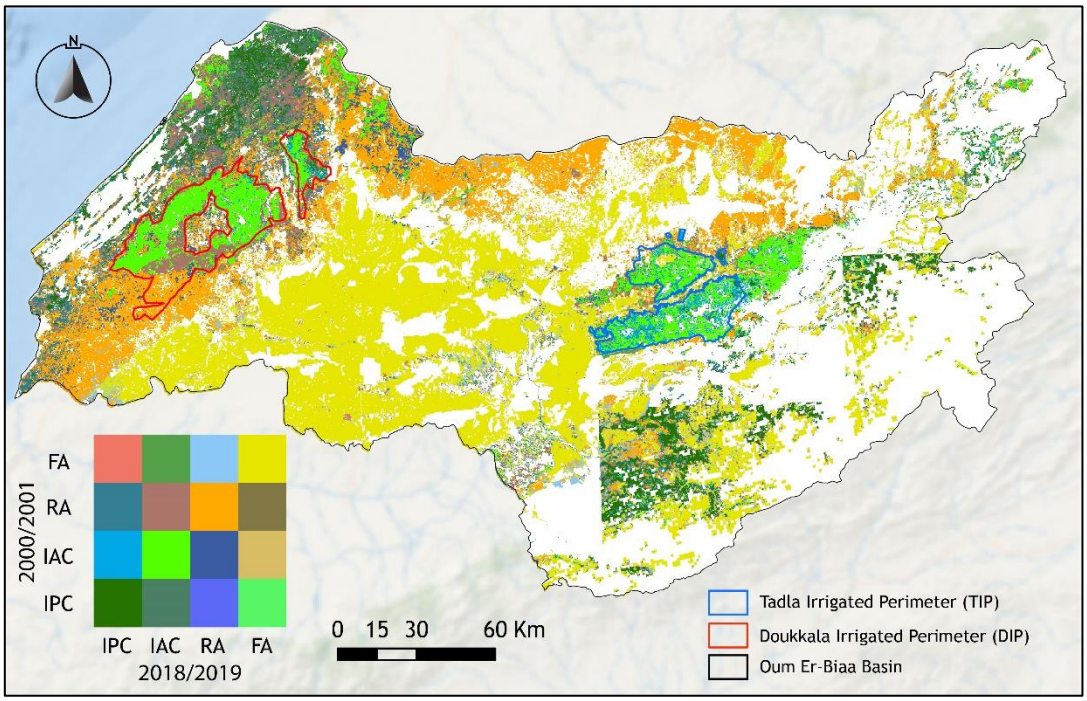

Figure 26: Change map of farming systems over the OER basin from 2000 to 2019. The diagonal of the square represents the unchanged classes of farming systems.

5.3.4 Trend analysis results

This research further analyzed the inter-annual trends for the four PhM (i.e., SOST, TEOS, LOS, and GINT). The Mann-Kendall test was used to identify significant trends at 90% confidence level and Sen's slope estimator was applied to compute the magnitude of trends for the period between 2000 and 2019 alternated between increasing and decreasing trends over the study area. For the start of season (TSOS).Figure 27 displays its trends obtained using Mann Kendall and sen's slope tests. Positive and negative values refer to delayed and advanced dates of TSOS.

Most areas in the OER basin did not show a significant trend during the past twenty years for TSOS, LOS, and GINT metrics ($p > 0.1$). Contrary, the TEOS shows a significant trend over most part of the study area ($p < 0.1$). In this section the signficant trend pixels are only considered for description and analysis. A significant negative TSOS trends was discovered

across small parts of Doukkala irrigated perimeter, Tadla irrigated perimeter, and in parts of the rainfed area. For the pixels with negative trends, over irrigated perimeters, sen's slope gives an average decrease in TSOS of approximately -0.2 day/year, outside the irrigated perimeters; the TSOS shows a decrease between -0.2 and -0.4 day/year. The early start of agricultural season in these zones could explain these results. Especially the irrigated annual crops where we found different crop types and irrigation systems. Hence, this implies that over the studied period of 20 years TSOS has delayed with more than 6 day (-6 day/20 years). Other regions of the OER basin showed a non signficant trend. These regions are not interpreted since the significance level is above 0.1.

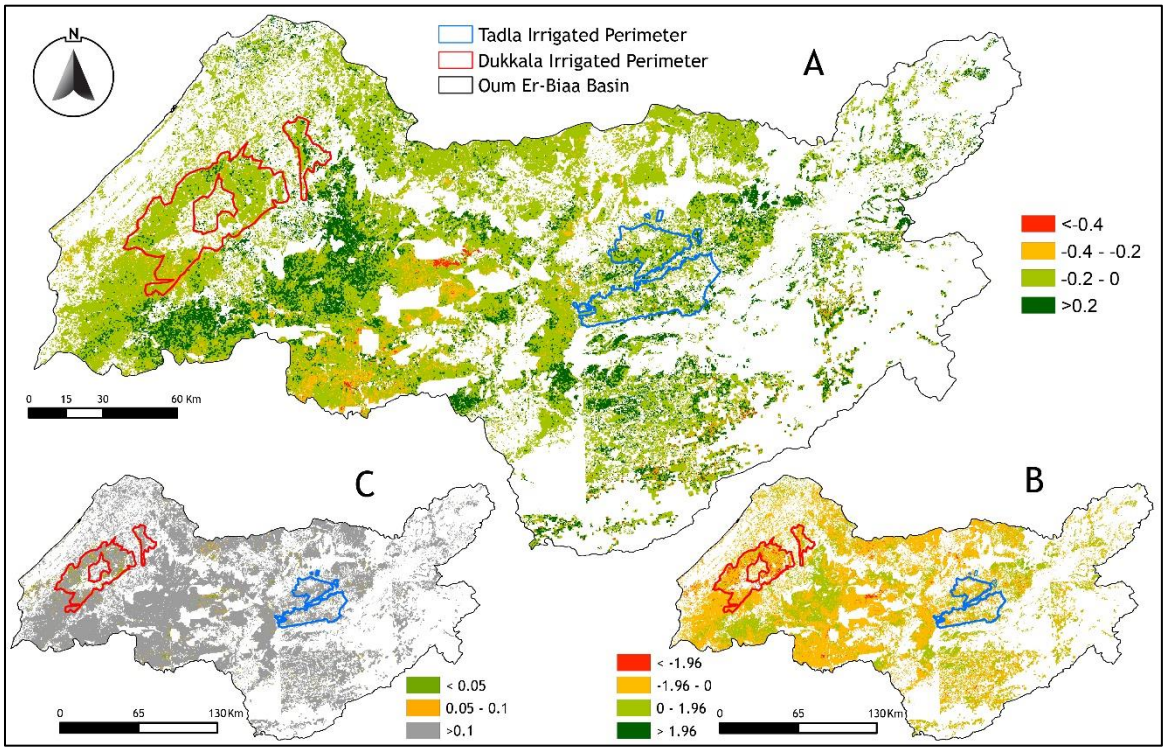

Figure 27: Start of season time (TSOS) trend: Sen's slope values (A); Mann-Kendall Z (B); and p value intervals (C).

On the other hand, we found significant positive trend for the TEOS across large parts of the OER basin and in a part of the Tadla irrigated perimeter. However, we found significant negative trend in the rainfed and fallow farming systems (Figure 28).

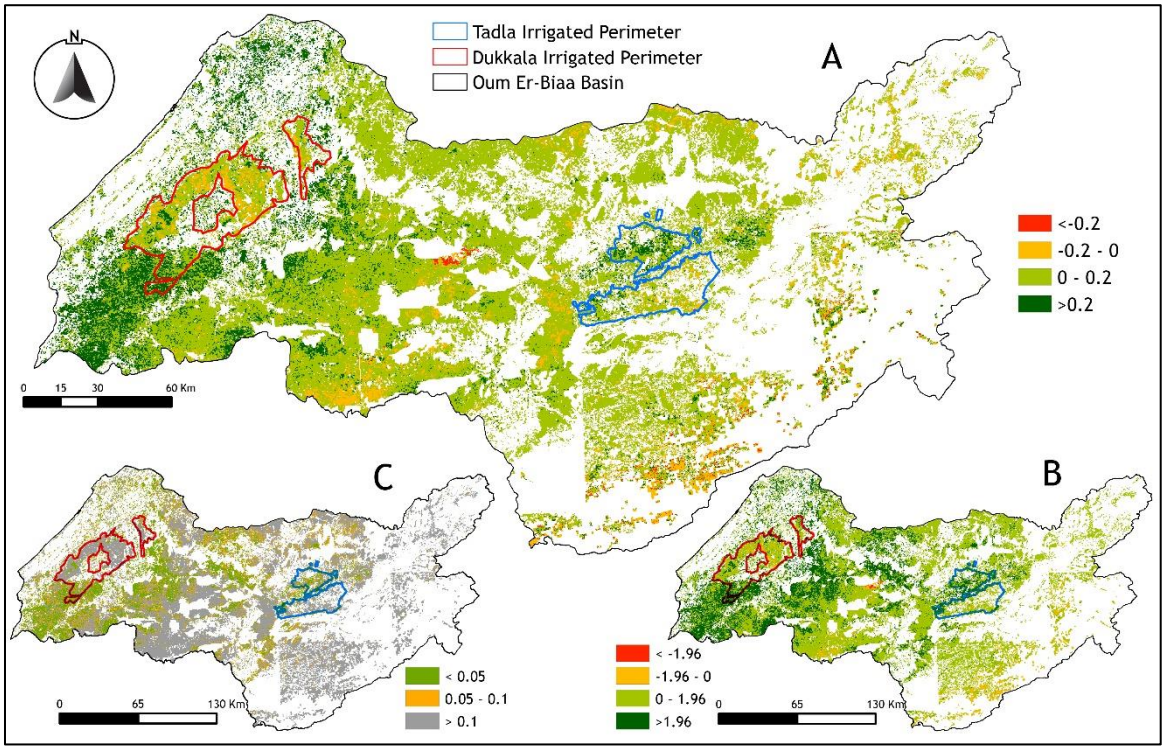

Figure 28: Spatial distribution of end of cropping season time (TEOS) trend. Maps A, B, and C represent sen's slope values, Kendall Z, and p-value intervals, respectively.

For the pixels with positive trends, Sen's slope gives an average increase in TEOS above 0.2 day/year, in the TIP and between 0 and 0.2 in rainfed area. The TEOS shows a decrease between 0 and -0.2 days/year in numerous part of the OER basin, especially in the southern part. These results could be explained by the satisfaction of plants requirements in the irrigated zones, where in other area the negative trend is essentially linked to climatic conditions and the poor land management. This signify that over the studied period of 20 years TEOS has changed with more than 3 days/20 year, in irrigated area and with -3 days/20 years in rainfed and fallow areas.

After the trend analysis of the TEOS metric, we directed our studies towards the analysis of trends in length of season (LOS) (Figure 29) to investigate the link between TEOS and TSOS with the LOS, since the LOS is the result of the difference between TEOS and TSOS. The results show a significant positive trend in LOS over the south parts of Doukkala and in north parts of Tadla irrigated perimeters. In addition, we found significant negative trend in the rainfed and fallow farming systems.

For the pixels with positive trends, Sen's slope gives an average increase in LOS above 0.1 day/year, in the Tadla irrigated perimeter and approximately between 0 and 0.1 days/year in DIP. The LOS shows a decrease between 0 and -0.1 day/year in numerous part of the OER basin. This signify that over the studied period of 20 years LOS has changed with more than 1.6 days/20 year, in irrigated areas and with -1.6 days/20 year in rainfed and fallow areas.

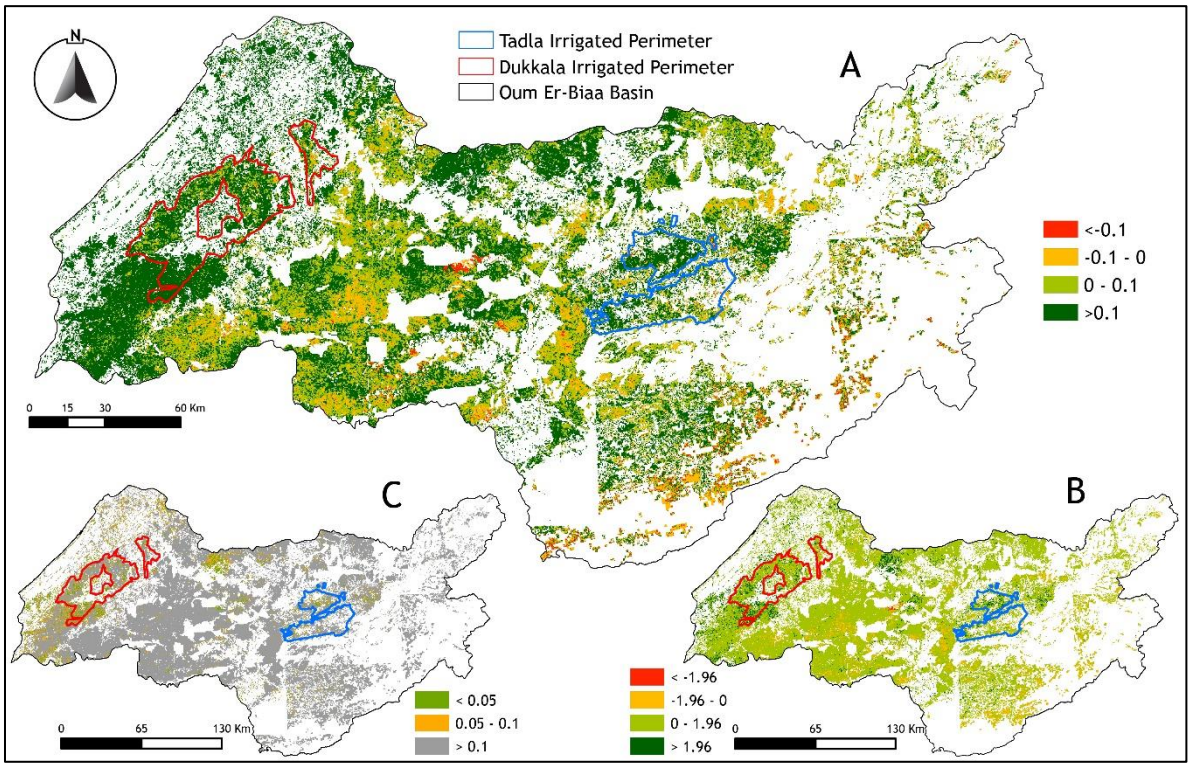

Figure 29: Spatial distribution of length of season (LOS) trend. Maps A, B, and C represent sen's slope values, Kendall Z, and p-value intervals, respectively.

Comparing these results with trends in TSOS and TEOS indicates that increases in TEOS and decrease in TSOS dates are mostly responsible for the positive LOS trends in irrigated perimeters of Doukkala and Tadla. Negative LOS trends in the rainfed area and fallow farming systems is related to a delay in TSOS dates and an early TEOS.

Finally, considering the GINT metric, the trend of this index was obtained using Mann-Kendall and Theil-Sen median trend tests (Figure 30). We found significant positive trends over large farming systems. These areas are specially located in the irrigated perimeters of Tadla and Doukkala, in addition to some zones with improved agricultural management practices.

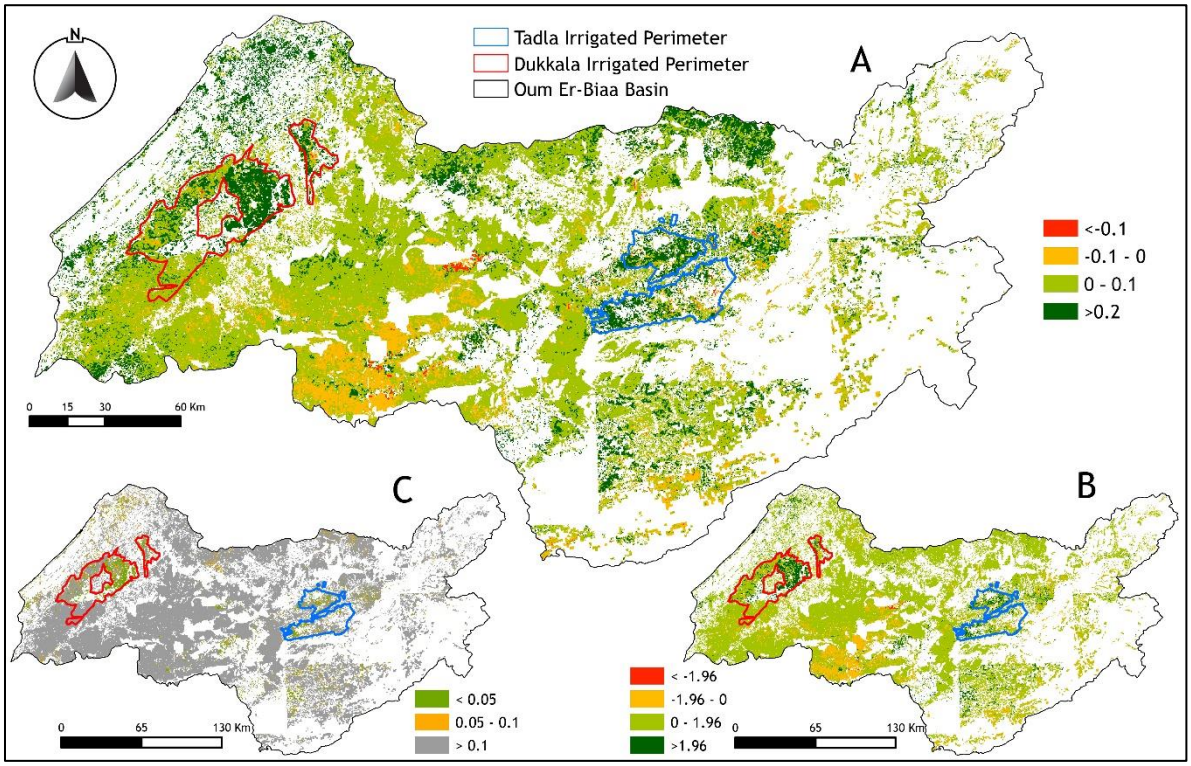

Figure 30 : Spatial Spatial distribution of great integral (GINT) trend. Maps A, B, and C represent sen's slope values, Kendall Z, and p value intervals, respectively.

Generally, significant positive trends are located in the western and eastern part of the OER basin. The central region is dominated by insignificant negative trends, while stable farming systems are dispersed over the study area. Irrigated perimeters show an increase in GINT with 0.2 /year, while the rainfed area shows an increase between 0 and 0.1/year. Generally, the trend results reveal an important variation between the different FS in the studied region.

In this study, we have demonstrated that the phenological pattern of vegetation cover across different farming systems and across different regions over the last 20 years have an important implication in the vegetation dynamics and climate changes. It provides an insight of the vegetation cover status of a region affected by climate risks. In our knowledge, this study is the first to demonstrate the ability of annual Phenological Metrics (PhM) and RF modelling to map and characterize changes over the major farming systems in Morocco. The use of TIMESAT for NDVI time series processing and analysis has provided a more comprehensive investigation of the NDVI behavior from a phenological perspective. As far as we know, this

study is the only one that has explored the phenological farming systems variability over North Africa at 250m spatial resolution.

Overall, The accuracies obtained in this study for the cassification of farming systems were reliable and consistent with those revealed for other MODIS-based land-cover classifications (Alcantara et al. 2012; Qiu et al. 2017). For comparison, the resulted overall accuracies of the RF classifications obtained over the OER basin scale (i.e., 90-96%) is similar to that obtained using MODIS time-series for mapping cropping intensity in China at a regional scale (i.e., 92%; (Qiu et al. 2017)). On the side of classification performance, the confusion between rainfed area and fallow, which was the main source of error, reflects the strong similarity between these two farming systems especially when the climatic conditions are critical. Consequently, our findings have confirmed the advantage of using a combination of PhM from MODIS time-series and RF classifier to discriminate between farming systems (Nitze et al. 2015). ***I***n addition to the influence of climate conditions on phenological changes, changes in crop type was also an important determinant in phenological changes and trends in the OER basin. For this reason in this study, we have used a mask layer to mask only unchanged area and eject the effect of annual land use change over farming systems.

In terms of PhM variability and trends, our study revealed substantial variability over the studied PhM. Generally, TSOS and TEOS shows high and low variability inside and outside the irrigated perimeters, respectively (Figure 26). The TSOS inside irrigated perimeters displayed early onset trends than other zones, which could be resulted due to the sowing date and irrigation (Figure 26). On the other hand, delayed TEOS could be explained by the variability of harvest time and, biological factors, and climatic conditions occurred during the cropping season. These delays and early onsets in time of occurrence between TSOS and TEOS were translated to a longer cropping season over the irrigated perimeters (Figure 27). The remarkable shift expressed by GINT and LOS over the irrigated perimeters is the result of an intensification plan and a change of agricultural practices with the encouragement of farmers to plant perennial crops. The question raised here is how much are sustainable the water and soil resources to support this mode of production under the growing pressure applied?

Our study has also revealed that annual variability outside the irrigated perimeters, especially in the center of the study area, where fallow and rainfed farming systems extend, is

strong. This high variability can be justified by the changes in rainfall amount and distribution received over these regions during the cropping season and the changes on the agricultural production potentiel. As identified by Ouatiki et al. (2019a) climatic stations located in these regions experienced a significant decreasing trend and receive a low rainfall amount during the season. Other factors leading to the high variability of PhM in these regions were the depletion of groundwater and the quality of agricultural management, since these regions considered as rainfed and fallow areas, where the accessibility to irrigation supplies is absent (Lebrini et al. 2020). A similar situation is observed in the variability of GINT metric (Figure 30-A), the same regions experience a high variability and low values of GINT, which signify a low biomass production and an unbalanced field for agricultural planning. Regarding the trend results, GINT increased during the studied period by 0.1/year in the most area of the basin, while for certain regions of FA and RA it decrease by -0.1/year (Figure 30). Therefore, we believe that all this factors affect the productivity of these two farming systems, which are translated in the short cropping season and the low biomass production (Figure 25-A and Figure 25-B, respectively).

The wide spatial distribution of annual variability of PhM found in this study is reliable with the outcomes from previous studies (Luo and Yu 2017; Vrieling et al. 2013; Yuan et al. 2019). For instance, Vrieling et al. (2013) identified that a higher variability of Length of Growing Period (LGP); represented here in our study by the Length of Season metric (LOS) is generally found in arid and semi-arid areas, with coefficients of variation above 0.25 (i.e., LOS in our study varied from 0.15 to 0.35). This slight difference between our both studies could be referenced to the higher spatial resolution of MODIS data (i.e., 250 m). Contrary, in the irrigated perimeters where land receive important amount of water and fertilizer, the variability of PhM remained lower. Further, the variability in crop types may had some influence on the variability of PhM. However, this hypothesis is most unlikely probable as our study focused only on unchanged farming systems of the OER basin.

Weather extremes and consecutive droughts in this region had strongly affected the vegetation cover dynamics and resulted in adaptations of farming system management in response to climatic variation. Socio-economic policies and improving farm practices were also a dominant drivers of farming systems change in addition to climate conditions. These factors

could all have affected the variability of the start, the end and the productivity of the cropping season, resulting in phenological changes over time. A good example of agricultural planning that made great changes in the agricultural sector in Morocco is the Green Morocco Plan strategy, which has aimed to encourage tree-growing extension that led to a high variability over some parts of the perennial farming system.

Notably, our finding showed that the variability of PhM are varied and related to farming system types. The results from this study are expected to constitute a background to other research about droughts monitoring and desertification studies in arid regions. The PhM datasets and the trends results could be integrated with climate data to perform an estimation of crop water requirement and offer a tool for managers and stakeholders to make decisions for the extension of agricultural areas according to the available water resources in a context of water stress.

5.4 Conclusion

Finally, variation in phenological metrics over FS was estimated at the OER basin level during 2000–2019 seasons using MODIS NDVI data and trend analysis tests. Our study finding are the following:

(1) Over irrigated perimeters (TIP and DIP) mean LOS GINT, and TEOS showed a low variability. On the other hand, moderate variability was observed for the mean TSOS during the studied period. Contrary to irrigated zones, PhM over rainfed and fallow farming systems showed a high variability. This variability over RA and FA is justified by the irregularity of rainfall amounts received over these farming systems.

(2) Trends over farming systems are not uniform at the OER basin level. Most areas in the OER basin did not show a significant trend during the past 20 years for TSOS, LOS, and GINT metrics ($p > 0.1$). Contrary to the TEOS where significant trend was observed ($p < 0.1$). TSOS shows early onset over the IPC and IAC (i.e., 0.2 days/year), while over RA and FA is delayed by -0.2 days/year, especially in the center of the basin. Other regions of the FA and RA shows extended TSOS by 0.2 days/year. TEOS shows early onset (i.e., -0.4 days/year) over the FA, RA, and part of the IPC. Other regions of the basin showed a TEOS extended by 0.2

days/year. LOS generally slightly increased over the farming systems except particular zones of the FA and did not advance markedly during the study period. GINT increased during the studied period by 0.1/year in the most area of the basin, while for certain regions of FA and RA it decrease by -0.1/year.

The investigation of changes on PhM over twenty years (19 cropping seasons) proved the ability of these metrics to characterize the spatiotemporal changes over the OER basin. Nevertheless, the need to take into accounts the perceptions and opinions of local populations is essential in order to reduce the process of vegetation cover degradation and better manage natural resources.

Chapter 6: Pheno-climatic classification of Morocco based on phenological and climatic features.

6.1 Introduction

Global changes like increasing food demand, population growth and degradation of arable land are a few challenges agriculture has to face (Nath et al. 2015). While agricultural practices have to be accurate to achieve constant yields, a sustainable use of resources and management schemes are becoming increasingly important to ensure a long-term food security (Spiertz 2009). In this context, studies on large vegetative area extent and systems are important to the sustainable productivity of these zones (Yang et al. 2007). The phenology of vegetation cover and its connection to climate is a key to understand ongoing global climate and land surface changes (Immitzer et al. 2012). Hence, phenology is usually influenced by many biotic and biotic factors such as soil temperature, solar illumination, precipitation and topography (Atzberger et al. 2013; Chapman et al. 2018). Besides, phenology has been studied using observation from multi satellite sensors. In this context, the advent of remote sensing data provides continuous spatial and temporal coverage to map and characterize phenological information at both local and regional scales (Boschetti et al. 2009; Lebrini et al. 2021). Further, Researchers have been able to define and quantify seasonal occurrences of plant phenological profiles using time series acquired from remote sensing image data (Pan et al. 2015). In comparison to older approaches based on single-image processing, several studies have demonstrated that time series of vegetation indices used provide accurate and robust information on vegetation cover (Buitre et al. 2019; Chen et al. 2004; Lebrini et al. 2019b).

Classification or zoning, also known as regionalization, is a sort of geographic

categorization that generalizes and maps terrain patterns in defined classes or zones (Adole et al. 2018; Bac-Bronowicz and Grzempowski 2018). In addition, regionalization produces a set of classes that reduce the complexity of a landscape to more manageable and understood patterns. For example, the world has been subdivided into climatic data in the köppen-Geiger classification (Beck et al. 2018).

Few studies have addressed the issues of pheno-climatic classification. Gu et al. (2010) have used a time series of MODIS NDVI data combined with a digital elevation model to produce a new pheno-class map for the United States. The study generated 40 pheno-classes characterized with similar phenological and topographic information. In the study of White et al. (2005) AVHRR time series of NDVI data between 1982 and 1999 combined with climatology data were used to generate a pheno-region zones where regions with a minimal probability of non-climatic forcing are represented. For this purpose, they have developed a global pheno-region database. Henebry and de Beurs (2013) used MODIS cumulative time series from 2002 to 2006 to derive 15 phenological ecoregions based on clustering the similarities between data. They used a cumulative MODIS time series of 22 images based on 23 composite per year.

Pheno-climatic classification, which characterizes and stratifies regions based on similar phenological and climatic patterns provide a tool for defining agricultural potential and climatic conditions prevails within a defined region. Furthermore, it improve the choice of production and facilitate the design of coherent agricultural development projects with regard to the pheno-climatic potential of the territories. In this chapter, we use the term "pheno-climatic classes" to describe the regions identified by similar phenological and climatic patterns.

The main goal of this chapter is to introduce a new pheno-climatic classification of Morocco that identifies regions with similar phenological and climatic patterns based on land surface phenological metrics (timing and productivity metrics), elevation gradients, slope and climate data. The production of such pheno-climatic classification help as a tool for monitoring sensitive environment and for making accurate decision related to phenology and climate issues.

6.2 Methods

This study focused on the production of a pheno-climatic classification of Morocco using phenological metrics derived from NDVI-MODIS data (MOD13A1), CHIRPS rainfall product, MODIS Land Surface Temperature product (MOD11A2) and digital elevation model (Chapter 2, Table 2). The use of topographic variable data, such as the digital elevation model (DEM) produces major classification enhancements as was proved by previous research (Lu and Weng 2007; Manandhar et al. 2009). Therefore, shuttle radar topography mission (SRTM) one-arc second DEM tiles were resampled to a 500 m spatial resolution by the bilinear interpolation. Digital elevation model and slope used in this chapter are shown within Figure 31.

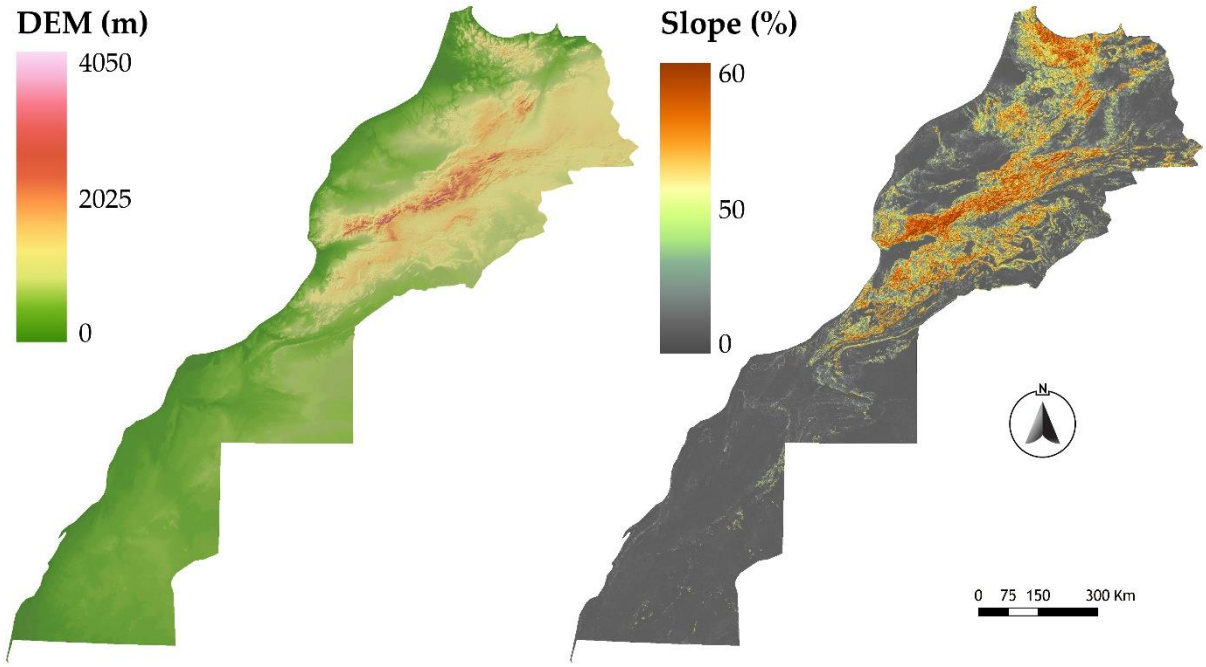

Figure 31: Topographical features used for the pheno-climatic classification of Morocco. a) Digital elevation model; b) Slope.

Concerning phenology data, we focused on timing and productivity phenological metrics to produce the pheno-climatic classification, these metrics are insightful about occurrence and development stages of vegetation cover (Zeng et al. 2020). Hence, median value of amplitude, base value, left derivative, large integral, length of season, middle value of season, right derivative, and small integral were used. Data used cover a study period of 21 years spanning from 2000 to 2021 (Chapter 2, Table 2).

The pheno-climatic classification methodology consisted of three steps. First, satellite data pre-processing and resampling to spatial resolution of 500m. Second, eight phenological metrics were derived from MOD13A1 product. TIMESAT software was used to calculate phenological metrics (See chapter 1). Third, the dataset was normalized and introduced as an input for an unsupervised learning classification based on K-means and random forest algorithms. More details on time series filtering and phenology extraction were provided in Chapter 2.

6.2.1 Data normalization

Because of the large variability of the units and ranges of data (e.g., the data for length of season ranges from 0 to 224 day and the data for the DEM ranges from 0 to 4050 m), data normalization was necessary to allow these datasets to be comparable (i.e., in a similar scale). This also resulted in a more even contribution of each input data layer into the classification process. All input variables were transformed to comparable units using a z-score:

$$z - score = \frac{x - \underline{x}}{\sigma} \qquad (6)$$

where x, $\underline{x}$, and σ represent each data value, dataset mean, and dataset standard deviation, respectively.

6.2.2 Pheno-climatic classes derivation using Random Forest and K-means classification.

The use of supervised classification or regression learning mode for predicting classes or values is frequent. Although, we confronted situations where unsupervised learning mode is needed to cluster raw data (Dehariya et al. 2010). When there is a lack of labelled data or it is difficult to categorize data based on ground truth labels (i.e., training data), classification using unsupervised learning provide a prominent alternative for unsupervised learning processes.

Classification method used for this study consisted on the combination of the unsupervised and supervised machine-learning algorithms K-means and Random Forest (RF), respectively. The RF is a non-parametric machine learning classifier that combines a random selection of training subsets of data with an ensemble of trees (Jin et al. 2018; Lebrini et al.

2020). Details of the random forest algorithm are provided within Chapter 5. However, the unsupervised K-means algorithm is a widely used clustering technique that classifies all pixels based on iterative recalculation of the cluster means (Reza et al. 2019). The K-means algorithm is an algorithm for placing data points in a multi-dimensional space into a defined number of clusters noted K where vector of mean values parameterizes each cluster (Venkata et al. 2020). The goal of K-means is to reduce the variability within the cluster. The summation of squares distances termed as errors, between each pixel and its assigned cluster centre is minimized and declared as objective function (Equation 7).

$$J = \sum_{j=1}^{k} \sum_{i=1}^{n} \left\| x_i^{(j)} - C_j \right\|^2 \quad (7)$$

Where $\left\| x_i^{(j)} - C_j \right\|^2$ is a selected distance measure between data point $x_i^{(j)}$ and cluster centre C_j.

Since the number of classes created by K-means is a user specified input we tested different numbers of K parameters (e.g., 5, 10, and 15) to determine the optimum number of pheno-climatic classes.

6.3 Results and Discussions

6.3.1 Climate data analysis

Generally, the study area is characterized by a Mediterranean climate with hot dry summer and cold wet winter with concentrated precipitation, it includes also arid and semiarid climate in Saharan region. The spatial distribution of rainfall from 2000 to 2020 is shown in Figure 32. Overall, the study area is characterized by a high variability of rainfall from south to north and from east to west. High amounts of rainfall are observed in the north part of Morocco and along of the Atlas Mountains. Over these regions, the rainfall amounts varies between 700 mm and 1100 mm. Rainfall between 300 mm and 600 mm is observed over lowlands areas. In the northwest part of the country the rainfall varies from 200 mm to 300 mm, other parts in the east also have the same values. Rainfall amounts start decreasing from northwest to northeast regions, values between 100 and 200 mm are observed in the eastern part and some presaharian regions. Going south, the rainfall amount observed is less than 100

mm. Over the past twenty years, latitudinal representation of rainfall shows a high seasonal variability with distinct periods (Figure 32). The same remarks are observed for longitudinal representation of rainfall as shown in Figure 32. High amounts of rainfall are observed around latitude 35°N. Hence, a strong contrast characterize the variability of rainfall. Observed rainfall amounts reach their maximum above 35°N and start decreasing to reach minimum values bellow 25°N. On the other hand, high amounts of rainfall are concentrated between longitudes 10°W and 1°W.

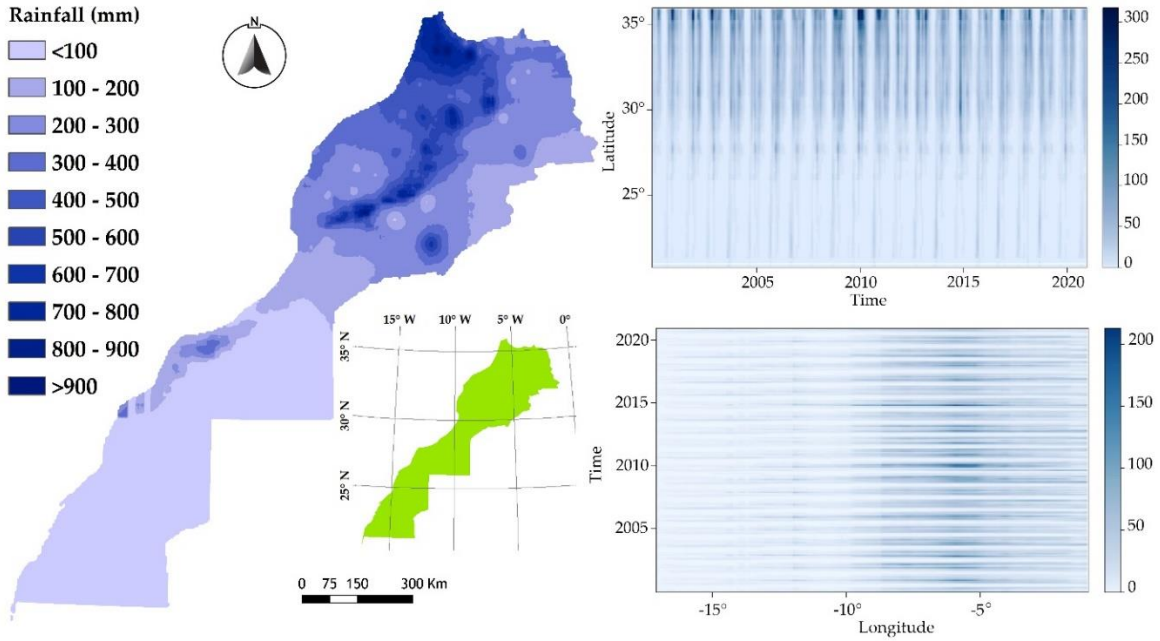

Figure 32: Rainfall distribution and variability over Morocco. a) Total annual median distribution of rainfall; b) latitudinal variability; c) Longitudinal variability.

The median annual LST was found to vary across the country during the study period, as shown in Figure 33. Overall, LST values varies between -3°C and 55°C. Low temperature values are observed in the north part of the country and over mountainous areas. In addition, lowlands situated to the west of the Atlas Mountains shows high degrees of surface temperature. However, high temperature values are extended over the southern and eastern parts of Morocco. Along to the Atlantic coastal area of Morocco from Tangier to Laguira cities, surface temperature is comprised between 23°C and 35°C. However, on the Mediterranean coastal area, temperature values are around 20°C and 26°C.

The incursion of extratropical weather systems from Europe and the Atlantic Ocean, brings colder air and cloudiness, which results in a declining temperature gradient from north

to south that is also influenced by the Atlas Mountains. This variability in temperature is due essentially to Morocco's proximity to the Atlantic Ocean and the vast area of Moroccan Sahara that affect the LST variability over the country (Verner et al. 2018). Consequently, two phenomena occur and influence the seasonality of temperatures, either when sirocco (i.e, Chergui wind) blows from the east creating heatwaves, or when cold damp air blows from the northwest, creating a cold wave or cold spell. However, these phenomena do not last for more than two to five days on average. In addition, vegetation cover has a strong effect on LST variability. Similar results about the effect of heatwaves, vegetation cover, and oceanic oscillation on LST variability was studied and confirmed by Yan et al. (2020). The study carried out by Yan et al. (2020) confirmed that Over North America, the El Nino and La Nina were the main drivers for the periodical highest and lowest LST, respectively. The same study report that the status of vegetation on the surface directly affects the amount of solar radiation received by the surface, and the vegetation also affects the change of LST through climate regulation during the growth process.

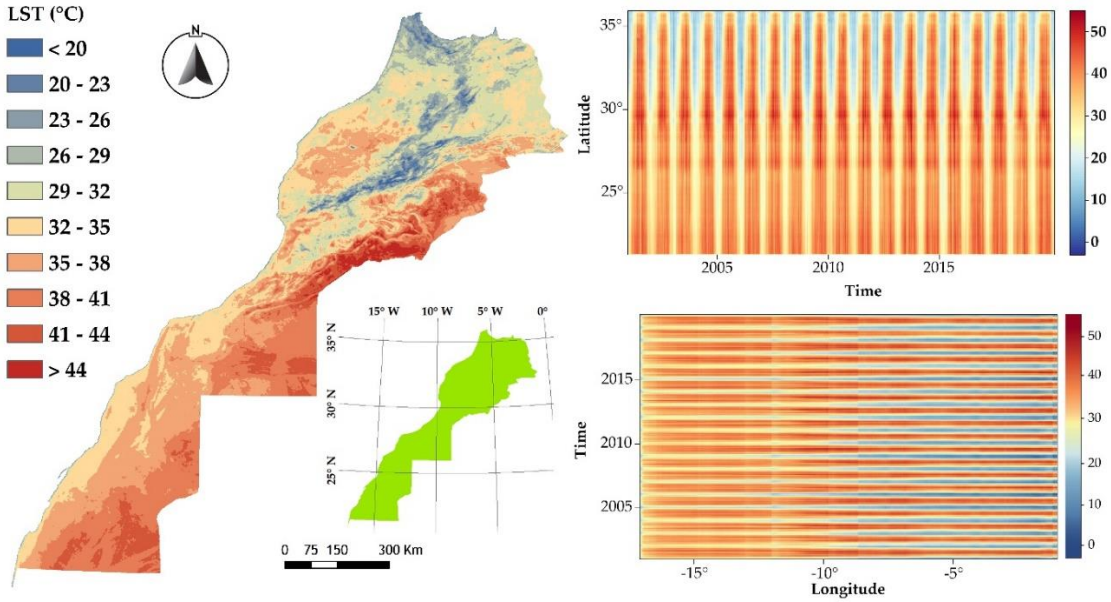

Figure 33: Land surface temperature distribution and variability over Morocco. a) Median 8 day distribution of LST; b) latitudinal variability of LST; c) Longitudinal variability of LST.

6.3.2 Phenological data analysis

In this section, we present 3 phenological metrics from all derived metrics based on NDVI time series. Computed metrics at pixel level are presented in Figure 34. Over Morocco, amplitude of season values are spanning between 0 in Saharan regions and 0.73 in regions

with a pronounced phenological activity. As observed in Figure 34, regions with high values of AOS are generally in area with strong variability of phenological phases during the season. These regions have values of AOS between 0.5 and 0.73. However, area with perennial vegetation are characterized with small values of AOS, these zones have values between 0.3 and 0.5. These areas are generally located in the Atlas Mountains and foothill areas where perennial forest cover is persistent. AOS values below 0.3 characterize zones with low vegetative development during the season. Pixels where no phenological activity occurred are replaced with 0. Concerning large integral metric (GINT), it is considered as a key metric, which characterize the quantity of biomass produced during a cropping season. Figure 34 shows GINT distribution over Morocco for the studied period. GINT values are comprised between 0 and 17. High values of GINT are situated in the north and the northwest of Morocco. However low values are located to the south and the southeast of the country (Figure 34). As result, GINT shows a high spatial variability and a contrasting level of phenological responses over the studied area. These differences are generally related to the agricultural activity since the Utile Agricultural Area (UAA) of the country is situated within this zone (El Mekki and Ghanmat 2015). In addition, forest cover make this contrast perceivable, the presence of forest cover along the Atlas and Rif Mountains makes of this zone a basin of biomass production (Chebli et al. 2018). The pheno-climatic classification of Morocco could not been achieved without implies of timing metrics, Length of Season (LOS) is an essential metric calculated based on Start of Season Time and End of Season Time metrics (SOST and EOST). Figure 34 shows the spatial distribution of LOS metric over Morocco. Long seasons are observed over the Atlas and Rif mountains, these zones have already described as arras with presence of forest canopy. Over these areas, LOS reach a maximum of 224 days. However, lands with agricultural activity presents a LOS values around 100 days. Over agricultural zones LOS highly depend on the irrigation scheme adopted and the rainfall amounts received. Generally, LOS values over rangeland and rainfed area depend on the distribution and the amounts of rainfall, this result was already confirmed by the study of Lebrini et al. (2019b). LOS values decrease where no phenological activity occurred, this is the case of the south of Morocco where LOS values are near 0 (Figure 34).

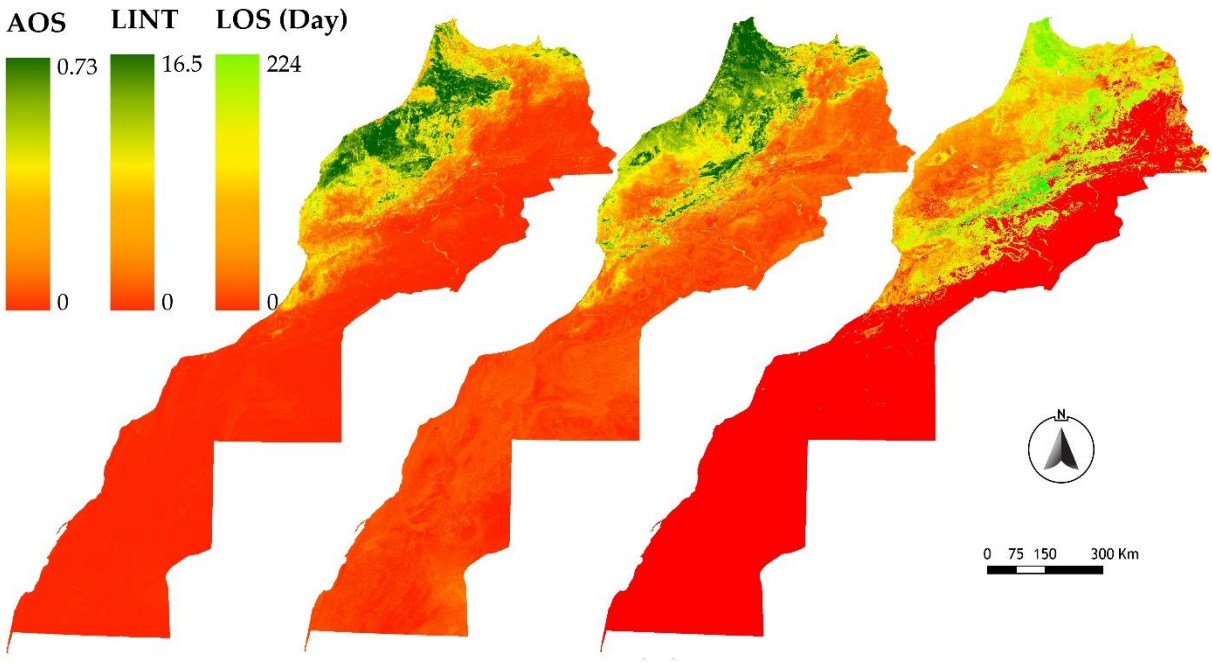

Figure 34: Examples of Phenological metrics; a) Amplitude of season; b) Large integral; c) Length of season.

6.3.3 Pheno-climatic classification of Morocco

In this section, we presents the result of the pheno-climatic classification of Morocco. The pheno-climatic classification consisted on 6 classes, which have similar climatic and phenological behaviour. The resulted pheno-climatic classes were labelled based on computed statistics on climatic and phenological features (Table 11). In addition, Google Earth images were used to visually validate the outputs of the pheno-climatic classification. Table 10 shows statistics on derived pheno-climatic classes. Over Morocco, SSDH (i.e., Sandy Stony land – Dry, Hot) is the largest class with an area of 439651 Km^2, which represents 61.86% of the total area of Morocco. LPMH (i.e., Low Productive, annual/grassland vegetation-Moist, Hot) and HPMW (i.e., High Productive, annual/grassland vegetation-Moist, Warm) classes represents both similar contribution to the total area of Morocco with 9.67% and 8.11%, respectively. PSDH (i.e., Pre-Saharan vegetation - Dry, Hot) class represents 9.67%. However, the DPHuC (i.e., Dense Perennial vegetation – Humid, Cold) and SPHuC (i.e., Sparse Perennial vegetation – Humid, Cold) classes are the smallest classes with a total contribution to the pheno-climatic classification of Morocco with 5.88% and 6.03%, respectively (Table 10).

Table 10: Superficies of pheno-climatic classes

Phenological classes	Significance	Area (km²)	Percentage (%)
PSDH	**P**re-**S**aharan vegetation - **D**ry, **H**ot	68788	9.67
LPMH	**L**ow **P**roductive, annual/grassland vegetation-**M**oist, **H**ot	59803	8.41
SSDH	**S**andy **S**tony land – **D**ry, **H**ot	439651	61.86
HPMW	**H**igh **P**roductive, annual/grassland vegetation-**M**oist, **W**arm	57695	8.11
DPHuC	**D**ense **P**erennial vegetation – **H**umid, **C**old	41831	5.88
SPHuC	**S**parse **P**erennial vegetation – **H**umid, **C**old	42872	6.03

Table 11 shows the mean values of CHIRPS data, land surface temperature and great integral metric over each pheno-climatic class. These data were used as support for the labelling process of the phenoclimatic classes as indicated in above. We have considered rainfall and surface temperature data as indicator for the climate aspect. 3 climate classes were considered which are, dry, moist, and humid for rainfall and hot, warm, and cold for surface temperature. However, concerning phenological aspect, the classes were labelled based on productivity, perennial/annual cover, and nature of the soil (presence/absence of vegetation cover). During this last step, Google earth images were used to support decisions on class labelling (Table 11).

Table 11: Mean values of rainfall, land surface temperature and large integral metric by pheno-climatic classes.

Pheno-climatic Classes	CHIRPS (mm)	LST (°C)	GINT
PSDH	250.80	31.66	2.30
LPMH	284.92	33.64	3.59
SSDH	98.54	38.39	1.46
HPMW	431.52	32.31	6.18
DPHuC	560.44	27.34	7.57
SPHuC	441.83	26.30	3.33

Figure 35, shows the result of the pheno-climatic classification of Morocco. DPHuC class is generally situated in the northern part of the country, it is observed along the Atlas and Rif Mountains. Small portion of this class is also observed in the eastern part, this area is the irrigated perimeter of Triffa in the northeast of Morocco, which is known by their perennial

crops, especially citrus trees (Htitiou et al. 2019a). Besides, SPHuC class has similar climatic patterns to DPHuC except the phenological characteristics. SPHuC shows the presence of sparse perennial vegetation cover and not a perennial one. These differences could be explained by the variability of altitude, slope, and the situation of this area in the east part of the Atlas Mountains where few rainfall event occur. In addition, the nature of the soil composition could be a key factor, which could affect the productivity and the perennial pattern of vegetation cover over this area. HPMW class represents a great portion of the UAA (i.e., Utile Agricultural Area) of Morocco. These zones are knowns by their agricultural activity, especially with the irrigation potential and the favourable soil composition (El Mekki and Ghanmat 2015).

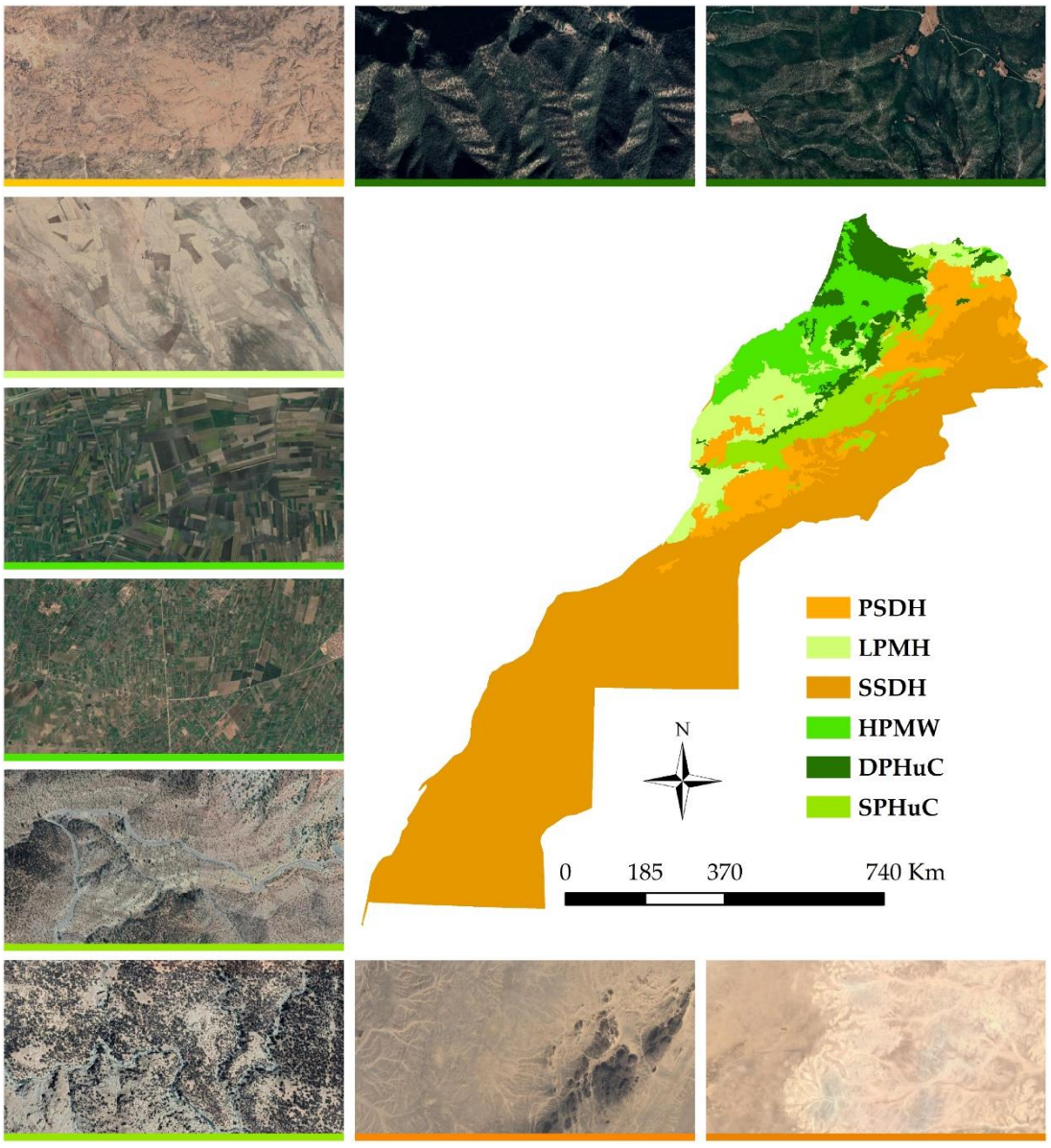

Figure 35: Pheno-climatic classes of Morocco, **PSDH**: Pre-Saharan vegetation - Dry, Hot; **LPMH**: Low Productive, annual/grassland vegetation-Moist, Hot; **SSDH**: Sandy Stony land – Dry, Hot; **HPMW**: High Productive, annual/grassland vegetation-Moist, Warm; **DPHuC**: Dense Perennial vegetation - Humid, Cold; **SPHuC**: Sparse Perennial vegetation – Humid, Cold

Based on climatic and phenology data, LPMH is considered as a low productive area with moist and hot climate. This result was confirmed by truth data images. Google earth data and previous knowledge over the study area, shows that rainfed area and grassland are located within this zone. Generally, vegetation cover in this area depend on the amounts of rainfall received and especially the spatiotemporal fluctuations of rainfall events. Finally, PSDH and SSDH are two classes characterizing Saharan land. Both classes have similar climate conditions. However, on the phenological aspect, SPDH class present a fragmented vegetation cover. This vegetation cover is mostly formed with scattered concentrations of grasses, shrubs, and trees (Figure 35).

6.4 Conclusion

Landscape monitoring is increasingly benefiting from the geo-spatial technologies, which can make a substantial contribution to the monitoring and the management of vegetation cover as providing accurate information at a large spatial scale. For this reason, the use of phenological metrics time series appears more efficient. This study introduces a new pheno-climatic classification of Morocco based on phenology and climate characteristics.

The new pheno-climatic classification map was generated based on thirteen phenological metrics, rainfall and land surface temperature data. The use of satellite phenological metrics and climatic features proved the ability of these features to map and characterize the pheno-climatic classes of Morocco over a large extent and a relatively long period.

The pheno-climatic classification presented within this study may facilitate better decision making around food production, livelihoods, and food security at national scale. The production of such results, in the appropriate time and with accurate way is important for researcher and policy makers. In addition, it can be used to further explore changes in agro-ecological patterns in response to environmental changes and variability.

The new pheno-class map may also provide a value as a national-scale support for other research and applications related to land surface assessment and monitoring, including agricultural and drought monitoring, ecological modelling of the impact of global changes on biodiversity, and biogeochemical modelling. The generated pheno-climatic classification provide a support for research because it provides information about the magnitude, timing, and spatial variability of biological phenomena. However, we believe that the new pheno-climatic classification map described in this study will be useful for multiple purposes.

General conclusion

Plants' life cycles are precisely adjusted to the seasonality of the ecosystems in which they live. Differences in the timing of their phenology will result from natural variations in climate and weather. However, abiotic impacts, could also have effects on the timing of their phenology. Late start of season or advanced end of season provides convincing evidences that there is and impact of climate change on vegetation cover (Baldi et al. 2008; White et al. 2009b). Agriculture sector is increasingly benefiting from the geo-spatial technologies, which can make a substantial contribution to the monitoring and the management of agricultural systems as providing accurate information at a large spatial scale. Data on semi-arid farming systems phenology are scarce and somehow difficult to produce, essentially because of lack of sufficient data. For this reason, the use of phenological metrics time series appears more efficient. The classification of agricultural systems may facilitate better decision making around food production, livelihoods, and food security. Within this thesis research, a reliable remote sensing approach was developed to monitor phenological dynamics at large scale with applications in farming systems management. In addition, phenological metrics were used besides climate data to provide a new pheno-climatic classification of Morocco.

The overall motivation of this research was to develop an approach based on phenology-based data and machine learning algorithms for monitoring farming systems over semi-arid areas, and to assess the spatial patterns of major pheno-climatic classes at national scale. The research objectives were as follows:

1. Assesses the performance of phenological metrics in the discrimination of farming systems using support vector machine classification over Beni Mellal-Khenifra region.
2. Compare the performance of phenological metrics and three machine-learning algorithms (i.e., Support vector Machine, random Forest, and K nearest neighbour) in the characterization of changes over farming systems over OER basin.

3. The use of Random Forest algorithm and phenological metrics to map trends over unchanged farming systems over OER basin.

4. Explore the importance of phenology and climate data to provide a new pheno-climatic classification of Morocco using unsupervised machine learning.

In the third chapter, this thesis examines the use of remote sensing data to characterize and map the spatio-temporal phenological metrics variability through Beni-Mellal-Khenifra region between 2012 and 2016. Phenology-based classification approach showed a high ability to identify and monitor the main agricultural system in the study area. The classification overall accuracy reached 88%, with a kappa coefficient of 0.83. The F1-score values for all classes were greater than 0.76. Analysing the results, the rainfed area shows a dependence to the spatio-temporal fluctuations of rainfall, this result can be extended in further studies on the characterization of drought in agricultural zones. Therefore, the phenological analysis provides information to deep our understanding of the spatio-temporal variability of land surface phenology in arid and semi-arid area. The results demonstrated the ability of phenological parameters to identify and monitor the main agricultural system classes in the study area and to control the illegal pumping zones and the irrigated area.

In the fourth chapter, phenological metrics of AS classes were mapped and studied over the OER-AGS area. Among the three classifiers, the RF classifier produced satisfactory accuracies. Mapping changes over the study area revealed important results, especially on the dynamics and the effect of regional policy on agricultural system changes. The use of satellite phenological metrics to classify AS and map changes over the sixteen years proved the ability of phenological metrics in characterizing the spatiotemporal changes over a large extent and a relatively long period.

In the fifth chapter, variation in phenological metrics over FS was estimated at the OER basin level during 2000–2019 seasons using MODIS NDVI data and trend analysis tests. Our study finding are the following:

(1) Over irrigated perimeters (TIP and DIP) mean LOS GINT, and TEOS showed a low variability. On the other hand, moderate variability was observed for the mean TSOS during the studied period. Contrary to irrigated zones, PhM over rainfed and fallow farming systems

showed a high variability. This variability over RA and FA is justified by the irregularity of rainfall amounts received over these farming systems.

(2) Trends over farming systems are not uniform at the OER basin level. Most areas in the OER basin did not show a significant trend during the past 20 years for TSOS, LOS, and GINT metrics ($p > 0.1$). Contrary to the TEOS where significant trend was observed ($p < 0.1$). TSOS shows early onset over the IPC and IAC (i.e., 0.2 days/year), while over RA and FA is delayed by -0.2 days/year, especially in the center of the basin. Other regions of the FA and RA shows extended TSOS by 0.2 days/year. TEOS shows early onset (i.e., -0.4 days/year) over the FA, RA, and part of the IPC. Other regions of the basin showed a TEOS extended by 0.2 days/year. LOS generally slightly increased over the farming systems except particular zones of the FA and did not advance markedly during the study period. GINT increased during the studied period by 0.1/year in the most area of the basin, while for certain regions of FA and RA it decrease by -0.1/year.

In the last chapter, we presents a new pheno-climatic classification of Morocco. This classification was generated based on thirteen phenological metrics, rainfall and land surface temperature data. The use of satellite phenological metrics and climatic features proved the ability of these features to map and characterize the pheno-climatic classes of Morocco over a large extent and a relatively long period. The pheno-climatic classification presented within this study may facilitate better decision making around food production, livelihoods, and food security at national scale. The production of such results, in the appropriate time and with accurate way is important for researcher and policy makers. In addition, it can be used to further explore changes in agro-ecological patterns in response to environmental changes and variability.

In perspective, while this thesis illustrates a number of substantial research contributions, there remains a large number of potential applications and some specific issues that require further analysis. Asses environmental, agronomic and socio-economic consequences of phenological changes can improve the awareness of stakeholders to adapt it to take decisions to limit the impacts of change on ecosystems and society.

The production of such results, in the appropriate time and with accurate way is important for decision-makers and the management of agricultural practices to help the most

vulnerable farms to continue their agricultural activities in the context of food insecurity and climate change and even crop insurance. Nevertheless, the need to take into accounts the perceptions and opinions of local populations is essential in order to reduce the process of vegetation cover degradation and better manage natural resources.

To conclude, the research objectives pretended in this thesis were successfully realized and a pheno-climatic classification of Morocco has been developed. The extensibility to observe past and present phenological patterns serves as a powerful tool for characterizing dynamics over farming systems, and provides a strategy that can aid management decisions at present and in the future.

References

Adole T, Dash J, Atkinson PM (2018) Characterising the land surface phenology of africa using 500 m modis evi Appl Geogr 90:187-199 doi:10.1016/j.apgeog.2017.12.006

Akhtar F, Awan UK, Tischbein B, Liaqat UW (2017) A phenology based geo-informatics approach to map land use and land cover (2003–2013) by spatial segregation of large heterogenic river basins Appl Geogr 88:48-61 doi:10.1016/j.apgeog.2017.09.003

Alcantara C, Kuemmerle T, Prishchepov AV, Radeloff VC (2012) Mapping abandoned agriculture with multi-temporal modis satellite data Remote Sens Environ 124:334-347 doi:10.1016/j.rse.2012.05.019

Almazroui M, Islam MN, Balkhair KS, Şen Z, Masood A (2017a) Rainwater harvesting possibility under climate change: A basin-scale case study over western province of saudi arabia Atmos Res 189:11-23 doi:https://doi.org/10.1016/j.atmosres.2017.01.004

Almazroui M, Nazrul Islam M, Saeed S, Alkhalaf AK, Dambul R (2017b) Assessment of uncertainties in projected temperature and precipitation over the arabian peninsula using three categories of cmip5 multimodel ensembles Earth Systems and Environment 1:23 doi:10.1007/s41748-017-0027-5

Archibald S, Scholes RJ (2007) Leaf green-up in a semi-arid african savanna-separating tree and grass responses to environmental cues J Veg Sci 18:583-594

Arvor D, Jonathan M, Meirelles M, Dubreuil V, Durieux L (2011) Classification of modis evi time series for crop mapping in the state of mato grosso, brazil Int J Remote Sens 32:7847-7871 doi:10.1080/01431161.2010.531783

Atkinson PM, Jeganathan C, Dash J, Atzberger C (2012) Inter-comparison of four models for smoothing satellite sensor time-series data to estimate vegetation phenology Remote Sens Environ 123:400-417 doi:10.1016/j.rse.2012.04.001

Atzberger C, Klisch A, Mattiuzzi M, Vuolo F (2013) Phenological metrics derived over the european continent from ndvi3g data and modis time series Remote Sens 6:257-284 doi:10.3390/rs6010257

Bac-Bronowicz J, Grzempowski PJEES (2018) Regionalization of geographical space according to selected topographic factors in reference to spatial distribution of precipitation: Application of artificial neural networks in gis 77:1-17

Bachoo A, Archibald S Influence of using date-specific values when extracting phenological metrics from 8-day composite ndvi data. In: 2007 International Workshop on the Analysis of Multi-temporal Remote Sensing Images, 18-20 July 2007 2007. pp 1-4. doi:10.1109/MULTITEMP.2007.4293044

Badeck FW, Bondeau A, Böttcher K, Doktor D, Lucht W, Schaber J, Sitch SJNp (2004) Responses of spring phenology to climate change 162:295-309

Bai Y, Yang Y, Jiang H (2019) Intercomparison of avhrr gimms3g, terra modis, and spot-vgt ndvi products over the mongolian plateau Remote Sens 11 doi:10.3390/rs11172030

Bai ZG, Dent DL, Olsson L, Schaepman ME (2008) Proxy global assessment of land degradation Soil Use and Management 24:223-234 doi:10.1111/j.1475-2743.2008.00169.x

Baldi G, Nosetto MD, Aragon R, Aversa F, Paruelo JM, Jobbagy EG (2008) Long-term satellite ndvi data sets: Evaluating their ability to detect ecosystem functional changes in south america Sensors (Basel) 8:5397-5425 doi:10.3390/s8095397

Barakat A, Ouargaf Z, Khellouk R, El Jazouli A, Touhami F (2019) Land use/land cover change and environmental impact assessment in béni-mellal district (morocco) using remote sensing and gis Earth Systems and Environment 3:113-125 doi:10.1007/s41748-019-00088-y

Barbosa HA, Lakshmi Kumar TV, Paredes F, Elliott S, Ayuga JG (2019) Assessment of caatinga response to drought using meteosat-seviri normalized difference vegetation index (2008–2016)

ISPRS J Photogramm Remote Sens 148:235-252 doi:https://doi.org/10.1016/j.isprsjprs.2018.12.014

Beck HE, Zimmermann NE, McVicar TR, Vergopolan N, Berg A, Wood EF (2018) Present and future köppen-geiger climate classification maps at 1-km resolution Scientific Data 5:180214 doi:10.1038/sdata.2018.214

Belgiu M, Drăguţ L (2016) Random forest in remote sensing: A review of applications and future directions ISPRS J Photogramm Remote Sens 114:24-31 doi:10.1016/j.isprsjprs.2016.01.011

Benabdelouahab T, Balaghi R, Hadria R, Lionboui H, Djaby B, Tychon B (2016) Testing aquacrop to simulate durum wheat yield and schedule irrigation in a semi-arid irrigated perimeter in morocco Irrigation and Drainage 65:631-643 doi:doi:10.1002/ird.1977

Benabdelouahab T, Balaghi R, Hadria R, Lionboui H, Minet J, Tychon B (2015) Monitoring surface water content using visible and short-wave infrared spot-5 data of wheat plots in irrigated semi-arid regions International Journal of Remote Sensing 36:4018-4036 doi:10.1080/01431161.2015.1072650

Benabdelouahab T et al. (2019a) Using sar data to detect wheat irrigation supply in an irrigated semi-arid area vol 11. doi:10.5539/jas.v11n1p21

Benabdelouahab T et al. (2018) Using sar data to detect wheat irrigation supply in an irrigated semi-arid area J Agric Sci 11:1916-9760 doi:10.5539/jas.v11n1pxx

Benabdelouahab T, Gadouali F, Boudhar A, Lebrini Y, Hadria R, Salhi A (2020) Analysis and trends of rainfall amounts and extreme events in the western mediterranean region Theor Appl Climatol doi:10.1007/s00704-020-03205-4

Benabdelouahab T, Lebrini Y, Boudhar A, Hadria R, Htitiou A, Lionboui H (2019b) Monitoring spatial variability and trends of wheat grain yield over the main cereal regions in morocco: A remote-based tool for planning and adjusting policies Geocarto Int:1-20 doi:10.1080/10106049.2019.1695960

Biggs TW, Thenkabail PS, Gumma MK, Scott CA, Parthasaradhi GR, Turral HN (2006) Irrigated area mapping in heterogeneous landscapes with modis time series, ground truth and census data, krishna basin, india Int J Remote Sens 27:4245-4266 doi:10.1080/01431160600851801

Boschetti M, Stroppiana D, Brivio PA, Bocchi S (2009) Multi-year monitoring of rice crop phenology through time series analysis of modis images Int J Remote Sens 30:4643-4662 doi:10.1080/01431160802632249

Boudhar A et al. (2020) Hydrological response to snow cover changes using remote sensing over the oum er rbia upstream basin, morocco. In: Rebai N, Mastere M (eds). Springer International Publishing, pp 95-102. doi:10.1007/978-3-030-21166-0_9

Breiman L (2001) Random forests Machine Learning 45:5-32 doi:10.1023/A:1010933404324

Buitre MJC, Zhang H, Lin H (2019) The mangrove forests change and impacts from tropical cyclones in the philippines using time series satellite imagery 11:688

Campbell JB, Wynne RH (2011) Introduction to remote sensing. Guilford Press,

Carrão H, Gonçalves P, Caetano M (2008) Contribution of multispectral and multitemporal information from modis images to land cover classification Remote Sens Environ 112:986-997 doi:10.1016/j.rse.2007.07.002

Castro CL, Beltrán-Przekurat AB, Pielke RA (2009) Spatiotemporal variability of precipitation, modeled soil moisture, and vegetation greenness in north america within the recent observational record J Hydrometeorol 10:1355-1378 doi:10.1175/2009jhm1123.1

Chandola V, Hui D, Gu L, Bhaduri B, Vatsavai RR Using time series segmentation for deriving vegetation phenology indices from modis ndvi data. In: IEEE International Conference on Data Mining, 2010. pp 202-208. doi:10.1109/icdmw.2010.143

Chapman CA, Valenta K, Bonnell TR, Brown KA, Chapman LJJB (2018) Solar radiation and enso predict fruiting phenology patterns in a 15-year record from kibale national park, uganda 50:384-395

Chebli Y, Chentouf M, Ozer P, Hornick J-L, Cabaraux J-FJAG (2018) Forest and silvopastoral cover changes and its drivers in northern morocco 101:23-35

Chen J, Jönsson P, Tamura M, Gu Z, Matsushita B, Eklundh L (2004) A simple method for reconstructing a high-quality ndvi time-series data set based on the savitzky–golay filter Remote Sens Environ 91:332-344 doi:10.1016/j.rse.2004.03.014

Chen JL, Wilson CR, Seo KW (2006) Optimized smoothing of gravity recovery and climate experiment (grace) time-variable gravity observations J Geophys Res Solid Earth 111:n/a-n/a doi:10.1029/2005JB004064

CHIRPS (2020). https://www.chc.ucsb.edu/data/chirps accessed on 13/05/2020. Accessed 13/05/2020

Clauss K, Yan H, Kuenzer C (2016) Mapping paddy rice in china in 2002, 2005, 2010 and 2014 with modis time series Remote Sens 8:434

Cleland EE, Chuine I, Menzel A, Mooney HA, Schwartz MD (2007) Shifting plant phenology in response to global change Trends Ecol Evol 22:357-365 doi:https://doi.org/10.1016/j.tree.2007.04.003

Coppin P JI, Nackaerts K, Muys B, Lambin E (2004) Digital change detection methods in ecosystem monitoring: A review Int J Remote Sens:1565-1596

CRI (2015) Centre régional d'investissement-béni mellal khénifra, monographie de la région de béni mellal-khénifra, octobre 2015.

Cui T, Martz L, Guo X (2017) Grassland phenology response to drought in the canadian prairies Remote Sens 9:1258 doi:10.3390/rs9121258

Cui T, Martz L, Lamb EG, Zhao L, Guo X (2019) Comparison of grassland phenology derived from modis satellite and phenocam near-surface remote sensing in north america Can J Remote Sens 45:707-722 doi:10.1080/07038992.2019.1674643

Davenport ML, Nicholson SE (1993) On the relation between rainfall and the normalized difference vegetation index for diverse vegetation types in east africa Int J Remote Sens 14:2369-2389 doi:10.1080/01431169308954042

de Moura YM et al. (2017) Spectral analysis of amazon canopy phenology during the dry season using a tower hyperspectral camera and modis observations 131:52-64

Defila C, Clot BJIjob (2001) Phytophenological trends in switzerland 45:203-207

DeFries RS, Field CB, Fung I, Collatz GJ, Bounoua L (1999) Combining satellite data and biogeochemical models to estimate global effects of human-induced land cover change on carbon emissions and primary productivity Glob Biogeochem Cycles 13:803-815 doi:doi:10.1029/1999GB900037

Dehariya VK, Shrivastava SK, Jain RC Clustering of image data set using k-means and fuzzy k-means algorithms. In: 2010 International Conference on Computational Intelligence and Communication Networks, 26-28 Nov. 2010 2010. pp 386-391. doi:10.1109/CICN.2010.80

del Barrio G et al. (2016) Land degradation states and trends in the northwestern maghreb drylands, 1998–2008 Remote Sens 8:603 doi:10.3390/rs8070603

Didan K (2015) Mod13q1 modis/terra vegetation indices 16-day l3 global 250m sin grid v006. Nasa eosdis land processes daac. doi:10.5067/MODIS/MOD13Q1.006.

Diouf AA, Djaby B, Diop MB, Wele A, Ndione JA, Tychon B Fonction d'ajustement pour l'estimation de la production fourragère herbacée des parcours naturels du sénégal à partir du ndvi s10 de spot-vegetation. In: XXVIIe Colloque de l'Association Internationale de Climatologie, Dijon, France, 2014.

Diouf AA, Faye G, Minet J, Djaby B, Ndione JA, Tychon B Zonage phénoclimatique et caractérisation des parcours naturels du sénégal avec les données de télédétection satellitaire. In: XXVIIIe Colloque de l'Association Internationale de Climatologie, Liège, Bélgique, 2015.

Dixon RK, Solomon AM, Brown S, Houghton RA, Trexier MC, Wisniewski J (1994) Carbon pools and flux of global forest ecosystems. Science 263(5144):185−190

Duro DC, Franklin SE, Dubé MG (2012) A comparison of pixel-based and object-based image analysis with selected machine learning algorithms for the classification of agricultural landscapes using spot-5 hrg imagery Remote Sens Environ 118:259-272 doi:10.1016/j.rse.2011.11.020

Eklundh L, Jönsson P (2015) Timesat 3.2 software manual. Lund and Malmö University, Sweden.,

El Mekki AA, Ghanmat E (2015) The challenges of sustainable agricultural development in southern and eastern mediterranean countries: The case of morocco. In: Sustainable agricultural development. Springer, pp 65-82

Estrella N, Sparks TH, Menzel AJGCB (2007) Trends and temperature response in the phenology of crops in germany 13:1737-1747

Evrendilek F, Gulbeyaz O (2011) Boosted decision tree classifications of land cover over turkey integrating modis, climate and topographic data Int J Remote Sens 32:3461-3483 doi:10.1080/01431161003749469

Farr TG et al. (2007) The shuttle radar topography mission Rev Geophys 45:n/a-n/a doi:10.1029/2005RG000183

Friedl MA, Sulla-Menashe D, Tan B, Schneider A, Ramankutty N, Sibley A, Huang X (2010) Modis collection 5 global land cover: Algorithm refinements and characterization of new datasets Remote Sens Environ 114:168-182 doi:10.1016/j.rse.2009.08.016

Fu Y, He H, Zhao J, Larsen D, Zhang H, Sunde M, Duan S (2018) Climate and spring phenology effects on autumn phenology in the greater khingan mountains, northeastern china Remote Sens 10:449 doi:10.3390/rs10030449

Gadouali F, Semane N, Muñoz ÁG, Messouli M (2020) On the link between the madden-julian oscillation, euro-mediterranean weather regimes, and morocco winter rainfall Journal of Geophysical Research: Atmospheres 125 doi:10.1029/2020jd032387

Gao F et al. (2008) An algorithm to produce temporally and spatially continuous modis-lai time series IEEE Geosci Remote Sens Lett 5:60-64 doi:10.1109/LGRS.2007.907971

Geng L, Ma M, Wang X, Yu W, Jia S, Wang H (2014) Comparison of eight techniques for reconstructing multi-satellite sensor time-series ndvi data sets in the heihe river basin, china Remote Sens 6:2024

Gill JA, Alves JA, Gunnarsson TGJPTotRSB (2019) Mechanisms driving phenological and range change in migratory species 374:20180047

Gu Y, Brown JF, Miura T, Van Leeuwen WJD, Reed BC (2010) Phenological classification of the united states: A geographic framework for extending multi-sensor time-series data 2:526-544

Gu Y, Brown JF, Verdin JP, Wardlow B (2007) A five-year analysis of modis ndvi and ndwi for grassland drought assessment over the central great plains of the united states Geophys Res Lett 34 doi:10.1029/2006GL029127

Hadria R et al. (2019) Derivation of air temperature of agricultural areas of morocco from remotely land surface temperature based on the updated köppen-geiger climate classification Modeling Earth Systems and Environment doi:10.1007/s40808-019-00645-4

Hadria R, Benabdelouahab T, Mahyou H, Balaghi R, Bydekerke L, El Hairech T, Ceccato P (2018) Relationships between the three components of air temperature and remotely sensed land surface temperature of agricultural areas in morocco Int J Remote Sens 39:356-373 doi:10.1080/01431161.2017.1385108

Hadria R et al. (2006) Monitoring of irrigated wheat in a semi-arid climate using crop modelling and remote sensing data: Impact of satellite revisit time frequency Int J Remote Sens 27:1093-1117 doi:10.1080/01431160500382980

Hadria R, Khabba S, Lahrouni A, Duchemin B, Chehbouni A, Carriou J, Ouzine L (2007) Calibration and validation of the stics crop model for managing wheat irrigation in the semi-arid marrakech/al haouz plain Arabian Journal for Science and Engineering 32:87-101

Hanamean Jr. JR, Pielke Sr. RA, Castro CL, Ojima DS, Reed BC, Gao Z (2003) Vegetation greenness impacts on maximum and minimum temperatures in northeast colorado Meteorol Appl 10:203-215 doi:https://doi.org/10.1017/S1350482703003013

Hao P, Zhan Y, Wang L, Niu Z, Shakir M (2015) Feature selection of time series modis data for early crop classification using random forest: A case study in kansas, USA Remote Sens 7:5347-5369 doi:10.3390/rs70505347

Henebry GM, de Beurs KM (2013) Remote sensing of land surface phenology: A prospectus. In: Schwartz MD (ed) Phenology: An integrative environmental science. Springer Netherlands, Dordrecht, pp 385-411. doi:10.1007/978-94-007-6925-0_21

Hentze K, Thonfeld F, Menz G (2016) Evaluating crop area mapping from modis time-series as an assessment tool for zimbabwe's "fast track land reform programme" PLoS One 11:e0156630 doi:10.1371/journal.pone.0156630

Hopkins AD (1918) Periodical events and natural law as guides to agricultural research and practice. vol 9. US Government Printing Office,

Hopp RJ (1974) Plant phenology observation networks. In: Phenology and seasonality modeling. Springer, pp 25-43

Hsu C-W, Chang C-C, Lin C-J (2003) A practical guide to support vector classification. Department of Computer Science and Information Engineering, University of National Taiwan, Taipei.,

Htitiou A, Boudhar A, Lebrini Y (2019a) The performance of random forest classification based on phenological metrics derived from sentinel-2 and landsat 8 to map crop cover in an irrigated semi-arid region Remote Sensing in Earth Systems Sciences 2:208–224 doi:10.1007/s41976-019-00023-9

Htitiou A, Boudhar A, Lebrini Y, Hadria R, Lionboui H, Benabdelouahab T (2020a) A comparative analysis of different phenological information retrieved from sentinel-2 time series images to improve crop classification: A machine learning approach Geocarto Int:1-24 doi:10.1080/10106049.2020.1768593

Htitiou A, Boudhar A, Lebrini Y, Hadria R, Lionboui H, Benabdelouahab T (2020b) A comparative analysis of different phenological information retrieved from sentinel-2 time series images to improve crop classification: A machine learning approach Geocarto International:1-24 doi:10.1080/10106049.2020.1768593

Htitiou A et al. (2019b) The performance of random forest classification based on phenological metrics derived from sentinel-2 and landsat 8 to map crop cover in an irrigated semi-arid region Remote Sensing in Earth Systems Sciences doi:10.1007/s41976-019-00023-9

Huang C, Davis LS, Townshend JRG (2010) An assessment of support vector machines for land cover classification Int J Remote Sens 23:725-749 doi:10.1080/01431160110040323

Immitzer M, Atzberger C, Koukal T (2012) Tree species classification with random forest using very high spatial resolution 8-band worldview-2 satellite data Remote Sens 4:2661-2693 doi:10.3390/rs4092661

James G, Witten D, Hastie T, Tibshirani R (2014) An introduction to statistical learning: With applications in r. New York : Springer Publishing Company,

Jed Wing MKC et al. (2018) Caret: Classification and regression training.

Ji L, Peters AJ (2007) Performance evaluation of spectral vegetation indices using a statistical sensitivity function Remote Sens Environ 106:59-65 doi:https://doi.org/10.1016/j.rse.2006.07.010

Jin Y, Liu X, Chen Y, Liang XJIjors (2018) Land-cover mapping using random forest classification and incorporating ndvi time-series and texture: A case study of central shandong 39:8703-8723

Jin Y, Sung S, Lee D, Biging G, Jeong S (2016) Mapping deforestation in north korea using phenology-based multi-index and random forest Remote Sens 8:997 doi:10.3390/rs8120997

Jönsson P, Cai Z, Melaas E, Friedl M, Eklundh L (2018) A method for robust estimation of vegetation seasonality from landsat and sentinel-2 time series data Remote Sens 10:635 doi:10.3390/rs10040635

Jönsson P, Eklundh L (2002) Seasonality extraction by function fitting to time-series of satellite sensor data IEEE Trans Geosci Remote Sens 40

Jönsson P, Eklundh L (2004) Timesat a program for analyzing time-series of satellite sensor data Computers & Geosciences 30:833-845 doi:10.1016/j.cageo.2004.05.006

Jung M, Henkel K, Herold M, Churkina G (2006) Exploiting synergies of global land cover products for carbon cycle modeling Remote Sens Environ 101:534-553 doi:10.1016/j.rse.2006.01.020

Kaptué A, Roujean J-L, De Jong SM (2011) Comparison and relative quality assessment of the glc2000, globcover, modis and ecoclimap land cover data sets at the african continental scale Int J Appl Earth Obs Geoinf 13:207-219 doi:https://doi.org/10.1016/j.jag.2010.11.005

Kariyeva J, van Leeuwen WJD (2012) Phenological dynamics of irrigated and natural drylands in central asia before and after the ussr collapse Agric Ecosyst Environ 162:77-89 doi:10.1016/j.agee.2012.08.006

Kendall MG (1975) Rank correlation methods London: Charles Griffin 35
Kuhn M (2008) Building predictive models in r using the caret package 2008 28:26 %J Journal of Statistical Software doi:10.18637/jss.v028.i05
Lambin EF, Turner BL, Helmut JG, al. (2001) The causes of land-use and land-cover change: Moving beyond the myths Glob Environ Chang 11:261–269
Laskin DN, McDermid GJ, Nielsen SE, Marshall SJ, Roberts DR, Montaghi AJNCC (2019) Advances in phenology are conserved across scale in present and future climates 9:419-425
Laskin DN, McDermid GJJEI (2016) Evaluating the level of agreement between human and time-lapse camera observations of understory plant phenology at multiple scales 33:1-9
Lebrini Y, Benabdelouahab T, Boudhar A, Htitiou A, Hadria R, Lionboui H Farming systems monitoring using machine learning and trend analysis methods based on fitted ndvi time series data in a semi-arid region of morocco. In: SPIE Remote Sensing, Strasbourg, France., 2019a. SPIE. doi:10.1117/12.2532928
Lebrini Y et al. (2019b) Identifying agricultural systems using svm classification approach based on phenological metrics in a semi-arid region of morocco Earth Systems and Environment doi:10.1007/s41748-019-00106-z
Lebrini Y, Boudhar A, Htitiou A, Hadria R, Lionboui H, Bounoua L, Benabdelouahab T (2020) Remote monitoring of agricultural systems using ndvi time series and machine learning methods: A tool for an adaptive agricultural policy Arab J Geosci 13:796 doi:10.1007/s12517-020-05789-7
Lebrini Y et al. (2021) Mapping and characterization of phenological changes over various farming systems in an arid and semi-arid region using multitemporal moderate spatial resolution data Remote Sens 13 doi:10.3390/rs13040578
Lessel J, Ceccato P (2016) Creating a basic customizable framework for crop detection using landsat imagery Int J Remote Sens 37:6097-6107 doi:10.1080/2150704X.2016.1252471
Li L, Friedl M, Xin Q, Gray J, Pan Y, Frolking S (2014) Mapping crop cycles in china using modis-evi time series Remote Sens 6:2473-2493 doi:10.3390/rs6032473
Liang L (2019) Phenology. In: Reference module in earth systems and environmental sciences. Elsevier. doi:https://doi.org/10.1016/B978-0-12-409548-9.11739-7
Lieth H (1974) Phenology and seasonality modeling vol 8. Springer-Verlag, New York,
Lionboui H, Benabdelouahab T, Elame F, Hasib A, Boulli A (2016a) Multi-year agro-economic modelling for predicting changes in irrigation water management indicators in the tadla sub-basin International Journal of Agricultural Management 5:96-105 doi:10.5836/ijam/2016-05-96
Lionboui H, Benabdelouahab T, Hasib A, Boulli A (2016b) Analysis of farms performance using different sources of irrigation water: A case study in a semi-arid area International Journal of Agriculture Management and Development 6:145-154
Lionboui H, Benabdelouahab T, Hasib A, Fouad E, Abdelali B (2018) Dynamic agro-economic modeling for sustainable water resources management in arid and semi-arid areas. In: Handbook of environmental materials management. doi:10.1007/978-3-319-58538-3_114-1
Lionboui H, Benabdelouahab T, Htitiou A, Lebrini Y, Boudhar A, Hadria R, Elame F (2020) Spatial assessment of losses in wheat production value: A need for an innovative approach to guide risk management policies Remote Sens Appl Soc Environ 18 doi:10.1016/j.rsase.2020.100300
Lionboui H, Fadlaoui A, Elame F, Benabdelouahab T (2014) Water pricing impact on the economic valuation of water resources International Journal of Education and Research 2:147
Liu J, Shangguan D, Liu S, Ding Y, Wang S, Wang XJAR (2019) Evaluation and comparison of chirps and mswep daily-precipitation products in the qinghai-tibet plateau during the period of 1981–2015 230:104634
Lotsch A, Friedl MA, Anderson BT, Tucker CJ (2003) Coupled vegetation-precipitation variability observed from satellite and climate records 30 doi:10.1029/2003gl017506
Löw F, Michel U, Dech S, Conrad C (2013) Impact of feature selection on the accuracy and spatial uncertainty of per-field crop classification using support vector machines ISPRS J Photogramm Remote Sens 85:102-119 doi:10.1016/j.isprsjprs.2013.08.007
Lu D, Mausel P, Brondizio E, Moran E (2004) Change detection techniques Int J Remote Sens 25:2365-2401

Lu D, Weng QJIjoRs (2007) A survey of image classification methods and techniques for improving classification performance 28:823-870

Luo Z, Yu S (2017) Spatiotemporal variability of land surface phenology in china from 2001–2014 Remote Sens 9:65

Manandhar R, Odeh IO, Ancev TJRS (2009) Improving the accuracy of land use and land cover classification of landsat data using post-classification enhancement 1:330-344

Marchane A et al. (2015) Assessment of daily modis snow cover products to monitor snow cover dynamics over the moroccan atlas mountain range Remote Sens Environ 160:72-86 doi:https://doi.org/10.1016/j.rse.2015.01.002

Matsushita B, Yang W, Chen J, Onda Y, Qiu G (2007) Sensitivity of the enhanced vegetation index (evi) and normalized difference vegetation index (ndvi) to topographic effects: A case study in high-density cypress forest Sensors (Basel, Switzerland) 7:2636-2651

McGill R, Tukey JW, Larsen WA (1978) Variations of box plots The American Statistician 32:12-16 doi:10.1080/00031305.1978.10479236

McVicar TR, Jupp DLB (1998) The current and potential operational uses of remote sensing to aid decisions on drought exceptional circumstances in australia: A review Agric Syst 57:399-468 doi:https://doi.org/10.1016/S0308-521X(98)00026-2

Menzel A, Sparks TH, Estrella N, Roy DJGE, Biogeography (2006) Altered geographic and temporal variability in phenology in response to climate change 15:498-504

Meyer H, Reudenbach C, Hengl T, Katurji M, Nauss T (2018) Improving performance of spatio-temporal machine learning models using forward feature selection and target-oriented validation Environmental Modelling & Software 101:1-9 doi:10.1016/j.envsoft.2017.12.001

Mottaleb KA, Gumma MK, Mishra AK, Mohanty S (2015) Quantifying production losses due to drought and submergence of rainfed rice at the household level using remotely sensed modis data Agric Syst 137:227-235 doi:https://doi.org/10.1016/j.agsy.2014.08.014

Moulin S, Kergoat L, Viovy N, Dedieu G (1997) Global-scale assessment of vegetation phenology using noaa/avhrr satellite measurements J Clim 10:1154-1170 doi:10.1175/1520-0442(1997)010<1154:GSAOVP>2.0.CO

Mountrakis G, Im J, Ogole C (2011) Support vector machines in remote sensing: A review ISPRS J Photogramm Remote Sens 66:247-259 doi:https://doi.org/10.1016/j.isprsjprs.2010.11.001

Myneni RB, Hall FG, Sellers PJ, Marshak ALJIToG, Sensing R (1995) The interpretation of spectral vegetation indexes 33:481-486

NASA LP DAAC 2017, mod13q1. Version 6. Nasa eosdis land processes daac, usgs earth resources observation and science (eros) center, sioux falls, south dakota (https://lpdaac.Usgs.Gov), accessed april 13, 2017, . http://dx.doi.org/10.5067/MODIS/MOD13Q1.006.

Nath R, Luan Y, Yang W, Yang C, Chen W, Li Q, Cui XJS (2015) Changes in arable land demand for food in india and china: A potential threat to food security 7:5371-5397

Nitze I, Barrett B, Cawkwell F (2015) Temporal optimisation of image acquisition for land cover classification with random forest and modis time-series Int J Appl Earth Obs Geoinf 34:136-146 doi:https://doi.org/10.1016/j.jag.2014.08.001

O'Loughlin FE, Paiva RCD, Durand M, Alsdorf DE, Bates PD (2016) A multi-sensor approach towards a global vegetation corrected srtm dem product Remote Sens Environ 182:49-59 doi:https://doi.org/10.1016/j.rse.2016.04.018

Ouatiki H, Boudhar A, Ouhinou A, Arioua A, Hssaisoune M, Bouamri H, Benabdelouahab T (2019a) Trend analysis of rainfall and drought over the oum er-rbia river basin in morocco during 1970–2010 Arab J Geosci 12:128 doi:10.1007/s12517-019-4300-9

Ouatiki H, Boudhar A, Ouhinou A, Arioua A, Hssaisoune M, Bouamri H, Benabdelouahab T (2019b) Trend analysis of rainfall and drought over the oum er-rbia river basin in morocco during 1970–2010 Arab J Geosci 12 doi:10.1007/s12517-019-4300-9

Ouatiki H, Boudhar A, Ouhinou A, Beljadid A, Leblanc M, Chehbouni A (2020) Sensitivity and interdependency analysis of the hbv conceptual model parameters in a semi-arid mountainous watershed Water 12:2440

Ouatiki H et al. (2017) Evaluation of trmm 3b42 v7 rainfall product over the oum er rbia watershed in morocco Climate 5:1 doi:10.3390/cli5010001
Pal M (2005) Random forest classifier for remote sensing classification Int J Remote Sens 26:217-222 doi:10.1080/01431160412331269698
Pal M, Mather PM (2005) Support vector machines for classification in remote sensing Int J Remote Sens 26:1007-1011 doi:10.1080/01431160512331314083
Pan Z et al. (2015) Mapping crop phenology using ndvi time-series derived from hj-1 a/b data 34:188-197
Peng J, Dan L, Dong W (2013) Estimate of extended long-term lai data set derived from avhrr and modis based on the correlations between lai and key variables of the climate system from 1982 to 2009 Int J Remote Sens 34:7761-7778 doi:10.1080/01431161.2013.826840
Qian Y, Zhou W, Yan J, Li W, Han L (2014) Comparing machine learning classifiers for object-based land cover classification using very high resolution imagery Remote Sens 7:153-168 doi:10.3390/rs70100153
Qiu B et al. (2017) Mapping cropping intensity trends in china during 1982–2013 Appl Geogr 79:212-222 doi:10.1016/j.apgeog.2017.01.001
R Core Team (2017) R: A language and environment for statistical computing.
Reed BC, Brown JF, VanderZee D, Loveland TR, Merchant JW, Ohlen DO (1994) Measuring phenological variability from satellite imagery J Veg Sci 5:703-714 doi:10.2307/3235884
René A, Nathalie R (2007) L'agriculture du maghreb au défi du changement climatique : Quelles stratégies d'adaptation face à la raréfaction des ressources hydriques ? Paper presented at the WATMED 3,3e conférence internationale sur les Ressources en Eau dans le Bassin Méditerranéen <halshs-00134115>, Tripoli 1 -3 novembre 2006
Reza MN, Na IS, Baek SW, Lee K-H (2019) Rice yield estimation based on k-means clustering with graph-cut segmentation using low-altitude uav images Biosystems Engineering 177:109-121 doi:https://doi.org/10.1016/j.biosystemseng.2018.09.014
Rodriguez-Galiano VF, Ghimire B, Rogan J, Chica-Olmo M, Rigol-Sanchez JP (2012) An assessment of the effectiveness of a random forest classifier for land-cover classification ISPRS J Photogramm Remote Sens 67:93-104 doi:10.1016/j.isprsjprs.2011.11.002
Rouse JW, Haas RH, Schell JA, Deering DW (1973) Monitoring vegetation systems in the great plains with erts. Paper presented at the Third ERTS Symposium, Washington DC: NASA,
Salhi A et al. (2020) Bridging the gap of perception is the only way to align soil protection actions Sci Total Environ 718:137421 doi:10.1016/j.scitotenv.2020.137421
Samworth RJ (2012) Optimal weighted nearest neighbour classifiers Ann Statist 40:2733-2763 doi:10.1214/12-AOS1049
Schilling J, Freier KP, Hertig E, Scheffran JJA, Ecosystems, Environment (2012) Climate change, vulnerability and adaptation in north africa with focus on morocco 156:12-26
Schmidt M, Lucas R, Bunting P, Verbesselt J, Armston J (2015) Multi-resolution time series imagery for forest disturbance and regrowth monitoring in queensland, australia Remote Sensing of Environment 158:156-168 doi:https://doi.org/10.1016/j.rse.2014.11.015
Schreier J, Ghazaryan G, Dubovyk O (2020) Crop-specific phenomapping by fusing landsat and sentinel data with modis time series Eur J Remote Sens:1-12 doi:10.1080/22797254.2020.1831969
Schwartz MD (2003) Phenology: An integrative environmental science. Tasks for vegetation science 39. Kluwer academic publishers, Dordrecht, The Netherlands.
Schwartz MD (2013) Phenology: An integrative environmental science. Second Edition edn. Springer, New York
Schwartz MD, Carbone GJ, Reighard GL, Okie WRJH (1997) A model to predict peach phenology and maturity using meteorological variables 32:213-216
Schwartz MD, Reed BCJIJoRS (1999) Surface phenology and satellite sensor-derived onset of greenness: An initial comparison 20:3451-3457
Shahriar PM, Budde M, Rowland J (2014) Mapping irrigated areas in afghanistan over the past decade using modis ndvi Remote Sens Environ 149:155-165 doi:10.1016/j.rse.2014.04.008

Shao Y, Lunetta RS (2012) Comparison of support vector machine, neural network, and cart algorithms for the land-cover classification using limited training data points ISPRS J Photogramm Remote Sens 70:78-87 doi:10.1016/j.isprsjprs.2012.04.001

Sishodia RP, Ray RL, Singh SK (2020) Applications of remote sensing in precision agriculture: A review Remote Sens 12:3136

Sobrino J, Raissouni NJIjors (2000) Toward remote sensing methods for land cover dynamic monitoring: Application to morocco 21:353-366

Spiertz JJSa (2009) Nitrogen, sustainable agriculture and food security: A review:635-651

Suepa T, Qi J, Lawawirojwong S, Messina JP (2016) Understanding spatio-temporal variation of vegetation phenology and rainfall seasonality in the monsoon southeast asia Environ Res 147:621-629 doi:10.1016/j.envres.2016.02.005

Sun H et al. (2018) Optimizing knn for mapping vegetation cover of arid and semi-arid areas using landsat images Remote Sens 10:1248 doi:10.3390/rs10081248

Sun H, Xu A, Lin H, Zhang L, Mei Y (2012) Winter wheat mapping using temporal signatures of modis vegetation index data Int J Remote Sens 33:5026-5042 doi:10.1080/01431161.2012.657366

Toth C, Jóźków G (2016) Remote sensing platforms and sensors: A survey ISPRS J Photogramm Remote Sens 115:22-36 doi:https://doi.org/10.1016/j.isprsjprs.2015.10.004

Tucker CJ (1979) Red and photographic infrared linear combinations for monitoring vegetation Remote Sens Environ 8:127-150 doi:https://doi.org/10.1016/0034-4257(79)90013-0

Tucker CJ, Vanpraet C, Boerwinkel E, Gaston A (1983) Satellite remote sensing of total dry matter production in the senegalese sahel Remote Sens Environ 13:461-474

Vancutsem C, Ceccato P, Dinku T, Connor SJ (2010) Evaluation of modis land surface temperature data to estimate air temperature in different ecosystems over africa Remote Sens Environ 114:449-465 doi:https://doi.org/10.1016/j.rse.2009.10.002

Vapnik VN (2006) Estimation of dependence based on empirical data: : Empirical inference science afterword of 2006. Information science and statistics. Springer-Verlag New York. doi:10.1007/0-387-34239-7

Venkata M, Reddy P, Chandra Mohan Reddy S (2020) Classification of remote sensing images based on k-means clustering and artificial bee colony optimization. In: Advances in cybernetics, cognition, and machine learning for communication technologies. Springer, pp 57-65

Verner D et al. (2018) Climate variability, drought, and drought management in morocco's agricultural sector vol https://openknowledge.worldbank.org/handle/10986/30603 License: CC BY 3.0 IGO. World Bank, Washington, DC. © World Bank

Viña A, Gitelson AA, Rundquist DC, Keydan G, Leavitt B, Schepers J (2004) Monitoring maize (zea mays l.) phenology with remote sensing Agron J 96:1139-1147 doi:10.2134/agronj2004.1139

Vrieling A, de Beurs KM, Brown ME (2011) Variability of african farming systems from phenological analysis of ndvi time series Clim Chang 109:455-477 doi:10.1007/s10584-011-0049-1

Vrieling A, de Leeuw J, Said M (2013) Length of growing period over africa: Variability and trends from 30 years of ndvi time series Remote Sens 5:982-1000 doi:10.3390/rs5020982

Wang D et al. (2018) Evaluating the performance of sentinel-2, landsat 8 and pléiades-1 in mapping mangrove extent and species Remote Sens 10:1468 doi:10.3390/rs10091468

Wardlow B, Egbert S, Kastens J (2007) Analysis of time-series modis 250 m vegetation index data for crop classification in the u.S. Central great plains Remote Sens Environ 108:290-310 doi:10.1016/j.rse.2006.11.021

Wessel M, Brandmeier M, Tiede D (2018) Evaluation of different machine learning algorithms for scalable classification of tree types and tree species based on sentinel-2 data Remote Sens 10:1419 doi:10.3390/rs10091419

Wessels KJ, Bachoo A, Archibald S (2009) Influence of composite period and date of observation on phenological metrics extracted from modis data. Paper presented at the 33rd International Symposium on Remote Sensing of Environment: Sustaining the Millennium Development Goals, Stresa, Lago Magglore, Italy, 4-8 May 2009

White MA et al. (2009a) Intercomparison, interpretation, and assessment of spring phenology in north america estimated from remote sensing for 1982–2006 15:2335-2359 doi:https://doi.org/10.1111/j.1365-2486.2009.01910.x

White MA et al. (2009b) Intercomparison, interpretation, and assessment of spring phenology in north america estimated from remote sensing for 1982-2006 Glob Chang Biol 15:2335-2359 doi:10.1111/j.1365-2486.2009.01910.x

White MA, Hoffman F, Hargrove WW, Nemani RR (2005) A global framework for monitoring phenological responses to climate change 32 doi:https://doi.org/10.1029/2004GL021961

White MA, Thornton PE, Running SW (1997) A continental phenology model for monitoring vegetation responses to interannual climatic variability Glob Biogeochem Cycles 11:217-234 doi:10.1029/97gb00330

Wielgolaski FEJIjoB (2001) Phenological modifications in plants by various edaphic factors 45:196-202

Winkler K, Gessner U, Hochschild V (2017) Identifying droughts affecting agriculture in africa based on remote sensing time series between 2000–2016: Rainfall anomalies and vegetation condition in the context of enso Remote Sens 9:831

Wu D, Qu JJ, Hao X (2015) Agricultural drought monitoring using modis-based drought indices over the USA corn belt Int J Remote Sens 36:5403-5425 doi:10.1080/01431161.2015.1093190

Xiaoyang Zhang et al. (2003) Monitoring vegetation phenology using modis Remote Sens Environ 84:471–475

Yan Y et al. (2020) Driving forces of land surface temperature anomalous changes in north america in 2002–2018 Sci Rep 10:6931 doi:10.1038/s41598-020-63701-5

Yang F et al. (2007) Developing a continental-scale measure of gross primary production by combining modis and ameriflux data through support vector machine approach Remote Sens Environ 110:109-122 doi:https://doi.org/10.1016/j.rse.2007.02.016

Yu L, Su J, Li C, Wang L, Luo Z, Yan B (2018) Improvement of moderate resolution land use and land cover classification by introducing adjacent region features Remote Sens 10:414 doi:10.3390/rs10030414

Yuan M, Wang L, Lin A, Liu Z, Qu S (2019) Variations in land surface phenology and their response to climate change in yangtze river basin during 1982–2015 Theor Appl Climatol 137:1659-1674 doi:10.1007/s00704-018-2699-7

Zeng L, Wardlow BD, Xiang D, Hu S, Li DJRSoE (2020) A review of vegetation phenological metrics extraction using time-series, multispectral satellite data 237:111511

Zhang X et al. (2003) Monitoring vegetation phenology using modis Remote Sens Environ 84:471-475 doi:https://doi.org/10.1016/S0034-4257(02)00135-9

Zhao Q, Brocks S, Lenz-Wiedemann VIS, Miao Y, Zhang F, Bareth G (2017) Detecting spatial variability of paddy rice yield by combining the dndc model with high resolution satellite images Agric Syst 152:47-57 doi:https://doi.org/10.1016/j.agsy.2016.11.011

Zhou L, Tucker CJ, Kaufmann RK, Slayback D, Shabanov NV, Myneni RB (2001) Variations in northern vegetation activity inferred from satellite data of vegetation index during 1981 to 1999 J Geophys Res Atmos 106:20069-20083 doi:10.1029/2000jd000115